INFRARED STUDIES OF TWO DARK CLOUDS

Thesis by

Jonathan H. Elias

In Partial Fulfillment of the Requirements

for the Degree of

Doctor of Philosophy

California Institute of Technology

Pasadena, California

1978

(Submitted February 3, 1978)

ACKNOWLEDGEMENTS

The projects described in this thesis involved a large amount of observing time on various telescopes, which could not have been carried out without the assistance of a large number of people. Nearly every member of the Caltech infrared group helped with the Mt. Wilson observations at one time or another; Dan Nadeau, Steve Beckwith, Dave Ennis, Eric Persson and Anneila Sargent provided the bulk of this assistance. A good deal of help was also provided by the Mt. Wilson night assistants, Jim Frazier, Gene Hancock and Howard Lanning. Thanks are also due Drs. H. C. Arp and G. W. Preston, for handling the scheduling problems involving the infrared equipment, and for arranging for clear weather.

The observations at CTIO would not have been possible without the assistance of Jay Frogel and of the Cerro Tololo mountain crew.

I am also particularly grateful to Gordon Forrester and Keith Matthews for assistance with equipment; none of this work would have been possible without their help. Jim Gunn, John Hoessel, and Bob Zinn provided the optical spectra and much of the photographic material used in the thesis.

Eric Becklin originally suggested the project which grew into the thesis. Various people have provided useful comments on the work as it progressed, including Eric Becklin, Gary Grasdalen, George Herbig, Steve Strom and Mike Werner, but chief among these was my advisor, Gerry Neugebauer, who has read and commented on more

versions of this thesis than either of us would care to remember. I am also grateful to Janine Boyer, Sharon Hage and Alice Pruett, who carefully typed the manuscript and the lengthy tables.

ABSTRACT

The IC5146 dark cloud complex has been surveyed in the infrared in order to identify and study associated young stellar objects. Most of the objects detected in the survey appear to be field stars, predominantly late-type giants. Three young objects were detected in the survey: The B0 star BD+46°.3474, the Ae star BD+46°.3471, and a previously unidentified object which appears to be a heavily obscured FU Ori star. The properties of the last two objects are examined in detail, and an attempt is made to produce reasonable models for them. It is suggested that FU Ori stars are binaries, and some consequences of this model are described. Photometry of the brighter stars in the IC5146 cluster has been used to establish a distance to the cluster of 900 ± 100 pc.

A near-infrared survey has also been conducted of nearly 18 square degrees of the Ophiuchus dark cloud complex. Additional observations have been made of selected objects found in this survey and of the brighter objects found by Grasdalen *et al.* and by Vrba *et al.* in this region, in order to identify and study the young stars associated with the cloud. These observations show that very recent star formation has been largely restricted to a small region no more than a few parsecs in extent at the center of the dark cloud complex. Most of the young stars do not appear to be main sequence stars. At least three of these objects appear to be surrounded by infrared reflection nebulae. Many of the objects studied are background K and M giants which can be used to determine the near-infrared extinction due to the dark cloud.

TABLE OF CONTENTS

CHAPTER 2 (continued)

INTRODUCTION

This thesis consists of two papers describing the results of two infrared investigations of dark cloud regions. The first paper (Chapter 1) describes a study of the dark cloud associated with the HII region IC5146. This is a small dark cloud complex located a few degrees from the galactic plane at a distance of approximately 900 parsecs. Two appendices are also included which describe the analysis of 2 μm spectrophotometry and the construction of a simple model for the distribution of field stars observed at 2.2 μm.

The second paper (Chapter 2) describes a more ambitious undertaking, a study of a large area comprising most of the Ophiuchus dark cloud complex. This region is located fifteen to twenty degrees from the galactic plane, at a distance of roughly 160 parsecs. It is one of the nearest regions where extensive recent star formation has occurred, and has been previously studied by several other investigators, whose results are also discussed in this paper.

This work was conducted in order to provide a reasonably unbiased sample of the young stars embedded in the two dark cloud complexes, down to a limiting 2.2 μm magnitude of roughly +7. In general, infrared studies of dark clouds have been conducted only in small selected areas -- peaks in molecular emission lines or in the radio continuum, or regions where visible objects already known to be young stars have been identified. Regions which show none of these characteristics have been largely ignored, and objects which produce little radio or optical emission may well have been missed.

The results of the studies in this thesis tend to show that there is a great variety in the stellar population of dark cloud regions, and that any simple picture of these regions is probably unduly simple. For this reason, the two papers are descriptive rather than analytical, and are intended as much as anything else to provide opportunities for additional investigations.

CHAPTER 1

A STUDY OF THE IC5146 DARK CLOUD COMPLEX

I. INTRODUCTION

The IC5146 open cluster is a young stellar cluster at the eastern end of a small dark cloud complex (Fig. 1a). Although the visible cluster itself appears quite young (Walker 1959), it seemed possible that even younger objects might lie embedded in the dark cloud. In order to find these, the whole region has been surveyed at 1.6 and 2.2 μm, and additional observations have been made of selected objects detected in the survey.

The work described here is part of a series of surveys of dark clouds done for the purpose of finding and studying young stellar objects. The IC5146 complex was chosen as the first region to be studied because it is small, and could therefore be used to test techniques quickly, and because it is optically well studied (Walker 1959; Herbig 1960a). The optical studies have been combined with the infrared observations to find the distance to the cloud complex and to identify associated visible stars. The IC5146 region has also been previously studied in the radio (e.g., Loren et al. 1973; Kuiper et al. 1976; Milman et al. 1975) and in the infrared (Strom et al. 1972; Cohen 1973a).

The infrared survey and the subsequent observations are described below in §II, and the results of both the survey and the subsequent work are given in §III. The identifications of the infrared sources are discussed in §IV, where it is shown that all but a few of the detected objects are late-type giants unrelated to the dark cloud complex.

Two interesting young objects were detected in the survey and were subsequently studied in detail. The first of these appears to be a newly discovered FU Ori star, and is discussed in §V. It is suggested that the star may be a binary (§Vb).

The second young object is the Ae star BD+46°3471, which is discussed in detail in §VI. The new observations agree with previous work (Strom et al. 1972, Cohen 1973a, Allen 1973); they also show the object to be slightly variable in the near-infrared.

Infrared photometric observations of stars in the vicinity of IC5146 are presented in §VII. These observations are combined with existing optical photometry to derive a distance to the cluster and the dark cloud of 900 ± 100 pc; the observations also serve to identify unusual stars.

II. INFRARED OBSERVATIONS

The present infrared survey was done using a two channel InSb detector system which measures a single point in the sky simultaneously at two wavelengths. One channel corresponds to the standard 2.2 μm (K) filter (2.0 μm < λ < 2.4 μm), while the second channel (1.35 μm < λ < 1.7 μm) corresponds approximately to the standard 1.6 μm (H) filter. The limiting K magnitude of the survey is fainter than +8, while at 1.6 μm it is only somewhat fainter than +7.5. An empirically determined color correction was applied to the 1.6 μm magnitudes to transform them to H magnitudes. At K = +8 the 1σ uncertainty in the survey magnitude is ±0.3; for brighter objects the uncertainty decreases to ±0.1.

Scans spaced 45" apart in declination were made at sidereal rate on the CIT 0.6 m telescope on Mt. Wilson using a 1' aperture. The signal and reference beams were separated by about 2' in right ascension.

Selected objects detected in the survey and several additional stars in the IC5146 cluster were studied using broadband photometry from 1.2 μm to 20 μm and low resolution 2 μm spectrophotometry. Most of these observations were made with the Mt. Wilson 1.5 m and 2.5 m telescopes, although a few measurements were made with the 5 m Hale telescope or the 0.6 m CIT telescope. The observations between 1.2 and 4.8 μm were mostly made with an InSb detector; the measurements at longer wavelengths were made with a germanium bolometer. The properties of the broadband filters and the flux calibration used are given in Wilson et al. (1972) and Beckwith et al. (1976). The calibration of the 2 μm spectrophotometry is described in Appendix A.

III. RESULTS

An area of 2.3 square degrees was scanned; in this area 113 objects brighter than K = +8 were found. The area mapped and the distribution of the objects detected are shown in Figure 1. Detections in adjacent scans were considered to be due to the same object if they were within 2' of each other in right ascension. The probability that a detectable object would lie close enough to a given detected object to be confused with it is about 0.08 at the limiting magnitude; the actual number of detected objects is therefore probably

somewhat greater than 120. The cumulative counts, corrected for this effect, are shown in Figure 2.

Of the objects detected in the survey, two groups were selected for further study. The first group contained the eight objects with K brighter than +5; the second nine objects with H-K redder than +0.5 and K brighter than +7, the faintest magnitude for which H-K could be reliably determined. This second group should contain cool or heavily reddened objects, and objects with circumstellar emission. Positions and observed magnitudes for these observed infrared magnitudes are listed in Tables 1 and 2; object 5 is a member of both groups. The objects were all identified with visible stars on the telescope; the positions given are those of the visible stars as measured from plates taken on the 1.2 m Palomar Schmidt and are accurate to ±1". Additional information on the optical identifications is given in the notes to the tables.

The results of the broadband photometry are also given in Tables 1 and 2. The values given are averages of all measurements; if there are possible variations or aperture effects these are mentioned in the notes to the tables. If the object was measured more than once, the number of days it was measured is indicated in the notes. All wavelengths were not always measured each time an object was observed; 1.6 and 2.2 μm were almost always measured. The magnitudes are given to two decimal places if the 1σ uncertainty is less than 0.10; otherwise only one decimal place is given and the uncertainty is given explicitly. All upper limits are 3σ upper limits.

The 2 μm spectra of the stars listed in Tables 1 and 2 are plotted in Figures 3 and 4 respectively. The uncertainties shown are relative uncertainties; the uncertainties in the fluxes are 5% or better.

IV. GENERAL DISCUSSION

The stars detected in the survey seem uniformly distributed, (Fig. 1) suggesting that they are mostly field stars, that is, stars not embedded in the cloud material and with no origin in the cloud. This is supported by a comparison, shown in Figure 2, of the observed cumulative counts with those predicted by calculations based on a model of the galactic stellar distribution. A description of the model, which was also used to predict the spectral type distribution of the observed field stars, is given in Appendix B.

As the observed sample contained many field stars it was necessary to develop a means of separating the stars associated with the cloud from the field stars. The best discriminant is direct evidence that a given star is embedded in cloud material. Examples would be the presence of reflection nebulae around the star, or of emission peaks in molecular lines or the far infrared.

Additional criteria for removing field stars are less precise. If the energy distribution of an object shows apparent strong circumstellar emission, this increases the probability that the object is a very young object associated with the dark cloud, though it may also be a giant of very late spectral type. Most of the field stars and,

conceivably, many of the young stars associated with the cloud should show essentially blackbody energy distributions.

Field stars were distinguished from young stars near the main sequence using 2 μm spectroscopy. In the IC5146 region, at the limiting 2.2 μm magnitude of the survey, roughly 95% of the field stars should be K or M giants according to the model described in Appendix B. In such stars the 2.3 μm CO band can be definitely identified in low resolution 2 μm spectra; the presence of the CO band in the spectrum of a star with no unusual characteristics was taken as indicating that it was a field star.

For stars showing circumstellar emission the nature of the circumstellar emission and the presence or absence of CO and H_2O features are used to distinguish between late type giants with circumstellar shells, presumed to be field stars, and young stars with circumstellar emission, presumed to be associated with the cloud.

The assumptions about the nature of the field stars were tested using the observations of the nine objects with K brighter than 5.0. These all show the CO band in their 2 μm spectra (Fig. 3) and have energy distributions like those of cool stars. All but object 3 can be identified with stars observed by Lee *et al.* (1947); the spectral types found by Lee *et al.* (given in the notes to Table 1) are consistent with the types inferred from the 2 μm spectra (Appendix A).

The red stars in Table 2 appear to include both field stars and young stars. One of the objects, BD+46°3471 (#15), does not show any significant features in its 2 μm spectrum, and a second, #12, also

shows a 2 μm spectrum different from the others. Herbig (1960b) identified BD+46°3471 as an emission-line star embedded in the dark cloud, but object 12 cannot be identified with a previously studied optical object. Details of the observations of these two objects are discussed below (§V, VI); their energy distributions are plotted in Figure 5.

The remaining objects in Table 2 appear to be field stars. Two of the objects have a bluer H-K than the survey cutoff at 0.5, a result of the fact that survey colors had uncertainties of ~ 0.15 magnitudes at K = +7. This suggests that the red object sample is probably complete only for H-K > 0.7.

V. OBJECT 12

a) Classification

Object 12 appears to be a newly discovered, fourth example of the FU Orionis eruptive variables described by Herbig (1966, 1967), based on its light curve and its spectrum.

FU Ori stars are objects embedded in dark clouds which undergo a substantial increase in visual brightness ($\sim$ 5 magnitudes) over a period of a few months to several years, and then remain near maximum for many years. The FU Ori stars all have similar spectra, both in the visual (Herbig 1977), and in the near-infrared (Cohen 1975), and their energy distributions are also similar to one another (Herbig 1977, and references therein).

The optical spectra show absorption features characteristic of F or G supergiants, and also show P Cygni profiles at Hα. The infrared spectra show strong absorption by H_2O and CO characteristic of much cooler material. The energy distributions show evidence for three components: the visible star, a cooler component with a color temperature of 1500-2000 K, and a still colder component with a color temperature near 200 K.

Object 12 currently has an R magnitude near +15.0, as derived from a measurement of the object using the multichannel spectrometer on the 5 m Hale telescope by R. J. Zinn (Fig. 5). There is no star brighter than 20th magnitude visible on the red Palomar Sky Survey print, though the star and an associated reflection nebula are visible on more recent but otherwise identical red plates (Fig. 6: Plate). A search of the Hale Observatories plate files revealed only one useful prediscovery plate, a near infrared ($\lambda \sim 7500$ Å) photograph taken on 1965 July 5 (UT), which shows the object near its present magnitude at this wavelength. There is no evidence for any substantial variations on recent plates; there is also no evidence for any substantial variations in the near infrared (Fig. 7a), over a period of almost three years. The star thus appears to have brightened by at least 5 magnitudes sometime between 1952 September -- the date of the Sky Survey plate -- and 1965 July, and to have remained at a relatively constant magnitude since then.

This object is much fainter visually than the other FU Ori stars, so optical spectra cannot be as readily obtained. A spectrum of the object is shown in Figure 8, taken 1976 September 22 (UT) by

J. E. Gunn using the SIT spectrograph on the 5 m Hale telescope. The only apparent feature is Hα, seen in absorption; though no classification is possible, the absence of other strong features is consistent with a relatively early spectral type and high luminosity. The Hα feature appears displaced to the blue by ~ 4 Å; this may indicate that it is an unresolved P Cygni profile.

The 2 μm spectrum (Fig. 4) is very similar to that of FU Ori itself and of V1057 Cygni (Cohen 1975) in that it shows strong CO and H_2O absorption features. Such a spectrum is characteristic of very late M giants (see Merrill and Stein 1976a,b) but not of T Tauri stars or other young objects (see Cohen 1975). The energy distribution is similar to that of the other FU Ori stars (e.g., Rieke et al. 1972; Cohen 1973a,b) except that this star appears more heavily reddened. In particular, there appear to be two emitting components, one with a color temperature between 1500 and 2000 K, the other with a color temperature near 200 K. A weak emission feature at 10 μm, attributable to silicates, is seen in the three identified FU Ori stars; this feature is weak or absent in object 12. There is thus good reason to believe that this object is in fact another FU Ori variable.

b) Model

The available information permits construction of a reasonable model of the object, which should be applicable to other stars of this class. The proposal is that the object is a binary star, consisting of a luminous star of probable spectral type F or G, and a somewhat

less luminous star of spectral type M8 or later. This binary is surrounded by a dust shell with a small optical depth and a temperature near 200 K. Additional dark cloud material in the line of sight may contribute extinction, but will produce no added flux outside of the far-infrared. The flux between 2 and 5 μm is mostly produced by the M star, while the flux below 1 μm is produced by the F star. The dust shell emission is important only at wavelengths longwards of 5 μm.

The model stellar parameters derived from the observations of object 12 are listed in Table 3. The spectral type of the hot star is uncertain, so values are listed for two alternate types, FOII and GOII; the model fits similarly for both. The model energy distribution for an assumed spectral type of the hot star of GOII is compared with the observations in Figure 9. The cool dust envelope is modeled assuming dust grains with emissivity proportional to λ^{-1} at a temperature of 170 K; this is intended only as a crude approximation. The model fits well out to 3 μm; the excess of the observed flux over the model at 3.5 and 4.8 μm may be due either to emission from the dust shell which produces the 10 and 20 μm flux, or to an overestimate of the temperature of the cool component. The model parameters which fit the 1971 observations at V1057 Cygni by Rieke et al. (1972) are also listed in Table 3.

It has generally been suggested that the flux attributed here to an M star is produced instead by a second circumstellar shell containing hot dust (e.g., Simon et al. 1972; Rieke et al. 1972; Cohen 1973a,b). The energy distributions of the FU Ori stars can

be fitted by either model, but the spectroscopic evidence seems inconsistent with the hot dust shell model. The 2 μm spectra show strong H_2O and CO absorption bands of a sort not seen in circumstellar shells, but generally seen in late-M giants. In addition, the optical spectra show no strong molecular absorptions, as would be expected if the 2 μm spectrum were produced in a circumstellar shell. If the molecular features seen at 2 μm are produced by absorption of light from the hot star by material in a circumstellar shell, one would expect to see related features in the visual spectra such as the H_2O band at 0.93 μm. If the models given in Table 3 are applicable, the fractions of the light which is due to the M giant will be roughly 25% at I(0.9 μm), roughly 6% at R(0.7 μm), and still less at shorter wavelengths. Consequently, only in the red will even the strongest features in the M giant be seen. The SIT spectrum in Figure 8 is essentially featureless, and the dereddened multichannel spectrometer scan in Figure 10 shows no pronounced features. There is a weak feature at 0.94 μm, about 0.1 mag deep, which could be due to strong 0.93 μm H_2O absorption in the M giant. Other possible late-type stellar features are marginally present. The spectra of the other FU Ori stars also show no evidence of strong absorption in the red or photographic infrared (Herbig 1977; Shanin et al. 1975).

A second piece of evidence which appears to favor the binary model is the lack of variability in the 2-5 μm region, both in object 12 (Fig. 7a) and in V1057 Cygni (Cohen 1973a; Simon 1975; Simon and Dyck 1977). In ojbect 12, there appear to have been no

recent variations at other wavelengths, but in V1057 Cygni, both the visible and 10-20 μm fluxes have decreased since the outburst. If the 2-5 μm flux is produced by material ejected from the hot star, one would expect the dust to have cooled and its luminosity to have decreased as it receded from the star. If the shell is stationary, the decrease in the hot star's luminosity should have caused a corresponding decrease in the luminosity reradiated by the hot dust. The constancy of the 2-5 μm flux seems most reasonably explained if it is produced by a luminosity source independent of the hot star.

If the FU Ori stars are in fact binaries, the radial velocities of the stars should be variable. There is no evidence for large variations in the radial velocities of the hot star; the most stringent limit is that set by Herbig's (1977) series of observations of V1057 Cygni, in which the amplitude of the hot star's radial velocity variations can be no larger than ±5 km/sec.

The amplitude of the hot star's radial velocity variations will be within this limit for separations as small as a few astronomical units if the hot star is more massive than the M star. As an example, if the system consists of a hot star of 5 solar masses and an M star of 1 solar mass, the hot star's velocity amplitude will be ±5 km/sec for a separation of 6 a.u. if the system is viewed edge-on. The period will be about 6 years. The variations in the M star radial velocity should be several times larger, and may be observable using high resolution spectroscopy near 2 μm.

If the model is correct, the FU Ori outbursts may be a consequence of the binary nature of the stellar systems, and the mechanism may be similar to that which produces slow novae such as RR Tel, where the secondary is also a late M giant (e.g., Glass and Feast 1974).

A difficulty with the binary model is that preoutburst FU Ori stars are probably luminous T Tauri stars (Herbig 1977), which have 2 μm spectra which are nearly featureless (Cohen 1975; Elias in preparation). In addition, the observed 2.2 μm absolute magnitudes of T Tauri stars are all fainter than those of the M-giant secondaries in the FU Ori models, which are about $M_K = -4$. A possible explanation of these discrepancies is that the secondary is also affected by the outburst, so that its luminosity and radius are increased; observations of the 2 μm spectrum of an FU Ori star during the early stages of its outburst could help resolve this problem.

VI. BD+46°3471 (OBJECT 15)

BD+46°3471 is one of a group of emission-line stars which Herbig (1960b) suggested might be pre-main-sequence stars. The observations of these stars have been reviewed by Strom et al. (1975); they seem to confirm their pre-main-sequence nature. Despite many observations, the detailed characteristics of these stars are not fully understood.

The extinction to BD+46°3471 derived from the visual colors is small ($A_V \sim 1.3$ magnitudes: Walker 1959; Strom et al. 1972) and the energy distribution (Fig. 5) cannot be fitted by that of an early type star. There is undoubtedly a hot circumstellar envelope

producing hydrogen recombination radiation, as indicated by the presence of hydrogen emission lines in the spectrum (e.g., Herbig 1960b; Andrillat and Swings 1976) and by a U-B color too blue for the observed spectral type (Strom et al. 1972), but this hot envelope is too weak to produce the observed infrared flux. This can be seen both from extrapolation of the continuum inferred from UBV photometry, and from the absence of the Bγ hydrogen line in the 2 μm spectrum of BD+46°3471 (Fig. 4).

The total observed luminosity is 140 solar luminosities if the distance is 900 pc (§VII). If the visual extinction to the star is 1.3 magnitudes, its photospheric luminosity is roughly 200 solar luminosities. This indicates that the infrared emission can be accounted for by reradiation by the envelope of the flux from the star. Both luminosity estimates are substantially in excess of the spectroscopic luminosity determined by Strom et al (1972) of 15 solar luminosities.

A reasonable model which accounts for the infrared flux is one in which hot gas flowing out from the star cools sufficiently to form dust, which absorbs light from the star and reradiates this energy in the near infrared. According to this picture, the emission line spectrum and ultraviolet excess are produced in a region close to the star; the dust forms at a greater distance. This model is similar to that proposed for other stars of this type by Allen and Penston (1973).

If the dust has a λ^{-1} emissivity, the infrared energy distribution is fitted by an envelope containing dust grains with temperatures up to 1,300 K. The bulk of the emission is from dust at a

temperature near 1,000 K. The stellar temperature is near 10,000 K (Strom et al. 1972), so the dust should be approximately 100 stellar radii from the star. The 2 μm optical depth of the envelope derived from the ratio of the envelope flux to the extrapolated stellar flux is less than 0.1, which is consistent with the observed visual extinction to the star.

The general agreement of the new data with previous observations (Strom et al. 1972; Cohen 1973a; Allen 1973) indicates that there are no large infrared flux variations on time scales up to several years. There is evidence of small variations on time scales of a few months, at least in the near infrared. Measurements made at 2.2 μm between 1975 and 1977 are plotted in Figure 7b. χ^2 for the nine 2.2 μm observations is 17: the probability that the star is in fact constant is 0.03. As a comparison, measurements of the nearby bright B star BD+46°3474 are shown in Figure 7c; χ^2 for these measurements is less than 1. The 1.2 and 1.6 μm data show similar behavior. There is additional supporting evidence for the small scale variations observed here: the 1.6 and 2.2 μm magnitudes reported by Strom et al. (1972) and by Allen (1973) are fainter than the mean values given in Table 2. Walker (1959) suggested that the star might be visually variable as well. Additional photoelectric photometry by Racine (1968) and by Strom et al. (1972) appears to support this suggestion. The mean amplitudes of both the optical and near infrared variations appear to be about 0.1 magnitudes. It is not known whether they are correlated; simultaneous observations should help indicate whether the

variations are due to changes in the envelope or in the stellar luminosity.

VII. OBSERVATIONS OF THE IC5146 CLUSTER

In addition to the objects selected in the survey, some of the brighter members of the IC5146 cluster were observed in the infrared. Observations at 1.2, 1.6 and 2.2 μm of nineteen of the stars studied by Walker (1959) are presented in Table 4. Several of the stars were observed more than once; the number of separate observations is indicated in the last column. Uncertainties are typically ±0.07 magnitude for a single observation. UBV photoelectric photometry and spectral types are also listed. Except as noted, the UBV photometry and the spectral types are taken from Walker (1959). Of the nineteen stars, only three were bright enough to have been detected in the survey: BD+46°3471, BD+46°3474 and W74. W74 is a G giant and its membership in the cluster is uncertain; BD+46°3474 is the earliest spectral type star in the cluster, with a spectral type of BOV (Crampton and Fisher 1974). BD+46°3471 has already been discussed in detail (§VI). BD+46°3474 is therefore the only 'normal' star known to be associated with the cloud which was detected in the survey.

The infrared photometry was combined with the visual photometry and observed spectral types to determine the cluster distance using the four early spectral type stars which showed normal energy distributions. The extinction to the stars was determined using the colors tabulated by Johnson (1966). The unreddened H-K color for all four

stars was assumed to be zero; J magnitudes (1.2 μm) were modified according to the transformation given by Frogel et al. (1978). The color excesses were fitted to the "standard" interstellar reddening law (Johnson 1968). The unreddened B-V colors and visual magnitudes are listed in Table 5, together with the visual extinctions, A_V, the inferred absolute visual magnitudes if the stars have not evolved off the zero-age main sequence (Blauuw 1963) and the derived distance moduli. The mean distance modulus, $m-M_v$ is 9.8, corresponding to a distance of 900 pc. If a greater distance to the Hyades is adopted (e.g., Hanson 1975), this value must be increased. The A_V values were derived using the visual and infrared photometry, minimizing the effects of deviations from a normal reddening law. The uncertainties in the individual A_V values are estimated to be 0.1 magnitude. The primary source of uncertainty in the distance is the uncertainty in the absolute magnitudes of the stars. The spectral classifications have an error of roughly ±1 subtype, as estimated from the agreement of the UBV observations with the spectroscopic classifications quoted by Walker (1959). These uncertainties correspond to absolute magnitude uncertainties of about 0.5 magnitudes, so the uncertainty in the mean distance modulus is about 0.3 magnitudes. The distance is then 900 ± 100 pc. This distance estimate is in agreement with that of Walker (1959) and Crampton and Fisher (1974).

The three remaining early-spectral-type stars in Table 4 all appear peculiar. BD+46°3471 and LkHα257 (W76) are emission line stars (Herbig 1960a,b) and also show excess infrared flux. The colors of W53 are inconsistent with its listed spectral type, near A1; the U-B,

B-V colors fit a main sequence spectral type near B6 or near F5. The near infrared reveals further inconsistencies, as the K magnitude is at least 0.5 magnitudes brighter than it should be for either of the two spectral types suggested by the UBV photometry, after dereddening, or for a spectral type of A1. W53 must be included with BD+46°3471 and W76 as an unusual member of the IC5146 cluster. Further observations of this star would be useful.

VIII. CONCLUSIONS

1) The stars associated with the IC5146 dark cloud complex which were detected at 2.2 μm appear to contain a high proportion of unusual objects -- that is, stars associated with the cloud which are not main sequence stars. The selection criteria are admittedly biased in favor of such objects, but it is worth noting that of the seven early-spectral-type members of the IC5146 cluster measured in §VII, only four appear to be completely normal main sequence stars.

2) Even the biased sample of red stars is strongly contaminated by field stars. Although this effect should be reduced for similar surveys at higher latitudes or where the dark clouds have large 2 μm optical depths, it would seem that considerable caution is required in interpreting the results of any undiscriminating 2 μm survey.

3) A newly discovered FU Ori variable is associated with the IC5146 dark cloud complex; the identification is based primarily on its past variability and on its spectroscopic similarity to the other FU Ori variables. Examination of the observations suggests that these

objects can be explained as binary stars, rather than as single stars with hot circumstellar shells. If this explanation is correct, radial velocity variations may be observable in these objects.

4) The present observations of the Ae star BD+46°3471 agree with earlier work. They show that the star has no strong spectral features at 2 μm, and that it is slightly variable in the near infrared. The observations suggest that the infrared excess is produced by hot dust condensed in a stellar wind.

I would like to thank the many people who helped with the observations, particularly S. Beckwith, D. Nadeau, S. E. Persson, J. Frazier, E. Hancock and H. Lanning. I am also grateful to R. J. Zinn and J. E. Gunn for providing optical spectra, to J. Huchra and C. Kowal for providing photographs, and to G. Herbig for helpful correspondence. I would especially like to thank my adviser, G. Neugebauer, for providing criticism of this work, in all its many versions. This work was supported in part by the National Science Foundation grant AST74-18555A2 and by the National Aeronautics and Space Administration grant NGL 05-002-207, and by the California Institute of Technology.

APPENDIX A
REDUCTION AND INTERPRETATION OF 2 μm SPECTRA

a) Reduction

The 2 μm spectra shown in this paper were reduced in a manner similar to that described by Neugebauer et al. (1976), with some additional refinements.

The observations were made with a low-resolution ($\Delta\lambda/\lambda \sim 0.015$) circular variable filter wheel, and covered the wavelength region between 2.0 and 2.5 μm. The primary purpose of the spectra was to identify the broad absorption features of H_2O shortwards (roughly) of 2.1 μm and longwards of 2.4 μm, the CO absorption feature longwards of 2.30 μm, and to measure the strength of the hydrogen Bγ line at 2.166 μm. The measurements were made at points spaced approximately 0.35 μm apart in wavelength, except near the Bγ line where the spacing was halved.

Observations of objects were reduced to fluxes by comparing the measured spectrophotometry to measurements of nearby standard stars made at similar air mass on the same night. Differential air mass corrections were applied; these corrections are mean Mt. Wilson corrections determined empirically from standard star observations on many nights (Fig. 11). The corrections applied to the spectra were seldom greater than 0.05 magnitudes; the uncertainties in the individual points include the effects of uncertainties in the differential corrections, using the dispersion in the extinction coefficients plotted in Figure 11.

The standard stars used are early type stars; they were assumed to have a narrowband-K color equal to 0.00 at all points in the 2 μm region outside of the hydrogen Bγ line; zero magnitude was assumed to be defined by a 10^4 K blackbody at all wavelengths, with the zero point set by equating the flux at 2.20 μm to that in the broadband K filter for zero magnitude (Beckwith et al. 1976). The relative errors in the spectrophotometry introduced by the various assumptions should be less than 2%. Since the standard stars usually showed significant Bγ absorption, a correction for this line was determined by comparing the standards to stars in which this line is absent. The corrections were individually determined, and range from nearly 20 Å down to zero (see below).

b) Accuracy

For bright objects, spectra appear to be reproducible to better than 5% absolute and 2% relative between 2.05 and 2.45 μm; the points outside this region are usually reproducible to 10%. Comparison of the spectrophotometry to broadband K magnitudes indicates a similar accuracy.

c) Interpretation

The strengths of the H_2O and CO absorption features are approximate indicators of spectral type for late type giants (e.g., Baldwin et al. 1973; Frogel et al. 1975). The depth of the CO band head near 2.3 μm can be determined from the spectra, unless they are extremely heavily

reddened or the 2.7 μm H_2O band overwhelms the CO band, as is the case for very late spectral types. Measurements of this band depth for a few bright G, K and M stars are plotted in Figure 12. There appears to be an intrinsic dispersion in the relation (Baldwin et al. 1973), since the typical measurement uncertainty is ~ 0.03 magnitudes. Measurements of the band depth should nonetheless provide an approximate spectral type for K and M giants if the luminosity of the star is known or assumed.

Early main sequence stars show almost featureless spectra, except for the Bγ hydrogen line. The Bγ equivalent width is less than 20 Å for main sequence stars, so that it produces a feature which is a few percent of the continuum at the resolution used. The small extinction coefficient at Bγ and its uniformity in the vicinity of the line made measurements possible with an observed reproducibility of ±2 Å for a single observation of a bright star. The results of observations of bright stars are plotted in Figure 13. For the later spectral types other spectral features affect the measured equivalent width. The important feature of the diagram is that main sequence stars with spectral types between roughly B0 and F5 should have measurable Bγ absorption, though spectral classification is probably not possible from measurements of this accuracy. Stars above the main sequence will have weaker lines than main sequence stars, so failure to detect Bγ is not easily interpreted.

APPENDIX B
FIELD STAR COUNTS

A simple model was constructed in order to predict the approximate numbers and distribution among spectral types of field stars at 2.2 μm. The stars were divided into 25 groups, each covering a small range in spectral type. For each type of star the luminosity function was assumed to take the form

$$\varphi(M,r,\ell,b) = n_o \exp\left[rs - (M-M_o)^2/(2\sigma^2)\right]/(2\pi\sigma^2)^{1/2} \qquad (1)$$

where

$$s = -(\sin|b|)/\beta + (\cos b \cos \ell)/\alpha \qquad (2)$$

and M is the 2.2 μm absolute magnitude of the stars, M_o is the absolute magnitude averaged over volume for stars of this type, and σ is their dispersion in absolute magnitude. n_o is the solar neighborhood space density of such stars, r is the distance along the line of sight, and ℓ and b are galactic longitude and latitude. β is the scale height of the stars perpendicular to the galactic plane and α is a scale length used to model the general stellar density increase toward the galactic center.

The distance, R, can be converted to an apparent magnitude, m, using the relation

$$m = M + 10 + 5 \log_{10}(r) + A_K\beta_D(1-\exp(-r\sin|b|/\beta_D))/\sin|b| \qquad (3)$$

The last term is a correction for interstellar absorption. r is in kpc, A_K is the 2.2 μm interstellar extinction coefficient in the galactic plane and β_D is the scale height of the obscuring matter. For the

model calculations, A_K was taken to be 0.2 magnitudes/kpc, and β_D was taken to be 0.1 kpc.

Using the equations given above, the number of stars of each type visible down to a given limiting 2.2 μm magnitude was obtained by numerical integration. The contributions of the different types were compared, and the total counts were estimated.

The parameters M_o, σ, n_o and β for the stellar types used in the model are listed in Table 6. The values for space densities and absolute magnitude dispersions were derived from McCuskey (1965, 1966, 1969), Blanco (1965), Hidajat and Blanco (1968) and Hughes (1969). The 2.2 μm absolute magnitudes were derived from visual absolute magnitudes (Blauuw 1962; Blanco 1965; Jung 1970, 1971; and Wilson 1976) using V-K colors (Johnson 1966; Lee 1970; and Frogel et al. 1978). The scale heights were derived from Upgren (1962), Blauuw (1965), Elvius (1965) and Hidajat and Blanco (1968). A single value of 2.0 kpc was used for α for all spectral types, (Elvius 1965; Blauuw 1965; McCuskey 1969; Hughes 1969).

Carbon stars and M dwarfs were both omitted from the computations. The luminosity function of carbon stars is poorly known (Blanco 1965), though they seem to have a distribution similar to that of the late-type giants. From the identifications of sources in the IRC (Neugebauer and Leighton 1969) as supplemented by the work of Grasdalen and Gaustad (1971), Vogt (1973) and Hansen and Blanco (1973, 1975) it appears that the carbon stars are roughly 3% of the total number of objects with apparent 2.2 μm magnitude brighter than +3, so they are unlikely to contribute significantly to the total counts in almost all cases.

The M dwarfs were also omitted from the model, largely for computational simplicity. An estimate of the counts due to M dwarfs can be made to justify this. If the early M dwarfs are assumed to have a uniform space density of 0.02 pc^{-3} (Sanduleak 1976) and an absolute 2.2 μm magnitude of +5 (Veeder 1974) there should be roughly one M dwarf per square degree brighter than an apparent 2.2 μm magnitude of 9.5, in any direction. Late M dwarfs should contribute less, though their space densities are not well known. Except near the galactic poles, therefore, the M dwarfs can safely be neglected.

A more serious source of error is the rather simple model of the stellar density variations, as well as uncertainties in the various parameters characterizing the luminosity functions. The model is unlikely to be accurate to better than a factor of 1.5 locally, and should be more unreliable when the counts are dominated by stars at distances of several kpc. The results of the calculations should therefore not be over-interpreted.

TABLE 1

OBJECTS WITH K < 5.0

Object	α(1950)	δ(1950)	[1.2]	[1.6]	[2.2]	[3.5]	[4.8]	[8.7]	[9.5]	[10]	[11.2]	[12.5]
1	$21^h45^m03^s.0$	+47°01'11"	6.03	5.04	4.71							
2	21 45 47.8	+47 05 59	5.55	4.64	4.33							
3	21 47 42.4	+47 32 43	6.29	5.35	5.00							
4	21 48 21.0	+47 33 58	5.73	4.68	4.20	3.67	3.8 ± 0.1	3.3 ± 0.2	3.5 ± 0.2	3.4 ± 0.1	3.6 ± 0.3	2.7 ± 0.3
5	21 50 33.5	+47 09 05	5.41	4.28	3.75	3.08	3.42	2.7 ± 0.2	2.9 ± 0.2	2.77	2.5 ± 0.2	2.4 ± 0.2
6	21 52 41.5	+47 15 06	5.68	4.86	4.60							
7	21 56 59.2	+47 33 08	5.85	5.02	4.84	4.70				4.2 ± 0.3		
8	21 57 01.0	+47 18 47	5.04	4.12	3.80							
9	21 58 02.8	+47 29 33	5.92	5.11	4.88	4.63				4.6 ± 0.3		

Notes (by object):

1. DO 40106 (Lee et al. 1947): Sp = M0
2. DO 40126: Sp = M2
4. DO 40203, V671 Cyg. Sp = C6-, 4 (Stephenson 1973). Measured on 10 dates between 1974 December and 1976 August. There is no evidence for infrared variations greater than ± 0.07 magnitudes.
5. DO 40268, Sp = C4, 3 (Stephenson 1973). Measured on 11 dates between 1975 May and 1976 August. There is no evidence for infrared variations greater than ± 0.05 magnitudes. This star also belongs in Table 2.
6. DO 40345: Sp = M4.
7. DO 40501: Sp = K5.
8. DO 40502: Sp = M3.
9. DO 40540: Sp = M1.

TABLE 2

OBJECTS WITH H-K > 0.5 AND K < 7.0

Object	α(1950)	δ(1950)	[1.2]	[1.6]	[2.2]	[3.5]	[4.8]	[8.7]	[9.5]	[10]	[11.2]	[12.5]	[20]
10	$21^h39^m34^s.4$	+47°12'59"	8.38	7.16	6.65								
11	21 42 03.5	+47 07 56	6.71	5.70	5.29								
12	21 45 26.9	+47 18 08	8.97	7.37	6.32	5.21	4.8 ± 0.1	3.5 ± 0.1	3.3 ± 0.1	3.05	2.8 ± 0.1	2.5 ± 0.2	0.4 ± 0.2
13	21 49 52.5	+47 25 08	7.97	7.00	6.71								
14	21 50 15.1	+47 35 05	7.95	6.83	6.21	5.67	> 5.4			> 4.9			
15	21 50 38.5	+46 59 34	8.44	7.54	6.58	5.33	4.8 ± 0.1			3.5 ± 0.1			> 1.4
16	21 54 57.0	+47 25 24	7.26	6.34	6.02								

Notes (by object):

12. Probable FU Ori star (see text). Measured on 15 dates between 1974 December and 1977 July. There appears to be a possible aperture effect in the near infrared:

	BEAM DIAMETER 9"	17"-20"	> 30"
[1.6]	7.44 ± 0.05	7.37 ± 0.02	7.26 ± 0.06
[2.2]	6.37 ± 0.04	6.32 ± 0.02	6.24 ± 0.05

There is no evidence for any variations as a function of time greater than ± 0.05 magnitudes.

14. Carbon star (Nassau and Blanco 1956). Measured on 7 dates between 1975 August and 1976 October. Possibly variable, but the variations must be less than ± 0.10 magnitudes at 2.2 μm.

15. BD+46°3471. Measured on 10 dates between 1975 May and 1977 July. The star is probably variable (see text). Spectral type A0e-A2e (Herbig 1960b; Racine 1968; Strom et al. 1972; Crampton and Fisher 1974).

TABLE 3

MODEL PARAMETERS FOR FU ORI STARS

	IC5146#12 (a)	IC5146#12 (b)	V1057 Cygni 1971 Observations
Hot star spectral type	FOII	GOII	F5II
Hot star dereddened K magnitude	+6.6	+6.8	+5.3
Cool star spectral type	~M8III	~M8III	later than M8III
Cool star dereddened K magnitude	+5.7	+5.8	+4.9
Visual extinction, magnitudes	10.8	9.9	3.2

TABLE 4

PHOTOMETRY OF IC5146 CLUSTER STARS

Star	Spectral Type	V	B-V	U-B	[1.2]	[1.6]	[2.2]	n
W2		13.40	0.84	0.22	12.13	11.72	11.71	1
BD+46.3471(W6)*	A0e	10.16	0.42	0.14	8.44	7.54	6.58	9
W8	A7	11.61	0.50	0.22	10.67	10.54	10.48	2
W9	F3	11.66	0.54	0.15	10.64	10.39	10.33	1
W11	F8-G0	11.05	0.49	-0.04	10.15	9.93	9.86	1
W14	F5	11.28	0.52	0.07	10.58	10.36	10.32	1
W18	F4	11.43	0.47	0.02	10.63	10.44	10.38	1
W32*		14.71	1.78	1.50	10.85	10.04	9.72	1
W35	B8-A3	13.14	0.69	0.33	11.63	11.30	11.11	3
BD+46.3474(W42)*	B0V	9.64	0.78	-0.15	7.82	7.63	7.56	4
W44*		14.34	1.21	0.75	11.75	11.27	11.04	1
BD+46.3475(W48)	G0V	9.64	0.59	0.03	8.51	8.23	8.20	2
W53	A1	11.76	0.65	0.10	9.92	9.52	9.41	3
W62	B8-B9	12.04	0.32	0.03	11.19	10.92	10.91	1
W64	B9	12.36	0.39	0.09	11.32	11.04	10.94	2
W66		13.90	1.12	0.57	11.08	10.51	10.17	1
W70		13.13	0.70	0.19	11.76	11.34	11.28	2
W74*	G5-G8III				8.46	7.94	7.82	1
LkHα257(W76)	B5-A2e	13.17	0.71	0.43	11.25	10.63	9.89	1

Notes:

BD+46.3471(W6). Discussed in §VI. UBV measurements mean of values from Walker (1959), Racine (1968), and Strom et al. (1972).

W32. Spectral type must be M3 or earlier (Blanco 1963).

BD+46.3474(W42). Spectral type from Crampton and Fisher (1974).

W44. Spectral type G or early K (Walker 1959).

W74. No photoelectric UBV photometry available.

TABLE 5

IC5146 DISTANCE

Star	Adopted Spectral Type	$(B-V)_o$	V_o	A_v	M_v	m-M
W35	B8-9 V	-0.07	10.75	2.40	+0.9	9.85
BD+46.3474	B0 V	-0.30	6.35	3.30	-3.3	9.65
W62	B8-9 V	-0.07	10.70	1.35	+0.9	9.80
W64	B8-9 V	-0.07	10.70	1.65	+0.9	9.80

TABLE 6

LUMINOSITY FUNCTION PARAMETERS

Spectral Type	M_o	σ	Log n_o (kpc^{-3})	β (kpc)
B0,1	- 3.12	0.5	2.90	0.04
B2,3	- 1.33	0.5	3.78	0.04
B5	- 0.53	0.5	4.04	0.04
B8-A0	0.34	0.5	5.28	0.07
A2-5	1.33	0.4	5.49	0.10
F0-5	1.87	0.5	6.04	0.15
F8-G2 V	3.14	0.3	6.34	0.25
G5 V	3.51	0.3	6.45	0.30
G8-K3 V	4.15	0.5	6.95	0.35
F8-G2III	0.45	1.0	4.60	0.50
G5III	- 0.08	1.0	4.60	0.50
G8III	- 0.56	0.8	5.15	0.25
K0,1III	- 0.80	0.7	5.54	0.20
K2,3III	- 1.66	0.7	5.18	0.20
K4,5III	- 3.36	0.6	4.23	0.30
M0 III	- 4.14	0.6	3.43	0.30
M1 III	- 4.40	0.6	3.08	0.30
M2 III	- 4.76	0.6	3.08	0.30
M3 III	- 5.23	0.6	3.08	0.30
M4 III	- 6.04	0.6	2.95	0.30
M5 III	- 6.90	0.5	2.95	0.30
M6 III	- 7.90	0.5	2.40	0.30
M7 III	- 8.90	0.5	2.04	0.30
M8 + III	- 9.90	0.5	1.60	0.30
MI (A11)	-10.00	1.0	1.11	0.05

REFERENCES

Allen, D. A. 1973, M.N.R.A.S., 161, 145.

Allen, D. A., and Penston, M. V. 1973, M.N.R.A.S., 165, 121.

Andrillat, Y., and Swings, J. P. 1976, Ap. J. (Letters), 204, L123.

Baldwin, J. R., Frogel, J. A., and Persson, S. E. 1973, Ap. J., 184, 427.

Beckwith, S., Evans, N. J., II, Becklin, E. E., and Neugebauer, G. 1976, Ap. J., 208, 390.

Blaauw, A. 1963, Basic Astronomical Data, ed. A. Blaauw and M. Schmidt (University of Chicago), p. 383.

_____. 1965, Galactic Structure, ed. A. Blaauw and M. Schmidt (University of Chicago), p. 435.

Blanco, V. M. 1963, Ap. J., 137, 513.

_____. 1965, Galactic Structure, ed. A. Blaauw and M. Schmidt (University of Chicago), p. 241.

Cohen, M. 1973a, M.N.R.A.S., 161, 85.

_____. 1973b, M.N.R.A.S., 161, 105.

_____. 1975, M.N.R.A.S., 173, 279.

Crampton, D., and Fisher, W. A. 1974, Pub. Dominion Astrophys. Obs., 14, #12.

Elvius, T. 1965, Galactic Structure, ed. A. Blaauw and M. Schmidt (University of Chicago), p. 41.

Frogel, J. A., Persson, S. E., Aaronson, M., Becklin, E. E., Matthews, K., and Neugebauer, G. 1975, Ap. J. (Letters), 195, L15.

Frogel, J. A., Persson, S. E., Aaronson, M., and Matthews, K. 1978, Ap. J., in press.

Glass, I. S., and Feast, M. W. 1974, M.N.R.A.S., 167, 81.

Grasdalen, G. L., and Gaustad, J. E. 1971, A. J., 76, 231.

Hansen, O. L., and Blanco, V. M. 1973, A. J., 78, 669.

_____. 1975, A. J., 80, 1011.

Hanson, R. B. 1975, A. J., 80, 379.

Herbig, G. H. 1960a, Ap. J., 131, 248.

_____. 1960b, Ap. J. Suppl., 4, 337.

_____. 1966, Vistas in Astr., 8, 109.

_____. 1977, Ap. J., 217, 693.

Hidajat, B., and Blanco, V. M. 1968, A. J., 73, 712.

Hughes, E. E. 1969, Ph.D. thesis, California Institute of Technology.

Johnson, H. L. 1966, Ann. Rev. Astr. and Ap., 4, 193.

_____. 1968, Nebulae and Interstellar Matter, ed. B. M. Middlehurst and L. H. Aller (University of Chicago), p. 167.

Jung, J. 1970, Astr. and Ap., 4, 53.

_____. 1971, Astr. and Ap., 11, 351.

Kuiper, T. B. H., Knapp, G. R., and Rodriguez Kuiper, E. N. 1976, Astr. and Ap., 48, 475.

Lee, O. J., Gore, G. D., and Bartlett, T. J. 1947, Ann. Dearborn Obs., 5, #1C.

Lee, T. A. 1970, Ap. J., 162, 217.

Loren, R. B., Vanden Bout, P. A., and Davis, J. H. 1973, Ap. J. (Letters), 185, L67.

McCuskey, S. W. 1965, Galactic Structure, ed. A. Blaauw and M. Schmidt (University of Chicago), p. 1.

_____. 1966, Vistas in Astr., 7, 141.

_____. 1969, A. J., 74, 807.

Merrill, K. M., and Stein, W. A. 1976a, Pub. A.S.P., 88, 285.

_____. 1976b, Pub. A.S.P., 88, 294.

Miller, J. S., and Mathews, W. G. 1972, Ap. J., 172, 593.

Milman, A. S., Knapp, G. R., and Knapp, S. L. 1975, A. J., 80, 101.

Nassau, J. J., and Blanco, V. M. 1956, Ap. J., 125, 195.

Neugebauer, G., Becklin, E. E., Beckwith, S., Matthews, K., and Wynn-Williams, G. G. 1976, Ap. J. (Letters), 205, L139.

Neugebauer, G., and Leighton, R. B. 1969, Two-Micron Sky Survey, NASA SP-3047 (Washington, D.C.).

Racine, R. 1968, A. J., 73, 233.

Rieke, G., Lee, T., and Coyne, G. 1972, Pub. A.S.P., 84, 37.

Sanduleak, N. 1976, A. J., 81, 350.

Shanin, G. I., Shevchenko, V. S., and Shcherbakov, A. G. 1975, Variable Stars and Stellar Evolution, ed. V. I. Sherwood and L. Plaut (Reidel: Dordrecht), p. 117.

Simon, T. 1975, Pub. A.S.P., 87, 317.

Simon, T., and Dyck, H. M. 1977, A. J., 82, 725.

Simon, T., Morrison, N. D., Wolff, S. C., and Morrison, D. 1972, Astr. Ap., 20, 99.

Stephenson, C. B. 1973, Pub. Warner and Swasey Obs., 1, #4.

Strom, S. E., Strom, K. M., and Grasdalen, G. L. 1975, Ann. Rev. Astr. Ap., 13, 187.

Strom, S. E., Strom, K. M., Yost, J., Carrasco, L., and Grasdalen, G. 1972, Ap. J., 173, 353.

Upgren, A. R. 1963, A. J., 68, 475.

Veeder, G. J. 1974, A. J., 79, 1056.

Vogt, S. S. 1973, A. J., 78, 389.

Walker, M. F. 1959, Ap. J., 130, 57.

Wilson, O. C. 1976, Ap. J., 205, 823.

Wilson, W. J., Schwartz, P. R., Neugebauer, G., Harvey, P. M., and Becklin, E. E. 1972, Ap. J., 177, 523.

FIGURE CAPTIONS

Fig. 1. The area surveyed is shown as a rectangle superposed on a red photograph of the IC5146 region (a). The sources detected are plotted in (b); sources brighter than K = +7 are shown as circles, those between K = +7 and +8 are shown as crosses. The objects listed in Tables 1 and 2 are shown in (c), identified by number.

Fig. 2. Observed cumulative counts per square degree, as a function of limiting 2.2 μm magnitude. The counts have been corrected for coincidence. Also shown is the curve predicted using the model in Appendix B. The lower dotted line indicates the predicted counts for M giants, while the upper dotted line indicates the predicted counts for K and M giants combined.

Fig. 3. 2 μm spectra of the stars from Table 1. The zero point of the vertical scale is arbitrary.

Fig. 4. 2 μm spectra of the red stars from Table 2.

Fig. 5. Energy distributions of objects 12 and BD+46°3471. The points for object 12 are shown as open circles, those for BD+46°3471 as filled circles. All data except the visual points for BD+46°3471 are from this paper; the UBV data are those listed in Table 4.

Fig. 6. Object 12 in 1952 September (a) on the Palomar Sky Survey red plate, and in 1975 August (b), on a similar exposure.

Fig. 7. Multiple observations at 2.2 μm of object 12 (a), BD+46°3471 (b) and BD+46°3474 (c). Measurements only a few days apart are shown averaged together. Filled circles are measurements with a 9" beam, open circles are measurements with a 17" beam

or 20" beam, and crosses are measurements with a beam larger than 30".

Fig. 8. SIT spectrum of object 12. The resolution is about 10 Å. The vertical scale is linear, but in arbitrary flux units, as the spectrum was taken through a slit.

Fig. 9. Comparison of observations of object 12 with the model. The solid line is the energy distribution of the reddened G0 supergiant; the dashed line is that of the reddened M8 giant, the alternating dots and dashes represent emission from cool dust and the dotted line is the sum of the three.

Fig. 10. The multichannel spectrometer observations of object 12, corrected for $A_V = 9.9$ according to the formulation of the Whitford reddening law given by Miller and Mathews (1972). The resolution is 360 Å in the red, 160 Å in the blue. Uncertainties less than ±5% are not shown.

Fig. 11. Mean Mt. Wilson extinction coefficients in the 2.2 μm window, given in magnitudes/air mass. The solid line represents the mean curve, and the dotted lines show the dispersion about the mean from night to night.

Fig. 12. CO band depths for representative stars as a function of spectral type. Giants are shown as filled circles, supergiants as crosses and dwarfs as open circles. Typical uncertainties are 0.03 magnitudes.

Fig. 13. Bγ equivalent width as a function of spectral type for representative stars. The triangle is a subdwarf, the open circles are dwarfs, the squares are subgiants, the filled circles are giants and the crosses are supergiants. The uncertainties are usually 1-2 Å. The measurements at spectral types of K5 and later are affected by absorption features other than Bγ.

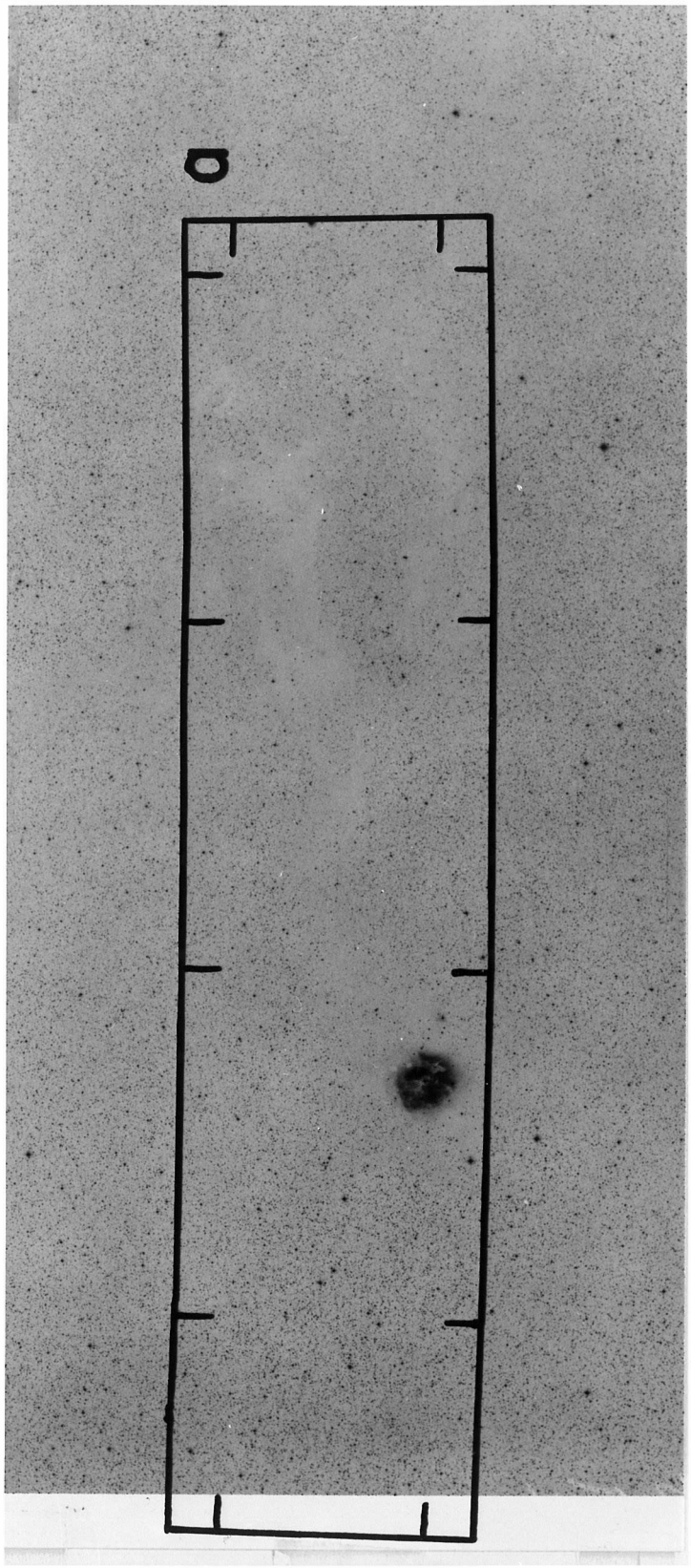

Fig. 1a

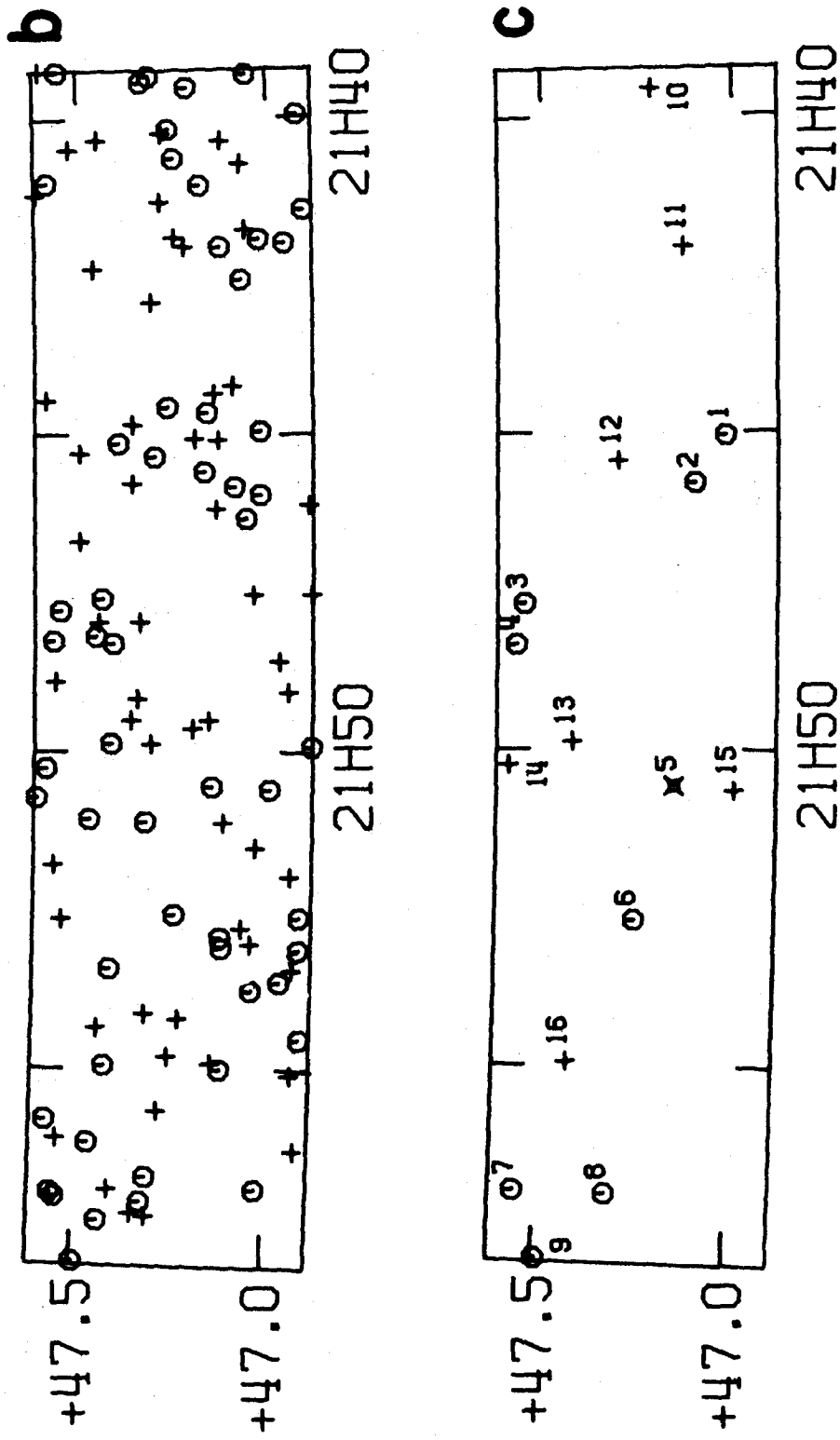

Fig. 1b,c

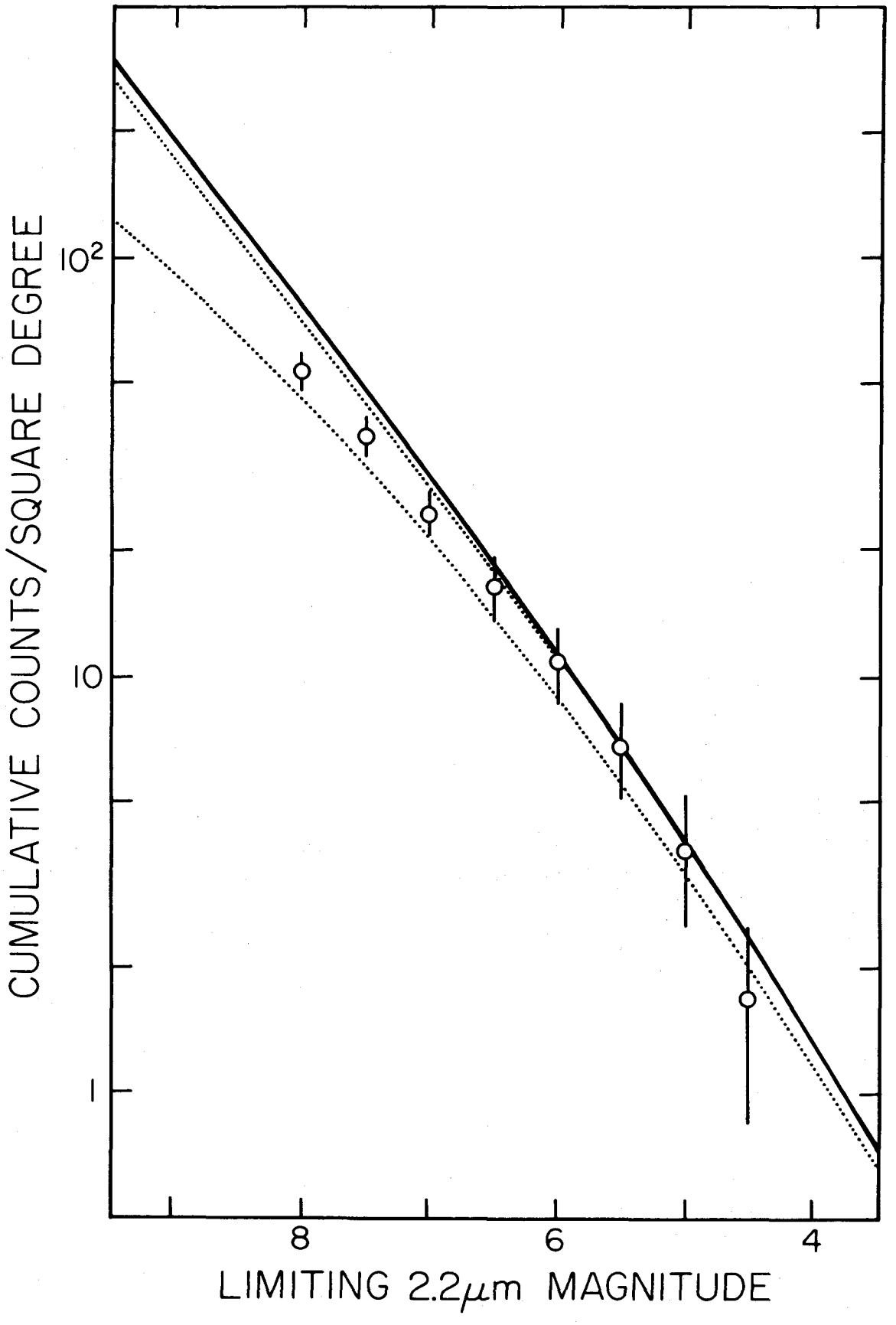
CUMULATIVE COUNTS/SQUARE DEGREE
10^2
10
1
8
6
4
LIMITING 2.2μm MAGNITUDE

Fig. 2

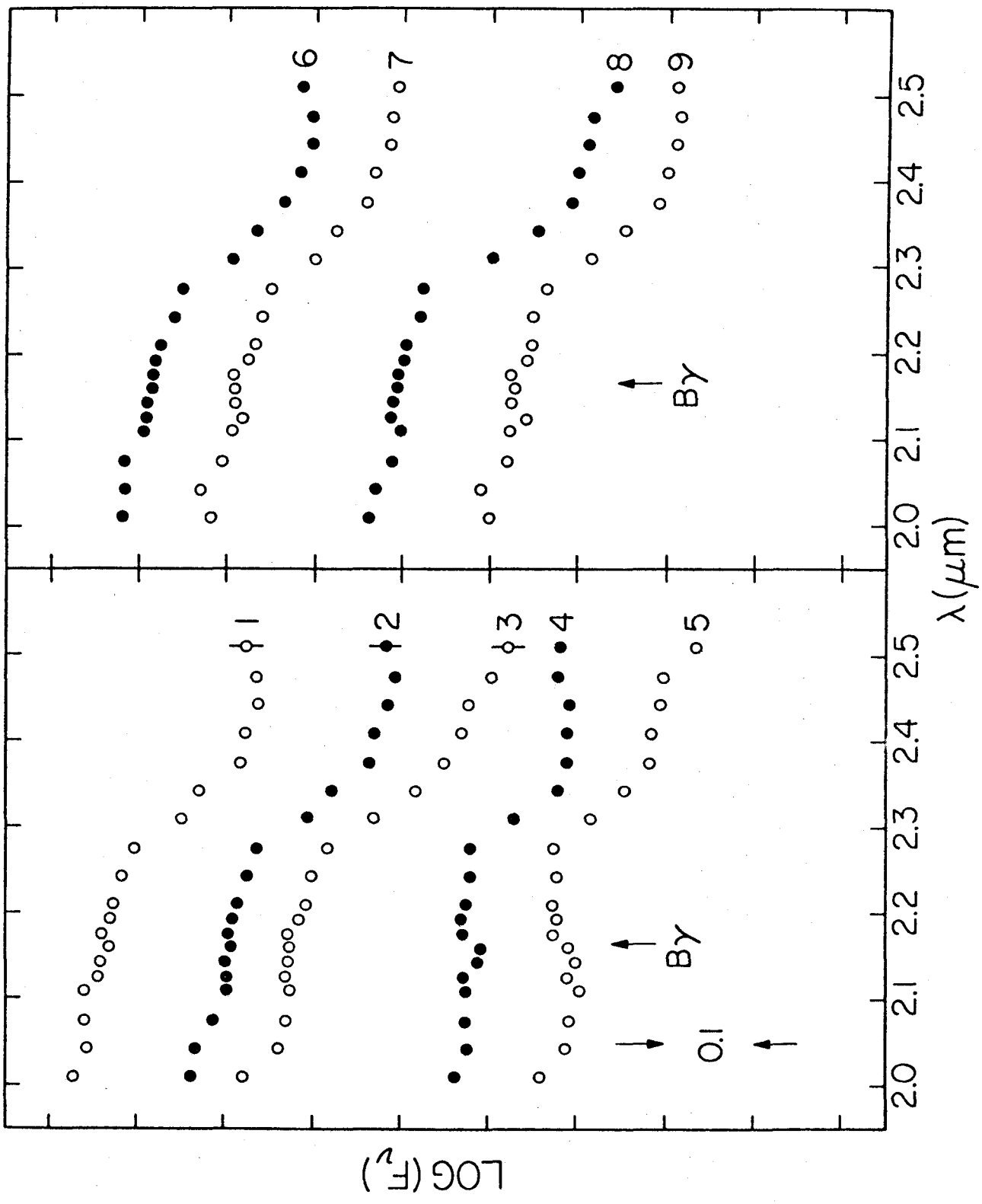

Fig. 3

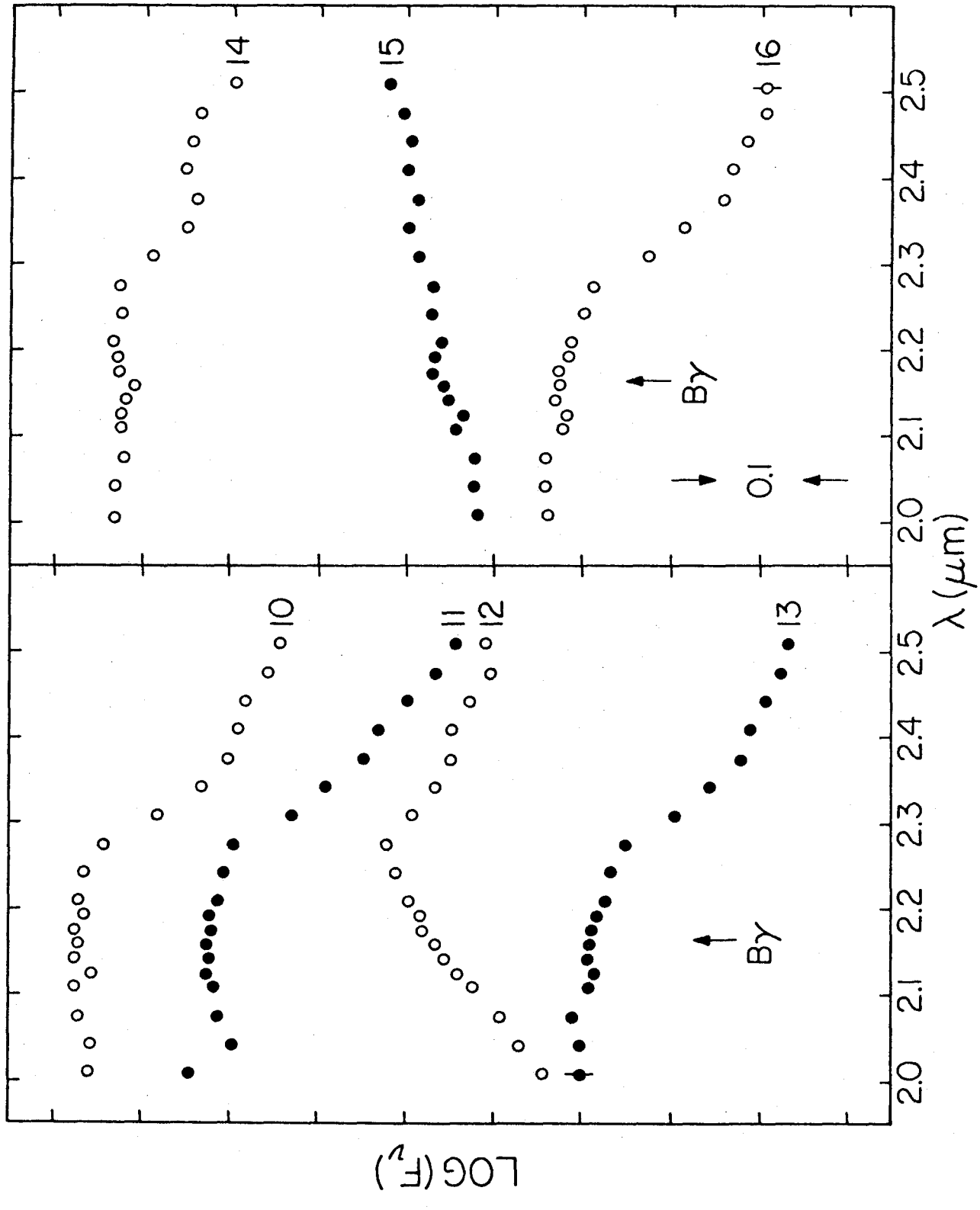

Fig. 4

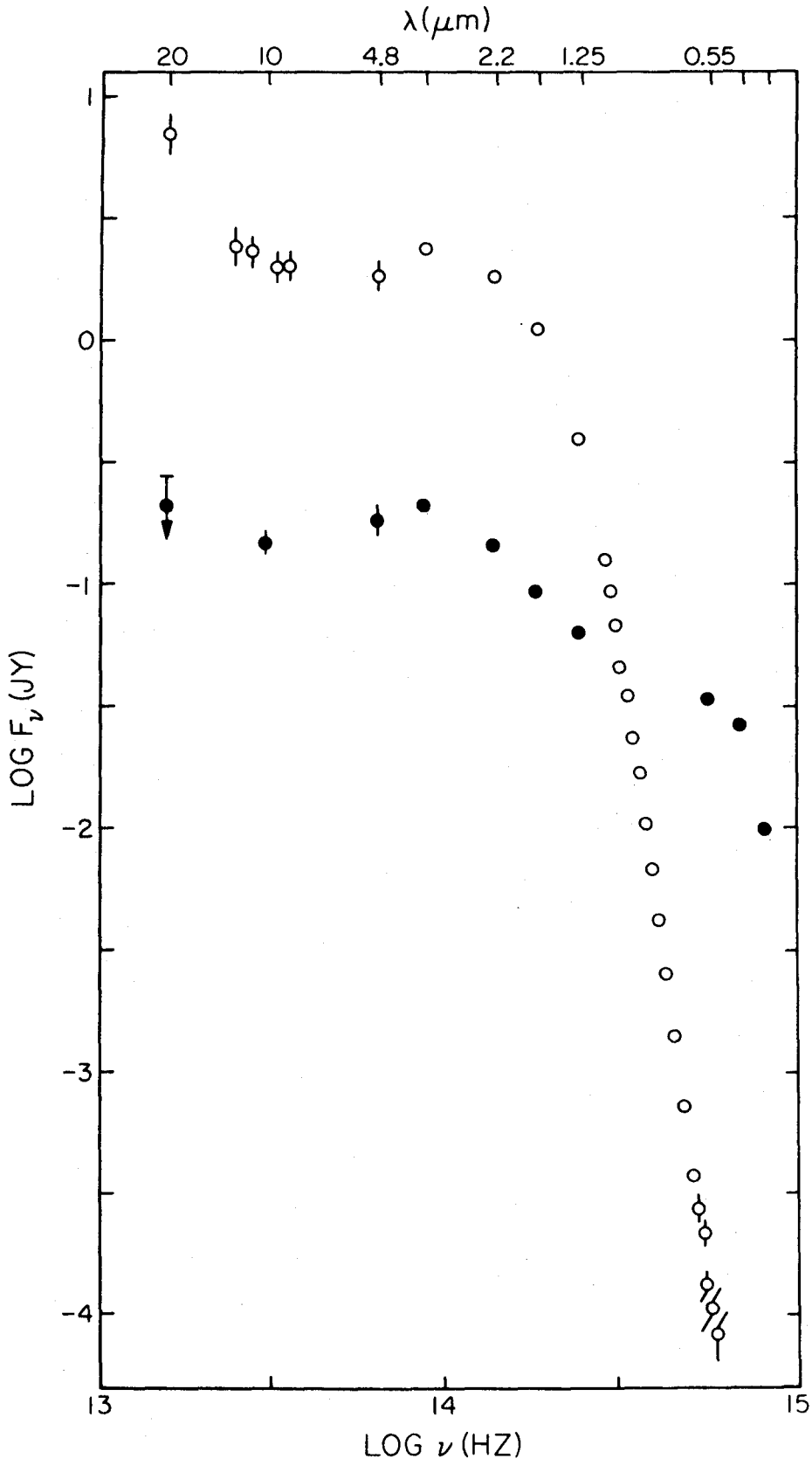

Fig. 5

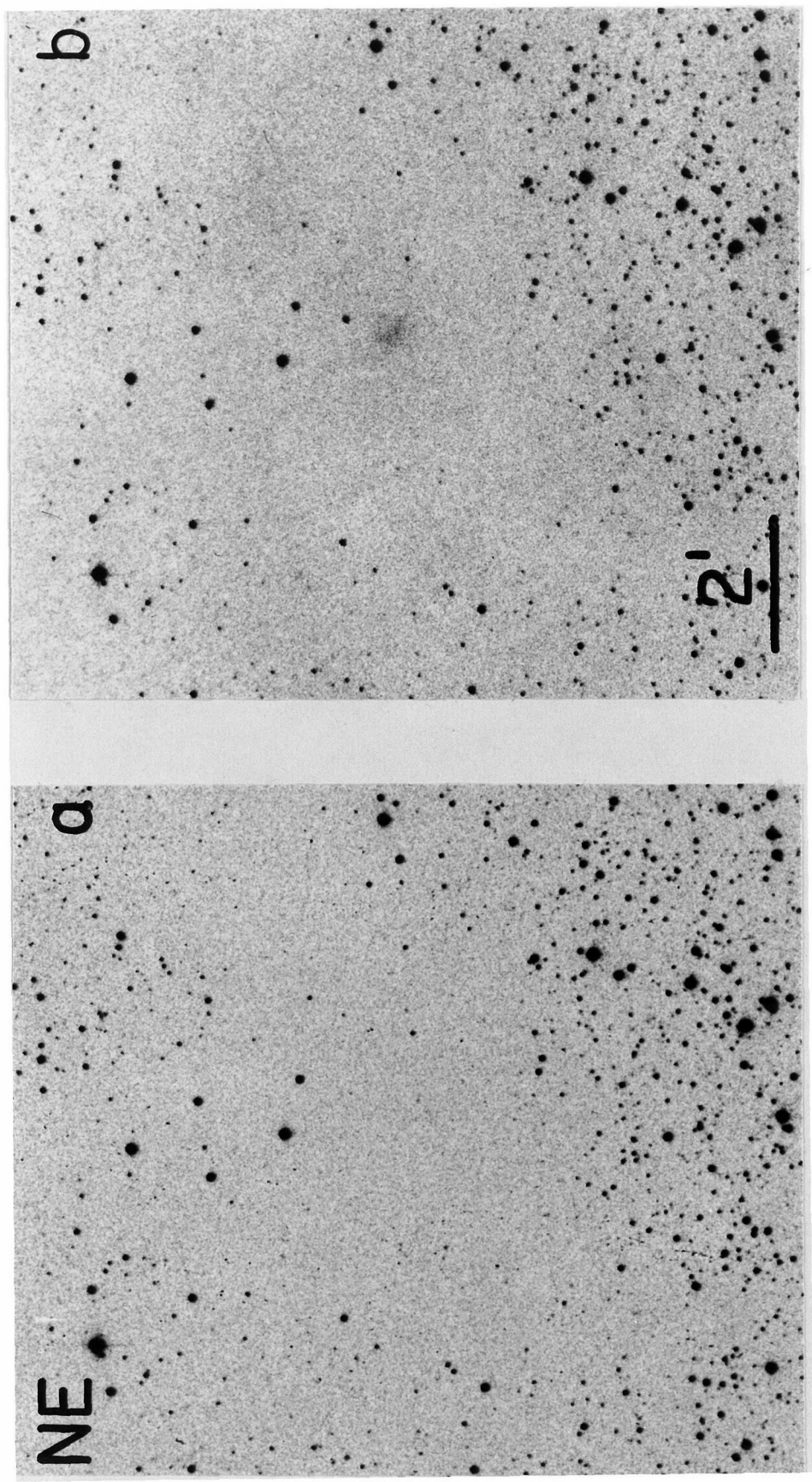

Fig. 6

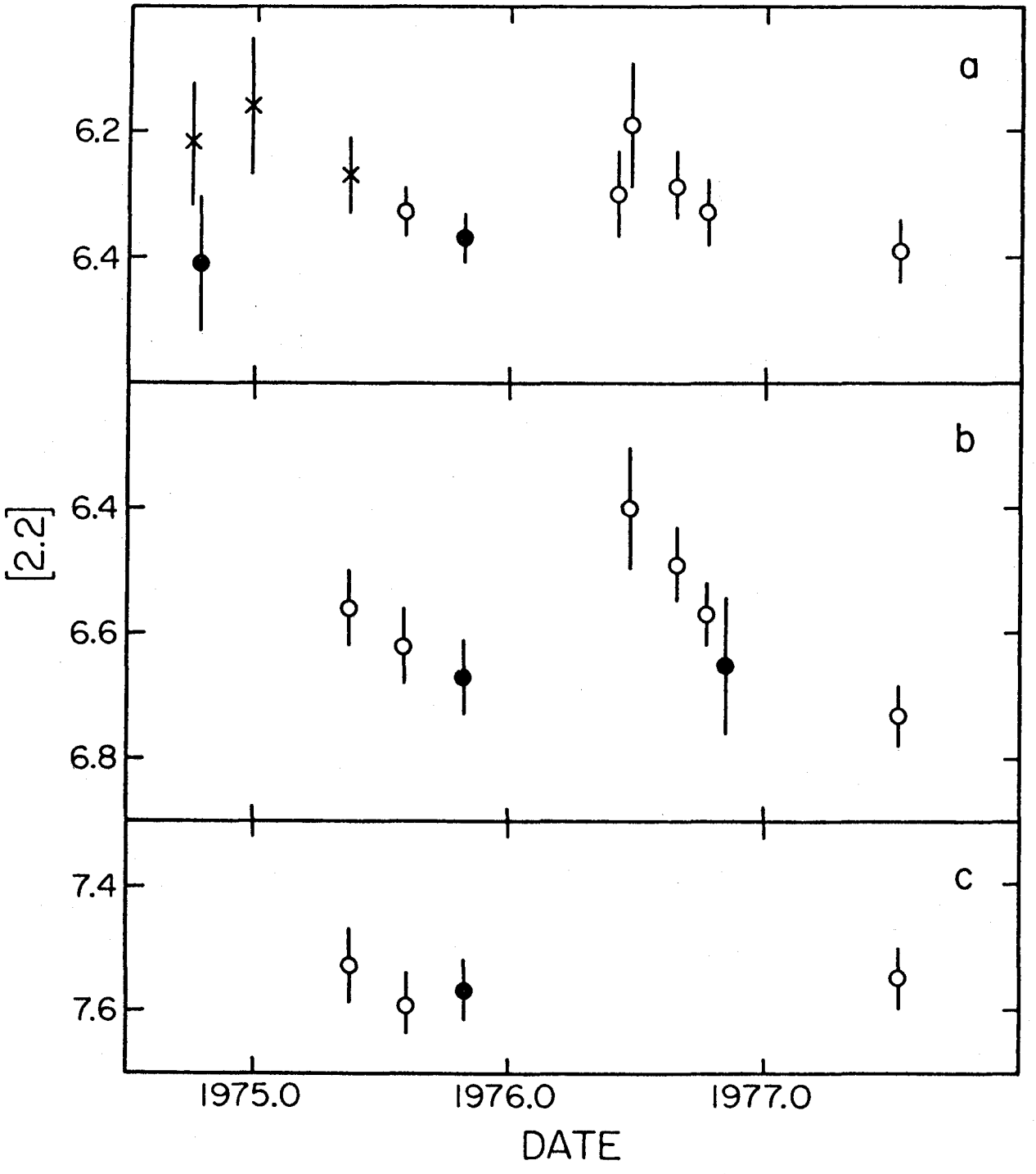

Fig. 7

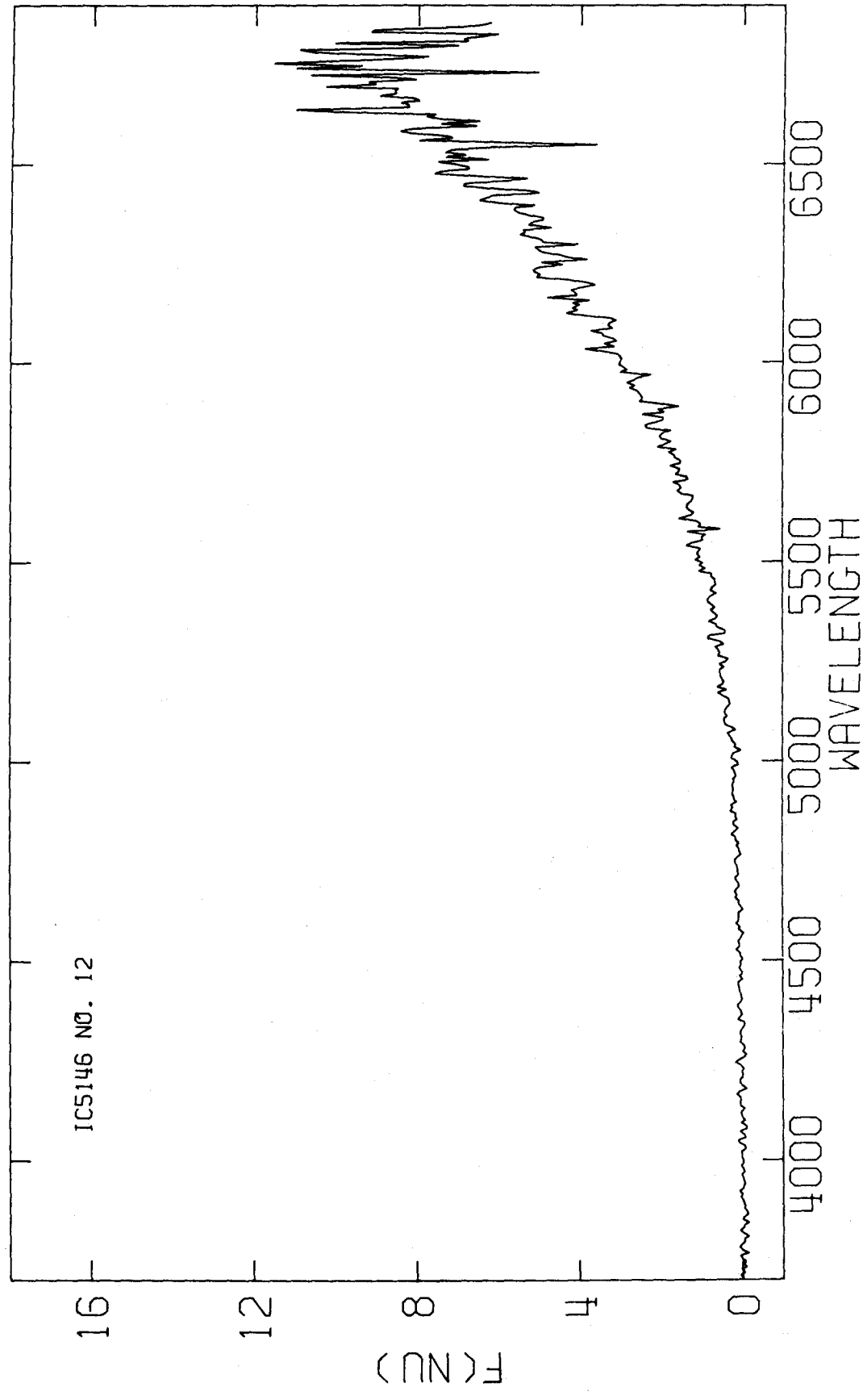
IC5146 NO. 12
F(NU)
0
4
8
12
16
4000
4500
5000
5500
6000
6500
WAVELENGTH

Fig.8

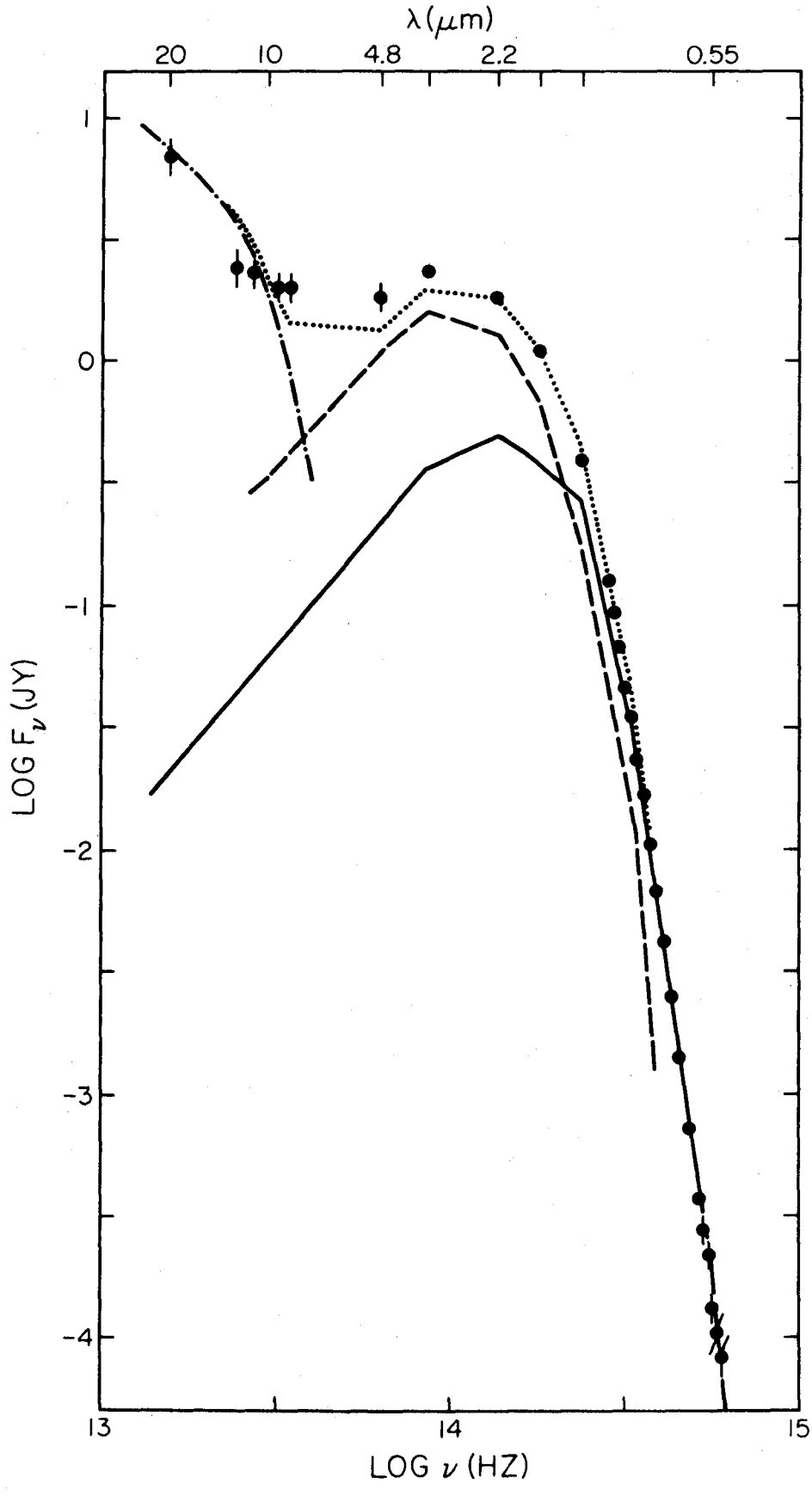

Fig. 9

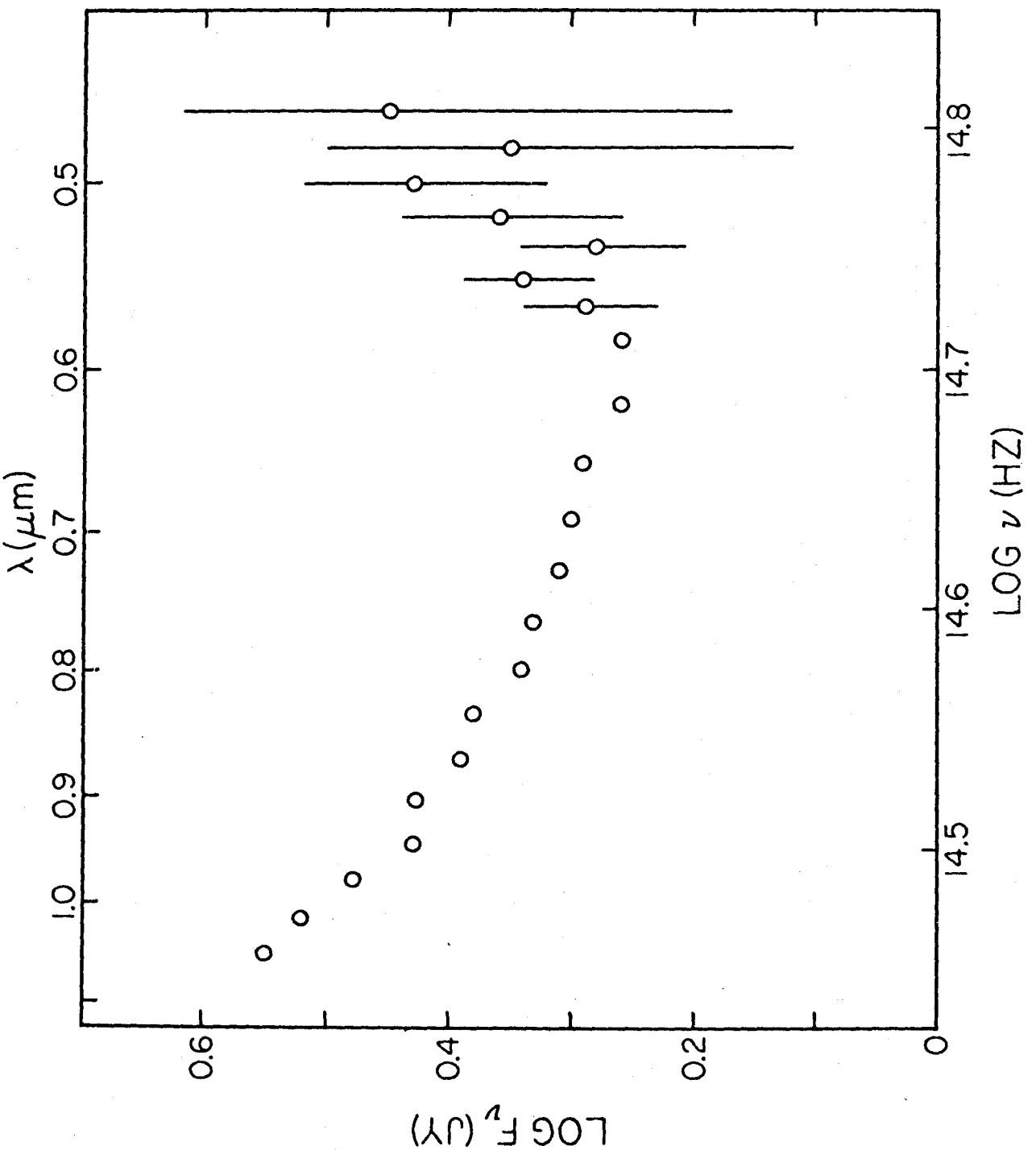

Fig. 10

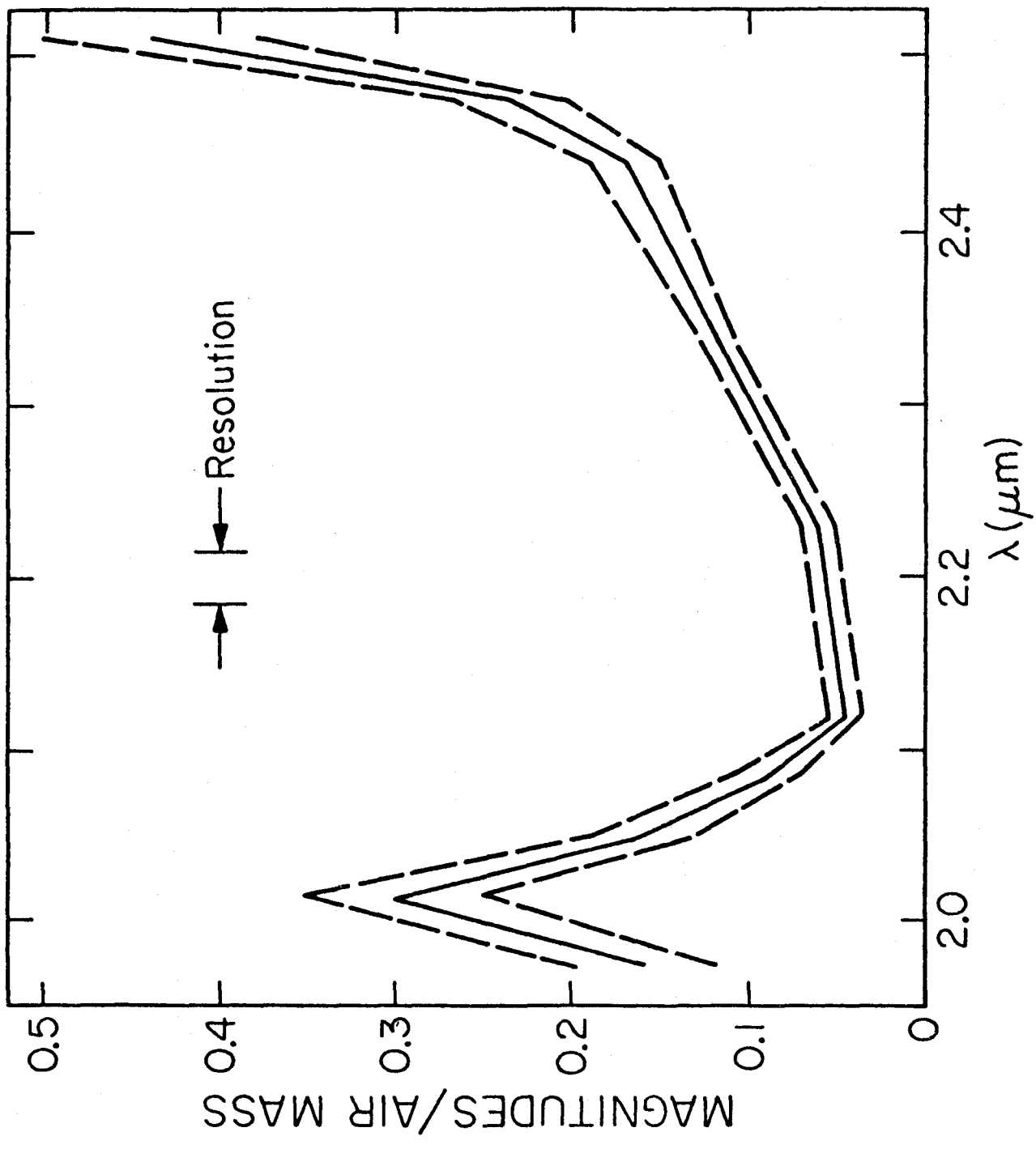

Fig. 11

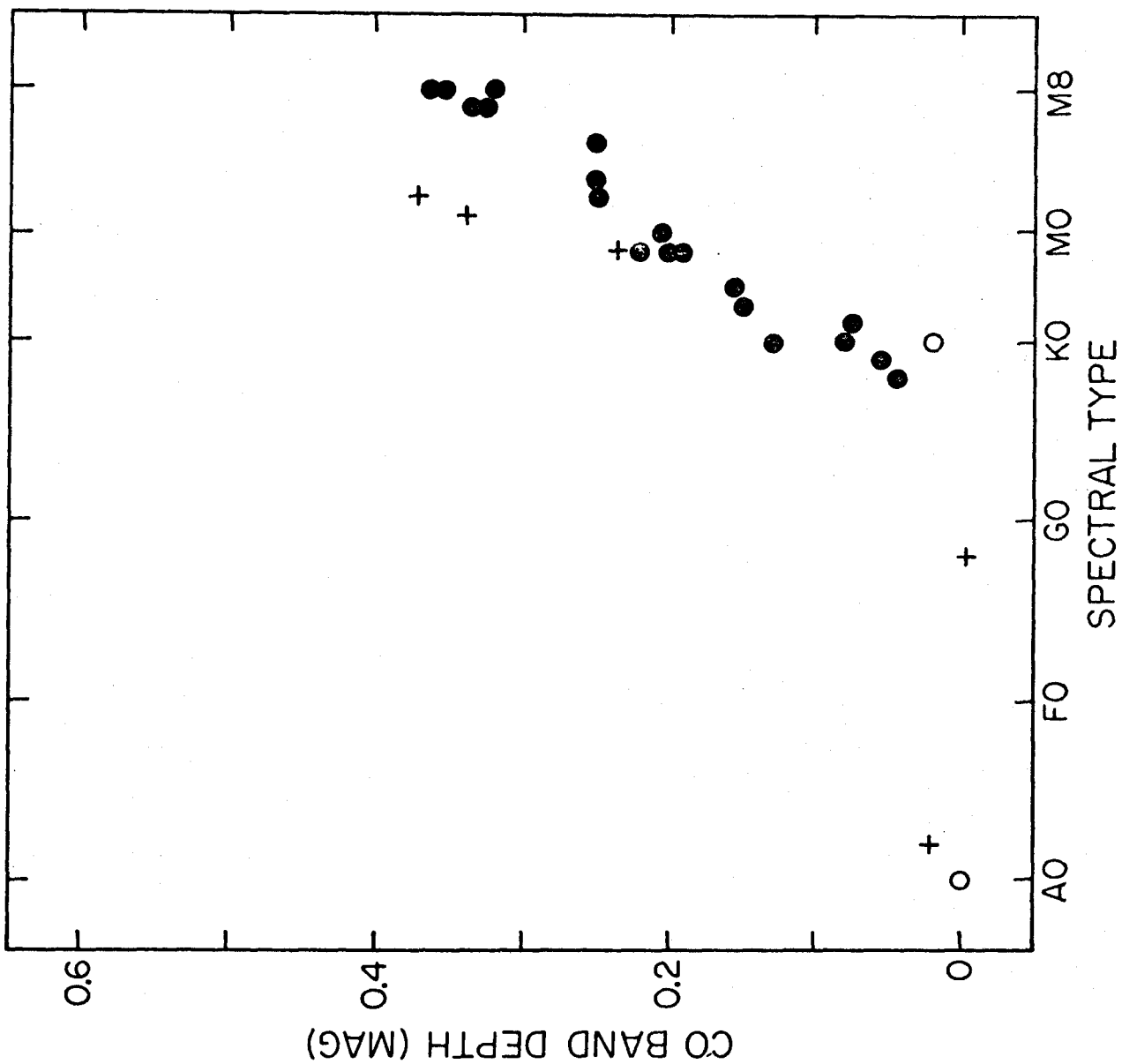

Fig. 12

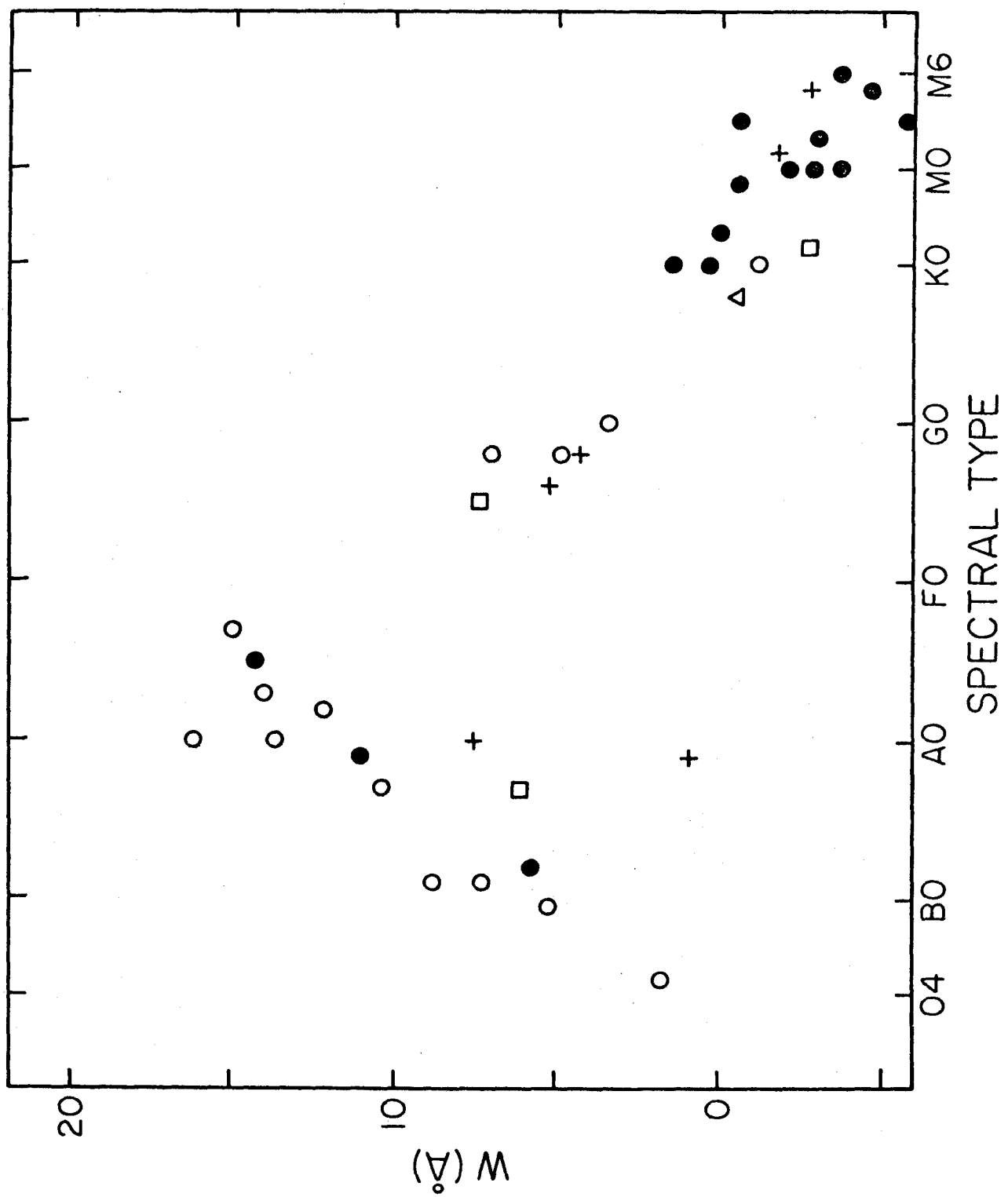

Fig. 13

CHAPTER 2

A STUDY OF THE OPHIUCHUS DARK CLOUD COMPLEX

I. INTRODUCTION

The Ophiuchus dark cloud complex is one of the closest major aggregates of dust and gas. Visual evidence for recent star formation is provided by its association with stars of the Scorpius OB2 association, and by the presence of T Tauri stars in its central regions.

These features led Grasdalen et al. (1973: henceforth, GSS) to search in the near-infrared for still more recently formed stars in the highly opaque region east of HD147889; this work was extended by Vrba et al. (1975a: henceforth, VSSG). In all, roughly 70 sources brighter at 2.2 μm than K = +10 were discovered in an area of 0.2 square degrees; at the center of the cloud these sources were taken to be upper main sequence members of a young cluster still embedded in and obscured by dark cloud material. Under this assumption, VSSG derived an initial mass function for the stars in the cloud (see also, Vrba 1977) and calculated various properties of the obscuring material. Although several of the 2.2 μm sources discovered by GSS and VSSG could be identified with known young stars, for most of the objects the identifications as main sequence stars were unverified. In addition to the survey work of GSS and VSSG, infrared studies of selected objects have been carried out; most notably the work on T Tauri stars by Rydgren et al. (1976: henceforth, RSS).

The intent of the work described in this paper was to complement the work of GSS/VSSG. A survey at both 1.6 and 2.2 μm was conducted, covering nearly 18 square degrees of the Ophiuchus dark cloud complex

at moderate sensitivity; nearly 400 sources brighter than K = +7.5 were detected. The purpose of the survey was to provide an initially unbiased set of objects from which a reasonable sample could be selected for further study, in order to determine both the spatial distribution of the young objects in the dark cloud, and the actual nature of these objects. In addition to the objects selected from the survey detections, a few fainter objects detected by GSS and VSSG were also observed.

The observations are discussed in §II, and the results of both the initial survey and the subsequent photometry and spectrophotometry are summarized in §III; these results are shown to be in good agreement with those of other investigators in §IV. The identifications of the objects which were studied in detail are discussed in §V, using two approaches. The primary approach, described in §Va, to make use of the photometry and spectrophotometry of the objects to classify them; this approach is identical to that described in an earlier paper (Elias 1978: Paper I). In addition, comparisons with optical surveys were made as described in §Vb, in order to verify that the objects selected for detailed study include most of the previously identified young objects which were detected by the survey.

It is shown that most of the youngest, newly-formed stars are concentrated in a small region less than 1°(3 pc) across near the center of the cloud, but that in all locations in the region surveyed a large proportion of the 2.2 μm sources are field stars -- objects unassociated with the dark cloud. Of the 50 objects studied in detail, 19 are thought

to be associated with the cloud and 17 are thought to be field stars; the remaining 14 objects cannot be definitely assigned to either group.

The properties of the 19 young objects are discussed in the subsequent sections. Three of them are very cool objects embedded in dense portions of the cloud (§VI) three are B or early A stars, (§VII) and six are known T Tauri stars (§III). The remaining seven objects have energy distributions which are similar to or intermediate between those of the T Tauri stars and the very cool objects; none appear to be luminous main sequence stars. As so few of the objects in the cloud are in fact stars on or near the main sequence, the total mass in stars cannot be readily estimated. In §IX, the extinction in various parts of the cloud is derived from photometry of field stars; these values are generally lower than those of VSSG.

II. OBSERVATIONS

The infrared survey was done using an InSb detector system on the CIT 0.6 m telescope on Mt. Wilson. Scans with a 2' beam were made at sidereal rate spaced by 1!5 in declination; each scan was done once at a wavelength of 1.6 μm and once immediately afterwards at a wavelength of 2.2 μm in order to provide color information on the sources detected. The chopping direction was parallel to the scan direction; the beam spacing was between 3' and 6'. The observations were made on 24 nights between 1975 May and 1976 June, and covered a total area of 17.9 square degrees (Figure 1a).

The limiting 2.2 μm magnitude was usually slightly brighter than K = +8; the limiting 1.6 μm magnitude ranged from H = +8 to nearly +9.5 as the detector was improved. The 1σ uncertainties in the measured magnitudes range from ±0.3 mag at the limiting magnitude to ±0.1 mag for the brighter objects.

GSS/VSSG reached a fainter limiting 2.2 μm magnitude--about +10--than could be reached practically when scanning the larger area. In order to obtain an idea of the field star density at faint magnitudes, two small unobscured areas were observed at a sensitivity comparable to that of GSS and VSSG. An area of 0.015 square degrees around the bright star HD148760 was scanned at 2.2 μm on the Mt. Wilson 1.5 m telescope, and an area of 0.021 square degrees around HD150714 was scanned on the Mt. Wilson 2.5 m telescope. These regions are indicated in Figure 1a.

The approximate boundaries of the region surveyed by GSS/VSSG are also shown in the figure. This area will be referred to as the 'central region,' and is defined as the region lying between $\alpha(1950) = 16^h22^m.0$ and $16^h25^m.2$ and between $\delta(1950) = -24°08'$ and $-24°30'$.

Selected objects detected in the present survey or by GSS/VSSG were studied using broadband photometry from 1.2 μm to 20 μm and low resolution 2 μm spectrophotometry. These observations were made using the Mt. Wilson 1.5 m and 2.5 m telescopes, and the CTIO 1.5 m telescope. Most of the observations between 1.2 μm and 4.8 μm and the 2 μm spectra were made with an InSb detector; the remaining measurements and the measurements at longer wavelengths were made with a germanium bolometer.

The properties of the broadband filters and the flux calibration used are given in Wilson et al. (1972) and Beckwith et al. (1976). Three sets of narrowband 10 μm filters were used. The first set is that described in Beckwith et al., the second set comprises these same filters operated at liquid nitrogen temperature, so their effective wavelengths are shifted to the blue by 0.2-0.3 μm. The third set is that described by Persson et al. (1976) with the addition of a sixth filter at 8 μm; these filters were also operated at liquid nitrogen temperature. The properties of the three filter sets are summarized in Table 1. The 2 μm spectra were taken and reduced using methods described in Paper 1; see also Neugebauer et al. (1976).

III. RESULTS

a) Main Survey

Figure 1b shows the distribution of the 382 objects with K < 7.5 detected in the main survey. Of these, 248 were brighter than K = 7.0. Detections in adjacent scans were considered to be due to a single source if they were coincident in right ascension by 2' or less. The actual counts must be corrected for pairs of stars occurring so close as to be considered one object; this coincidence correction is 7% for all sources brighter than K = 7.5, and 5% for the sources brighter than K = 7.0. The total number of sources brighter than K = 7.5 is therefore probably about 400. The cumulative counts, corrected for coincidence, are shown in Figure 2.

In addition to the point sources, two extended objects were detected; these were identified with the globular clusters M4 and NGC 6144.

b) Unobscured Regions

Six sources brighter than K = 10 other than the two locating stars were found in the two areas surveyed at high sensitivity; ten sources brighter than K = 11 were found in the area around HD150714.

The area in Figure 1 west of 16^h17^m (1950) and the area east of $16^h28^m.5$ and south of -26° both appear fairly free of local obscuration. The detections in these areas from the main survey can therefore be combined with the small-area, high-sensitivity survey results to determine the properties of the field stars, unaffected by the dark cloud

material. The resulting cumulative count distribution corrected for coincidence is shown in Figure 3.

c) Photometry and Spectrophotometry

Two overlapping sets of objects were observed more extensively. All stars with $H-K \geq 0.7$ and $K < 7.0$ found in the main survey were reobserved, as well as all objects with $K \leq 8.0$, independent of color, inside the central region. A few fainter objects inside the central region were also observed. The objects with H-K $\geq$ were chosen because their spatial distribution appears correlated with that of the dark cloud material (§Va, Fig. 1).

The results of the photometry of all three sets of objects are listed in Table 2, together with positions and identifications. Red and near-infrared plates were taken on the Palomar 48 inch Schmidt in 1975 and 1977 in order to provide optical identifications for the objects found in the survey. Optical positions measured from these plates are accurate to roughly ±1". Where available, accurate positions from the literature were used. The positions of objects without optical counterparts were derived from offset guider settings and the measured positions of guide stars. All the observed 2.2 μm spectra are shown in Figure 4, and energy distributions of selected objects are plotted in Figure 5.

Most of the objects detected in the main survey with $K < 5.0$ were also subsequently reobserved. There are 41 objects in this sample; positions and infrared magnitudes are listed in Table 3 except for the four

objects listed in Table 2. Several of the objects in Table 3 appear variable, as is expected if they are mainly late-M giants. If objects were measured more than once, and appeared variable, results from one day only are listed in the table and additional measurements are given in the notes. For apparently constant objects, all observations were averaged to obtain the values given in the table. Non-variable stars are taken to be those with a maximum measured magnitude variation at 2.2 μm of < 0.15 mag; variability is fairly certain only for amplitudes greater than 0.2 mag at 2.2 μm.

IV. COMPARISON WITH OTHER WORK

Inside the region observed for this paper, there are six sources in the 2.2 μm sky survey (IRC) of Neugebauer and Leighton (1969), and seven sources found at 4, 11, 20, or 27 μm in the AFGL survey (Price and Walker 1976). The six IRC stars were all detected in the present work, and are included in Table 3. The AFGL sources include detections of the two bright stars o Sco (GL 1843) and α Sco (GL 1863). The remaining five sources were seen only at 11 μm or longer wavelengths, and have color temperatures of 400 K or less (GL 1845, 1850, 1855, 4222, and 4224). All but GL 1850 are at or near positions of B stars associated with nebulosity; they will be discussed in §VIa. The three AFGL sources GL 1855, 4222, and 4224 can also be identified with the three sources found in the far infrared ($40 < \lambda < 250$ μm) survey of the Ophiuchus region of Fazio et al. (1976). As no identification of GL 1850 can be made at 2.2 μm, it will not be discussed further.

The 2.2 μm surveys of GSS and VSSG covered only the central region of the dark cloud. Most of the sources found by them are fainter than K = +8 and were therefore not detected by the present survey. All of the 2.2 μm sources known to be brighter than K = +8 were seen in the present survey. Three objects (#13, #24, and #34) were found inside the central region by the present survey which were not listed in GSS or VSSG. Objects #13 and #34 are T Tauri stars (Herbig and Rao 1972) which were observed by RSS who found them to have infrared magnitudes comparable to those measured in the present work.

Photometry in Table 2 of objects in the central region is generally in agreement with that reported by GSS, VSSG, RSS, and with other published photometry of these objects (e.g., Carrasco et al. 1973, Chini et al. 1977). The discrepancies can mostly be attributed to variability of the objects, or to the presence of extended emission components (see §VII). The agreement of the measured positions is also good.

V. ASSOCIATION MEMBERS

The criteria used to select objects from the survey for further study were intended to preferentially select young stars associated with the dark cloud. It is necessary to determine which of these objects are field stars before they are discussed in detail. It is also useful to estimate the number of stars associated with the cloud which were detected in the survey but were not observed further.

a) Infrared Identifications of Young Stars

Most of the objects detected in the present survey appear to be field stars. This can be seen from the observed spatial distribution of the detections (Fig. 1b) and from the agreement of the cumulative counts over the whole region with the counts from the unobscured regions (Fig. 3). The agreement of the observed field stars counts with those predicted by the model of the galactic stellar distribution described in Paper I (Fig. 3) indicates that the distribution of field star spectral types predicted by this model is probably reliable.

The sources with $H-K \geq 0.5$ and $K < 7.0$ are plotted in Figure 1c. The spatial distribution of the objects with $0.5 \leq H-K < 0.7$ is weakly correlated with that of the dark cloud material, while the distribution of the objects with $H-K \geq 0.7$ shows a much stronger correlation. This probably indicates that the objects with $0.5 \leq H-K < 0.7$ include a substantial number of red field stars, whereas the objects with $H-K \geq 0.7$ are predominantly background

field stars reddened by intervening dark cloud material and very red stars associated with the dark cloud complex.

Roughly 90% of the field stars brighter than K = 7.0 in this region are expected to be K or M giants. Another 5% are expected to be G giants, and the remainder should be mainly main sequence A and F stars. The K and M giants and many of the G giants should have a CO absorption band longwards of 2.3 μm strong enough to be distinguished in 2 μm spectra such as those in Figure 4. In contrast, young stars do not show such CO absorption; this means that most field stars can be distinguished from young stars associated with the dark cloud by the presence of the 2.3 μm CO band in their spectra. The field stars without CO bands in their spectra should be largely foreground stars, which will not be appreciably reddened, and can be distinguished from stars in or behind the cloud on the basis of their relative blueness.

Using these criteria, supplemented by available optical data, the stars in Table 2 were divided into three groups: field stars, stars associated with the dark cloud, and uncertain cases. The group to which each object belongs is indicated in the last column of Table 2. The stars in the third group--uncertain cases--are mostly objects for which 2 μm or optical spectra have not been obtained. The spatial distribution of the stars with $H-K \geq 0.7$ and $K < 7.0$ is shown in Figure 6, with the three groups of stars distinguished by different symbols. Note that fainter objects or those with $H-K < 0.7$ are not shown in the figure. It is evident that the infrared-bright stars associated with the dark cloud are strongly concentrated in a small

region only a few pc in extent; those objects which do not show a CO band are all within a 1° square box centered to the west of HD147889, with the exception of object #49 (MWC 863). This provides additional confirmation that there is a young stellar cluster in this region, as was previously concluded by GSS and VSSG.

Even within this 1° square region, there appears to be some contamination of the samples by field stars. Inside the central region surveyed by GSS/VSSG are 27 objects which were observed here; of which 17 are probably associated with the cloud and 7 very probably are not. The remaining three objects are ambiguous cases. Of the objects inside the central region, 8 have H-K $\geq$ 0.7 and K < 7.0 (Fig. 6); of these, 3 are field stars and 5 are associated with the cloud..

b) Optical Identification of Young Stars

The objects detected in the survey for which photometry and 2 μm spectra were obtained were intended to include a major fraction of the young stars in the cloud. As a check on the success of the selection procedures, optical surveys of T Tauri stars and of B stars were examined; these two groups of stars constitute most of the visually bright young stars known to be associated with the cloud.

i) T Tauri Stars

An attempt was made to identify known T Tauri stars with 2.2 μm sources from the survey. Definite optical identifications of all the T Tauri stars in the area surveyed do not exist, although a substantial

number have been identified by Herbig and Rao (1972) and RSS. In order to supplement the definite identifications, lists of stars with Hα in emission were examined (Struve and Rudkjøbing 1949, Haro 1949, Dolidze and Arakelyan 1959, Hidajat 1961, The and Lim 1964). As late-type giants may also show Hα in emission, identification of a 2.2 μm source as an Hα emitter does not guarantee that it is a T Tauri star.

Fifteen stars with Hα emission can be tentatively identified with infrared sources brighter than K = 7.0. Of these, four are definite or probable T Tauri stars which are listed in Table 2 (objects 14, 22, 28, and 34), while three more stars are probably very late-type giants (objects 43, 82, and 83). An eighth object (object 49) is the peculiar star MWC 863. The remaining identifications are with infrared sources of unknown characteristics; some of these may be due to chance coincidence. It is evident that there cannot be great numbers of T Tauri stars detected in the present infrared survey which are not included in either of the two samples represented in Table 2. This conclusion is reinforced by an examination of the photometry of RSS; the T Tauri stars measured by RSS which are not included in Table 2 are mostly fainter than K = 7.5.

ii) Main Sequence Stars

An estimate of the number of early-type main sequence stars associated with the dark cloud in the area surveyed can be made from optical studies; most of these stars should have H-K colors near zero and will not have been included in Table 2. Unobscured main sequence stars of spectral type ~ B9 or earlier should be brighter than K = 7

if the distance to the dark clouds is 160 pc (e.g., Bertiau 1958, Racine 1968, Whittet 1974).

Garrison (1967) has published spectral types and photometry for most of the stars of spectral type A or earlier, with V brighter than about +10, and data are available for fainter stars. Moderately obscured B stars embedded in the dark cloud should be surrounded by visible reflection nebulae, so as a check on the completeness of the data for V > 10, the Palomar Sky Survey prints covering the region surveyed in the infrared were examined for reflection nebulae which could not be attributed to identified stars of early spectral type associated with the cloud. No such nebulosity was found, so it would seem that most of the early-spectral-type stars associated with the dark cloud have been identified. A list of all the stars inside the survey region known to be of spectral type A0 or earlier is given in Table 4. Also included are α Sco and o Sco, which are stars of later spectral type which have probably already evolved off the main sequence (e.g., Garrison 1967). Nearly all of the 17 early-type stars in Table 4 with K < 7.0 appear to be associated with the cloud. These constitute roughly 6% of the total detections in the survey. Probable pre-main-sequence ojbects from the region around HD 147889 are therefore included in Table 4.

The spatial distribution of the stars listed in Table 4 is plotted in Figure 7. It is interesting to note that the probable association members seem to be located preferentially in the western half of the cloud, but that the concentration is not so pronounced as that of the very young, red objects (Fig. 6).

VI. VERY RED OBJECTS

There are several objects in the cloud which appear very red, in that they have H-K colors greater than about +2 magnitudes, and have no optical counterpart visible on infrared places (e.g. Chini et al. 1977). The best-observed cases in Table 2 are objects 21, 32, and 33. The near-infrared colors of these objects do not resemble those of heavily obscured main-sequence stars unless a reddening law is adopted which differs substantially from that observed elsewhere in the Ophiuchus region; the absence of far-infrared luminosity peaks at the positions of these objects tends also to indicate that they are intrinsically cool objects. In addition to their probably low temperatures, these objects have a number of other interesting properties, which are discussed below.

a) Infrared Reflection Nebulae

Objects 21, 29, and 32 are all extended at 1.6 and 2.2 μm (Fig. 8); object 21 is extended at 1.2 μm also, while the other two objects are too faint for a similar effect to be measured. Object "A" of VSSG was seen by them to be extended at 2.2 μm, and is probably a similar object. The three objects observed in the present work are all more extended at 1.6 μm than at 2.2 μm, and object 21 is still more extended at 1.2 μm than it is at either 1.6 or 2.2 μm. This can be seen from Figure 9, where the color is plotted as a function of beam size: colors measured with large beams are bluer than those measured with

small beams. The surface brightness of the emission decreases strongly as a function of increasing distance from the object (Fig. 10). Object 21 is the only object which has been measured with different beam sizes at 10 μm; it is not observed to have a significantly different flux when observations with a 7" beam are compared to measurements with a 14" beam.

A plausible explanation of the observations is that the extended emission is reflection nebulosity produced by scattering of light from the central objects by circumstellar dust. As the scattering cross-section of the dust must increase with decreasing wavelength, the scattered light should be generally bluer than the light from the central object itself. This explanation is preferred to one which postulates a separate emission mechanism to account for the extended component. Hydrogen recombination radiation should produce an observable Bγ emission line and a radio continuum source, neither of which is seen in any of the objects (Fig. 4; Brown and Zuckerman 1975). If the extended emission is from heated dust, neither the general blueness relative to the objects nor the compactness of object 21 at 10 μm is easily explained.

The presence of reflection nebulosity around these three objects implies a high local matter density, as the scattering efficiency of the dust grains is fairly low. A rather crude demonstration of this can be made by means of a calculation of the minimum column density required to produce the observed scattering. The ratio of the flux in a large beam to that in a small beam provides an approximate

value for the scattering optical depth within a column whose length is equal to the projected radius of the large beam. For object 21 at 2.2 μm this value is ~ 0.8 mag inside a 15" radius; this number is a lower limit to the total extinction. The values for objects 29 and 32 are similar though somewhat smaller. The reddening law obtained by VSSG implies a visual extinction for object 21 within 15" of the object of at least 8 mag. The minimum hydrogen column density can then be derived using the value for N_H/A_V of Spitzer and Jenkins (1975), corrected for the increased extinction efficiency of the grains in the dark cloud for a given hydrogen column density compared to those in the interstellar medium. Carrasco et al. (1973) have used polarimetry to show that the grain sizes in the central regions of the cloud are 1.5 - 2 times as large as those in peripheral regions; if this effect is purely due to grain growth, the increase in efficiency for a given hydrogen column density is roughly a factor of three. The molecular hydrogen column density must therefore be greater than 3×10^{21} molecules/cm^2 along a column of projected length 15", or $\sim 4 \times 10^{16}$ cm at a distance of 160 pc. The minimum molecular hydrogen density is thus about 10^5 molecules/cm^3.

This estimate of a high density around object 21 is supported by the observation at this point of a number of radio molecular lines which require high densities to be excited (e.g. Gottlieb and Ball 1973, Encrenaz 1974, Gottlieb et al. 1978). Gottlieb et al. (1978) mapped the $3_2 \rightarrow 2_1$ transition of sulfur monoxide in the Ophiuchus dark cloud, and found two emission peaks. The first is the one near object

21, while the second is located slightly to the west of objects 32 and 33. Object 29, in contrast, is not near a position of strong SO emission.

b) Object 29

Object 29 is far redder shortward of 3.4 μm than any other object in Ophiuchus, and is also the only object which is observed to have a strong 10 μm absorption feature. The object does not appear to be a peak of molecular line emission, and the extended 1.6 and 2.2 μm emission around this object is weaker than that around object 21. This suggests that the column density of material in the general vicinity of object 29 is less than that near object 21, and that it is insufficient to account for the extreme redness and the strength of the 10 μm absorption. It seems more plausible that the extreme redness and the 10 μm absorption feature are intrinsic to the object itself and that object 29 is a small, cool object which is optically thick in the 10 μm silicate feature. The inferred temperature is $\sim$ 350 K; the size of the object is of the order of 0.1". Doubtless the internal structure of the source is less simple than this, but it must be characterized by similar temperatures and sizes.

Another interesting property of object 29 is its variability. The 2.2 μm data for this object, corrected to a beam size of 9", are plotted in Figure 11. In contrast, the observations of object 21, also in Figure 11, do not seem to show similar variability.

c) Suggestions for Further Study

If the extended emission in these very red objects is in fact due to reflection nebulosity (§ VIa), two effects should be observable. The first and most significant effect is that the extended emission should be polarized, with the electric vector in each part perpendicular to the radius vector from the central object. This effect is similar to that seen in some Herbig-Haro objects (e.g., Strom et al. 1974a,b, Vrba et al. 1975b).

The second effect which should be observable is that the extended emission should be redder at its edges than it is toward the center. This is because the light from the central object will be reddened at the edges by intervening material. The multiple-aperture data obtained in the present study are not sufficiently accurate to measure this effect; high-resolution maps at 1.6 and 2.2 μm are probably required.

The very red objects observed in this study appear to exhibit a variety of characteristics, so it probably misleading to treat them as a single group of objects. In particular, objects 21 and 29 appear quite different, and further observations aimed at understanding these differences should be interesting. Observations of other, similar, objects should also be helpful. In particular, objects 32 and 33 are separated by only 40", so it is likely that differences observed between the two are intrinsic to the objects and are not due to differences in the intervening dark cloud material.

VII. LUMINOUS OBJECTS IN THE CLOUD

The must luminous objects in the dark cloud can best be found using far-infrared data, as the bulk of the energy from the stellar sources of the luminosity will be absorbed by the cloud and re-radiated at infrared wavelengths > 20 μm. The three far-infrared sources in the Ophiuchus region found by Fazio et al. (1976) can be identified with the three early type stars HD 147889, S-R 3, and S 1 (objects 9, 16, and 25 in Table 2). Optical spectra exist for all three stars, and both HD 147889 and S 1 are associated with H II regions (Brown and Zuckerman 1975, Matsakis et al. 1976). HD 147889 has a well established spectral type of B2V (e.g. Garrison 1967). The spectral type of S 1 is probably B3 or B5 (GSS, Brown and Zuckerman 1975), and its apparent luminosity is that of a star on the zero-age main sequence. The spectral type assigned S-R 3 by Struve and Rudkjøbing (1949) is A0, but the observed luminosity and the small observed equivalent width of Bγ in absorption (8 ± 3 Å) are more consistent with a star of earlier spectral type. Brown and Zuckerman (1976) did not detect an H II region around this star, so its spectral type must be later than B3. A best estimate of the spectral type is B6.

The AFGL survey (Price and Walker 1976) detected three objects associated with the dark cloud in regions not covered by the observations of Fazio et al. (1976). Of these, the detections of o Sco and α Sco are measurements of the stellar radiation, while the

detection associated with σ Sco is much brighter than the star itself, and probably represents radiation from cool dust, similar to that from the three far-infrared sources.

There are no strong far-infrared sources in the central regions of the dark cloud other than those identified with known early-type stars. This indicates both that there are no heavily obscured B stars in the cloud which have not been identified, and that there are no other high luminosity objects. Most of the objects in Table 2 which are bright at 2.2 μm must therefore be less luminous objects with infrared excesses, or objects with effective temperatures of a few thousand degrees or less. As Fazio et al. (1976) have noted, the radio continuum sources of Brown and Zuckerman (1975) which are not identified with known B stars are probably not compact H II regions in the dark cloud.

As most of the bright 2.2 μm sources are probably not early main sequence stars, the calculations of the total mass in stars and of the stellar initial mass function by VSSG and by Vrba (1977) may be seriously in excess of the true values. It is not possible to provide a reasonable set of improved estimates for these quantities, since the masses and luminosities of the pre-main-sequence objects are poorly known.

VIII. EMISSION-LINE STARS

a) T Tauri Stars

A number of T Tauri stars in the cloud were measured in this study, as were a number of objects with similar energy distributions and similar 2 μm spectra. All these objects display rather similar characteristics, in that they have rather flat infrared energy distributions, occasionally rising toward 20 μm (Fig. 5) and their 2 μm spectra are essentially featureless (Fig. 4). The photometric results are similar to those reported for these stars by RSS. The 2 μm spectra are similar to those reported for other T Tauri stars by Cohen (1975), who noted that the absence of Bγ and other emission lines in the 2 μm spectra of T Tauri stars indicates that the infrared continua of these objects are not produced by hydrogen recombination radiation. This suggestion is supported by the similarity of the energy distributions of stars such as object 30 (VS23=S-R 21), which has no Hα emission (Struve and Rudkjøbing 1949), to those of T Tauri stars such as S-R 4 (#13) and S-R 24 (#28).

b) MWC 863

MWC 863 (object #49) is one of the more enigmatic objects detected in the survey. It is known to show Hα emission (Merrill and Burwell, 1949), and was assigned a spectral type of A0. The infrared energy distribution shows a prominent silicate emission

feature, indicating that the infrared emission is from an optically thin dust envelope. No By emission is seen at 2 μm. Although the peculiarity of the object suggests its association with the dark cloud, it is not obviously interacting with it, and is in addition several degrees from any other unusual objects. Its proper motion is only approximately known (Schlesinger and Barney 1943) but is consistent with association with the dark cloud.

IX. BACKGROUND OBJECTS

a) Late M Giants

Some of the field stars found in the survey are of interest. Object #1 appears to be a Mira variable, (Fig. 12a), with a period of $\sim$ 320 days; although a period of $\sim$ 160 days is not altogether excluded by the data. Its apparent faintness suggests a distance of several kpc; if this estimate is valid, it must be several hundred pc below the galactic plane.

Object #43 has a 2 μm spectrum and infrared energy distribution similar to those of Object #1, but it does not appear as variable (Fig. 12b). Judging by the depths of the CO and H_2O bands, these two objects are the field stars of latest spectral type found in the survey.

b) Reddening

The background objects can be used to find the amount of intervening reddening material. The spectral types of the objects were estimated from the depths of the 2.3 μm CO band in their spectra, a procedure which provided a spectral type accurate to $\sim$ 3 subtypes for K and M giants (see Paper I or Baldwin et al. 1973). J-H, H-K, and K-L color excesses were found using these spectral types and the intrinsic colors compiled by Johnson (1966), Lee (1970), and Frogel et al. (1978). The results are listed in Table 5.

Two checks on the accuracy of these procedures were performed. The ratio of the color excesses, E_{J-H}/E_{H-K}, should differ significantly from the mean value for all stars for a star whose spectral type was grossly misestimated. In fact, the ratios were found to be consistent with the mean value of 1.59 ± 0.05 to within the accuracy implied by the uncertainties in the photometry and in the spectral types. As a second check, the same reddening calculations were performed for the three heavily reddened B stars HD 147889 (#9), S-R 3 (#16), and S 1 (#25), to see if a different value for E_{J-H}/E_{H-K} resulted. The weighted mean ratio for the B stars, 1.68 ± 0.10 was similar to that for the background stars. These values are also similar to the interstellar value toward the galactic center of 1.50 ± 0.10 (Becklin et al. 1978). A value for E_{K-L}/E_{H-K} of 0.56 ± 0.04 was found, using all stars in Table 5 with measured 3.4 μm magnitudes; this ratio is not significantly different from the interstellar value of 0.65 ± 0.06 (Becklin et al. 1978).

In order to convert the color excesses to visual extinction values the visual photometry of S 1 (#25) reported by VSSG was used to obtain the ratio A_V/E_{J-K}. This value, 4.6, is marginally different from the value found by VSSG, and probably reflects the uncertainties in the photometry and slight differences in the photometric systems. The visual extinction inferred from the J-K color excess is listed for each star in Table 6. The values for the B stars are similar to those found by VSSG and Carrasco et al. (1973). It is important to realize that the measured quantity is E_{J-K}, so variations in the A_V/E_{J-K} ratio over the cloud may affect the results. Exclusive of this effect, the uncertainties in the A_V values are slightly less than ± 1 mag. The measured extinction is probably all in the cloud itself, as the reddening of nearby globular clusters indicates a field A_V of $\sim$ 1 mag (Arp 1965, Lee 1977).

The average visual extinction at the center of the cloud appears to be roughly 10 mag, judging from the results of Table 5. It is of course true that background stars will be seen preferentially though less opaque regions of the cloud, and that stars very recently formed in the cloud may be expected to have especially thick condensations immediately in their vicinity. Nevertheless, it is clear that the extinction given by the background stars cannot be severely in error.

VSSG concluded that the extinction in the central region of the cloud was roughly twice as great as that derived here. This is undoubtedly due to their assumption that the bulk of the objects they detected were main-sequence stars, whereas nearly all of the objects observed in common appear to be intrinsically substantially redder than main sequence stars.

c) Globular Clusters

Two globular clusters, M4 (NGC 6121) and NGC 6144, are within the area surveyed. Of the two, M4 was considerably the brighter, and was more extended. Its peak brightness was $K \sim 5.0 \pm 0.1$ in a 2' beam; its extent in declination was roughly 10'. Its extent in right ascension is similar. Within this area there is considerable structure, suggesting that individual stars in the cluster may be as bright as K = +5 or +6. These stars can be tentatively identified with the brighter giant branch stars measured by Eggen (1972) and Lee (1977).

NGC 6144 had a peak brightness of $K = 7.3 \pm 0.1$ in a 2' beam and appeared to be only alightly larger than the beam at 2.2 μm.

X. CONCLUSIONS

A reasonable general description of the young stars in the Ophiuchus dark cloud can be produced. The observations clearly confirm the conclusion of GSS/VSSG that there is a young stellar cluster in a small area in the center of the Ophiuchus dark cloud, but they also show that there is a considerably greater range of stellar types present than these authors supposed. The major sources of luminosity--indicated by peaks in the far-infrared emission--are associated with the three known B stars in the center of the cloud. Of the remaining objects in the center of the cloud,

roughly one third are background objects; all or most of the remainder are probably pre-main-sequence objects.

At least three of these pre-main-sequence objects appear to be intrinsically very cool objects. They are surrounded by what seems to be infrared reflection nebulosity, which indicates a high local density of dust and gas. The reddest of these objects, #29, appears to be variable, and shows a strong 10 μm absorption feature which is probably intrinsic to the object.

The spectra and photometry of the background objects were combined to determine the average visual extinction in the center of the cloud. This was found to be approximately 10 magnitudes, although more opaque regions doubtless occur around a few individual objects.

ACKNOWLEDGEMENTS

These observations would not have been possible without the assistance of a great number of people. Chief among these were S. Beckwith, J. Frogel, D. Nadeau, and A. Sargent, and the Mt. Wilson night assistants, J. Frazier, E. Hancock and H. Lanning. I would also like to thank G. Grasdalen and S. Strom for useful conversations, and G. Neugebauer for extensive criticism. This work was partially supported by NASA Grant 05-002-207, NSF Grant AST74-18555A2, and the California Institute of Technology.

TABLE 1

10 μm NARROWBAND FILTERS

Filter Set	λ_o* (μm)	$\Delta\lambda$† (μm)	log $(F_{o,o})$‡
1	8.7	1.2	-24.30
	9.5	1.5	-24.38
	11.2	1.5	-24.52
	12.5	1.3	-24.62
2	8.5	1.2	-24.28
	9.3	1.5	-24.36
	10.9	1.5	-24.50
	12.2	1.3	-24.60
3	7.8	0.6	-24.21
	8.6	1.0	-24.30
	9.6	0.9	-24.39
	10.4	1.7	-24.46
	11.4	2.6	-24.54
	12.3	1.2	-24.61

*Center wavelength of the filter. Uncertainty is ± 0.1 μm

†Width of filter. Uncertainty is ± 0.05 μm

‡Log of adopted flux (W-m^{-2}-Hz^{-1}) of a 0-mag star at the filter center wavelength. The calibrations for Set 1 are from Beckwith et al. (1976); the calibrations for the other filters are derived by interpolation.

TABLE 2

MEASUREMENTS OF SELECTED OBJECTS

OBJECT	IDENTIFICATION	α(1950)	δ(1950)	POSITION	INFRARED MAGNITUDES							10 μm FILTER SET	2 μm SPECTRA	SAMPLE	ASSOCIATION
					[1.2]	[1.6]	[2.2]	[3.4]	[4.8]	[10]	[20]				
1*		$16^h14^m12^s.9$	$-24^o56'56"$	O	6.33	5.34	4.62	3.85	3.6±0.1	2.2±0.1			1	RS	F
2		16 15 29.0	-23 43 42	O	8.61	7.33	6.86						0	RS	U
3		16 18 10.7	-23 36 25	O	7.41	5.93	5.28	4.69		4.3±0.2			1	RS	F
4		16 18 12.9	-24 38 05	O	8.51	7.28	6.88	6.6±0.1					1	RS	F
5		16 20 40.0	-25 36 35	O	8.06	7.00	6.34	5.63					0	RS	U
6*	CoD-24^o12683 = GSS5	16 22 17.8	-24 20 03	O	8.40	7.91	7.82						1	CR	F
7*	S3 = GSS6	16 22 18.6	-24 22 28	O	9.82	8.06	7.04	6.2±0.1					2	CR	F
8*	S4 = GSS8	16 22 20.6	-24 23 25	O	8.84	7.18	6.50	6.09		>5.7			2	RS,CR	F
9*	HD147889 = GSS9	16 22 22.8	-24 21 07	SAO	5.38	4.81	4.55	4.36					1	CR	A
10		16 22 31.4	-23 47 15	O	7.92	6.46	5.79						1	RS	F
11*	S16 = GSS15	16 22 33.9	-24 27 13	O	9.39	7.36	6.48						1	RS,CR	F
12		16 22 36.7	-24 06 56	O	9.49	7.68	6.85						0	RS	U
13*	S-R4	16 22 54.8	-24 14 01	HRC	9.20	8.13	7.50						1	CR	A
14	Do-Ar21 = GSS23	16 23 01.7	-24 16 50	O	7.90	6.72	6.13						1	CR	A
15		16 23 04.0	-24 36 09	O	8.36	6.34	5.26	4.29	4.1±0.2	3.8±0.2			1	RS	F
16*	S-R3 = GSS25	16 23 07.7	-24 27 26	O	7.70	6.91	6.46						1	CR	A
17		16 23 11.6	-23 11 54	O	6.86	5.74	5.39	5.16	5.7±0.3	5.5±0.3			1	RS	F
18*	S28 = GSS29	16 23 15.5	-24 15 38	O	10.95	9.07	8.10						2	CR	A
19*	Do-Ar24 = GSS28	16 23 15.8	-24 13 37	O		8.7±0.3	8.1±0.2						0	CR	A
20*	VS1	16 23 $17.5±0^s.4$	-24 12 33±5"	IR	12.9±0.1	10.37	8.44						1	CR	U
21*	S29 = GSS30	16 23 19.9±0.2	-24 16 18±2	IR	>13.4	10.49	8.04	6.1±0.2	4.4±0.3	1.40	-1.7±0.2	1	1	CR	A
22*	Do-Ar24E = GSS31	16 23 22.0	-24 14 15	O	8.80	7.46	6.57						1	RS.CR	A
23*	S2 = GSS32	16 23 22.6	-24 18 04	O	10.52	8.36	7.02						1	RS.CR	A
24*		16 23 22.9	-24 09 29	O	10.34	8.39	6.86	5.26	5.0±0.1	3.00	+1.2±0.3		1	RS.CR	A
25	S1 = GSS35	16 23 32.8	-24 16 44	O	8.82	7.26	6.29	5.82		>5.3			1	RS,CR	A
26*	VS2 = GSS37	16 23 41.5	-24 13 47	O	10.71	8.95	7.94						1	CR	U
27*	GSS39	16 23 43.3±0.4	-24 16 24±5	IR	13.3±0.2	10.53	8.75						1	CR	A
28*	S-R24	16 23 56.5	-24 38 53	HRC	9.24	7.73	6.59	5.48	4.8±0.2	3.02	+1.0±0.4		1	RS	A
29*		16 24 07.7±0.2	-24 30 40±3	IR	14.7±0.2	10.79	6.78	3.88	2.13	0.63	-1.3±0.2	2.3	2	RS	A
30*	VS23 = S-R21	16 24 08.9	-24 12 31	O	8.76	7.56	6.84	6.08	5.5±0.2	3.4±0.1	-0.0±0.2		1	RS.CR	A
31*	VS25	16 24 25.4±0.4	-24 24 34±5	IR	12.36	10.43	9.31						1	CR	U
32*	VS18	16 24 26.9±0.3	-24 20 37±5	IR	13.7±0.1	11.63	9.66						0	CR	A
33*	VS17	16 24 28.6±0.3	-24 21 00±5	IR	>14.8	11.42	8.83						1	CR	A
34*	S-R9	16 24 38.8	-24 15 24	HRC		7.6±0.1	7.0±0.1						0	CR	A
35	VS13	16 24 45.2	-24 16 43	O	10.61	8.37	7.32						1	CR	F
36	VS14	16 24 48.3	-24 19 02	O	9.39	8.15	7.34	6.8±0.2		>5.4			1	CR	A
37	VS16	16 25 02.2	-24 19 54	O	8.54	7.09	6.50						1	CR	F
38*	VS15	16 25 07.8	-24 16 44	O	9.44	7.85	7.14	6.8±0.1					2	RS.CR	F
39		16 25 46.9	-25 40 01	O	8.00	6.86	6.49	6.21					0	RS	U
40		16 26 21.8	-25 46 13	O	6.79	5.73	5.20	4.64	4.5±0.1	3.5±0.2			0	RS	U

TABLE 2 (CONTINUED)

OBJECT	IDENTIFICATION	α(1950)	δ(1950)	POSITION	INFRARED MAGNITUDES [1.2]	[1.6]	[2.2]	[3.4]	[4.8]	[10]	[20]	10 μm FILTER SET	2 μm SPECTRA	SAMPLE	ASSOCIATION
41		$16^h27^m01^s.5$	$-23°44'40''$	O	8.88	7.52	6.98	6.6±0.1					0	RS	U
42		16 28 17.4	-24 31 02	O	8.98	7.65	7.13	6.7±0.1					1	RS	F
43*		16 29 44.1	-26 16 48	O	5.68	4.67	3.89	3.14	3.02	1.74	+0.7±0.2	1	1	RS	F
44		16 30 00.8	-24 16 24	O	9.73	7.84	7.02						1	RS	F
45		16 30 20.5	-23 44 06	O	8.76	7.15	6.42	5.87					0	RS	U
46		16 34 46.5	-24 20 09	O	8.95	7.41	6.77						0	RS	U
47		16 35 53.0	-24 05 26	O	7.94	6.10	5.19	4.56	4.2±0.1	3.6±0.1			0	RS	U
48*		16 36 48.9	-24 00 19	O	5.70	4.26	3.57	2.84	2.71	2.0±0.1			1	RS	F
49*	HD150193 = MWC863	16 37 16.4	-23 47 56	SAO	6.97	6.17	5.40	4.30	3.8±0.1	0.98	-0.4±0.2	3	1	RS	U
50		16 38 04.6	-24 03 26	O	7.64	6.02	5.25	4.93					0	RS	U

Description of Table 2

Column 1 Object. Object number used for identification in the text. An asterisk following the number indicates a note for the object follows the table.

Column 2 Identification. Previous identification of the object. Abbreviations are as follows:
S: Object detected by Grasdalen et al. (1973:GSS) for which photometry is given in GSS or Vrba et al. (1975a: VSSG).
GSS: Object detected by GSS. Number refers to entry number in Table 1 of GSS. Entry numbers for S28 and S29 given in VSSG are incorrect (Strom, private communication).
VS: Object detected by VSSG.
S-R: Struve and Rudkjøbing (1949).
Do-Ar: Dolidze and Arakelyan (1959).
MWC: Merrill and Burwell (1949).

Columns 3-5 α(1950), δ(1950), Position. Coordinates for equinox 1950. The origin of the position is given in (5):
O: Optical position measured from 48-inch Schmidt plates, taken in 1975-7.
SAO: Position taken from SAO catalog and given for epoch 1950.
HRC: Position taken from Herbig and Rao (1972).
IR: No definite optical counterpart, position determined from photometer offset guider settings.

Columns 6-12 Infrared Magnitudes. Magnitudes given to two decimal places are uncertain by less than ±0.10 mag. Uncertainties are given explicitly for magnitudes given to one decimal place. Upper limits are 3σ upper limits.

Column 13 10 μm Filter Set. Filter set or sets used for narrowband 10 μm photometry (Table 1). Measured magnitudes are given in the notes.

Column 14 2 μm Spectra. Number of 2 μm spectra obtained.

Column 15 Sample. RS: Object has survey $K < 7.0$, and survey $H-K \geq 0.70$. If two or more objects were confused in the survey measurement, only the brightest is included in the sample.
CR: Object is inside central region defined in text.

Column 16 Association. A: Associated with the dark cloud.
F: Field star.
U: Uncertain case.
See §Va for definitions.

Remarks (by object number)

1. This star is quite variable. The measurements in the table are for 1977 April 13, (UT) when the star was of intermediate brightness. Magnitudes near maximum observed brightness are: [1.2] = 6.1 ± 0.1, [1.6] = 5.03, [2.2] = 4.38, [3.4] = 3.67, [4.8] = 3.5 ± 0.2 and [10] = 2.2 ± 0.2. At minimum observed brightness, typical magnitudes are: [1.2] = 7.06, [1.6] = 6.04, [2.2] = 5.26, [3.4] = 4.44, [4.8] = 4.1 ± 0.2, and [10] = 2.9 ± 0.1. See §IXa.

6. S-R2; has spectral type = G8. The position given is preferred to the SAO position, because of large uncertainties in the proper motions. The [2.2] value agrees with that of Chini et al. (1977). This star must be a foreground object because of its color.

7. This object may be variable, with a total amplitude of ~ 0.2 mag at 2.2 μm. The means of 3 days' observations are given. The results are in agreement with those of VSSG.

8. These results agree with those of VSSG.

9. These results agree with those of Carrasco et al. (1973).

11. May be variable, as these results are ~ 0.5 mag. brighter than those reported by VSSG.

13. T Tauri star. The measurements in the table were taken 1977 April 20 (UT). Results from 1977 May 27 (UT) are: [2.2] = 7.26, [3.4] = 6.32, [4.8] = 5.6 ± 0.2 and [10] = 4.1 ± 0.1

16. These results agree with those of Carrasco et al. (1973).

18. These results are ~ 0.3 mag fainter than those of VSSG; if significant, these differences imply that the object is variable or extended.

19. T Tauri star. No photometry of this object was done, so the survey magnitudes are given. See RSS for representative photometry.

20. These values disagree with those of VSSG; possibly variable. Measurements made with a 20" beam only. A faint stellar object is seen at $\alpha(1950) = 16^h23^m17^s.2$, $\delta(1950) = -24^o21'34"$; this was also seen by Chini et al. (1977).

21. Extended at 1.2 - 2.2 μm. 10 μm narrowband magnitudes are: [8.7] = +2.2 ± 0.2, [9.5] = +2.0 ± 0.2, [11.2] = 0.9 ± 0.1, [12.5] = +0.3 ± 0.1. See §VIa.

22. T Tauri star.

23. The [1.2] value is much brighter than the upper limit in VSSG. The tabulated value was measured twice, so it is unlikely to be in error.

24. This star is apparently within the region surveyed by VSSG.

26. The position shown by VSSG for this object is incorrect; the position tabulated by VSSG is correct. This explains the failure of Chini et al. (1977) to identify this star optically.

27. The position of this object given in the table is significantly different from the position of continuum source 5 of Brown and Zuckerman (1975).

28. This is a pair of T Tauri stars; it is not possible to tell from the infrared positions which star is the source of the infrared flux. The 20 μm measurement is a 3σ detection.

29. This source is both extended and variable (§VIa,b). The 1.2 μm measurement is with a 20" beam; all others are with a 9" or 10"

beam, and all were taken 1977 May 21 and 27 (UT). 10 μm narrowband magnitudes and additional measurements with a 9" beam are: 1976 Sept. 5 (UT), [1.6] = 11.6 ± 0.1, [2.2] = 7.22, [3.4] = 3.7 ± 0.1, [4.8] = 2.4 ± 0.2, [10] = 0.9 ± 0.1, [8.5] = 1.2 ± 0.2, [9.3] = 1.2 ± 0.2, [10.9] = 0.8 ± 0.2, [12.2] = 0.3 ± 0.2; 1977 Apr 15 (UT), [1.2] > 13.8, [1.6] = 10.78, [2.2] = 6.69, [3.4] = 3.50, [4.8] = 2.08, [10] = 0.7 ± 0.1, [20] = − 1.6 ± 0.3, [8.5] = + 0.7 ± 0.1, [9.3] = + 1.1 ± 0.1, [10.9] = + 0.6 ± 0.1, [12.2] = − 0.2 ± 0.1; 1977 May 27 (UT), [7.8] = + 0.6 ± 0.1, [8.6] = + 0.8 ± 0.1, [9.6] = + 1.4 ± 0.1, [10.3] = + 0.9 ± 0.1, [11.4] = + 0.4 ± 0.1, [12.3] = − 0.1 ± 0.1.

30. This star is not known to have Hα emission. There is a faint companion 7" to the south, which is definitely not the dominant source of infrared flux.

31. A faint stellar object is seen at $\alpha(1950) = 16^h24^m25^s.7$, $\delta(1950) = 24^\circ24'36"$; this was also seen by Chini et al. (1977).

32. VS17 is 23" ± 2" S and 23" ± 2" E of VS18. VS18 measured with 10" beam at 1.6 and 2.2 μm, and with a 20" beam at 1.2 μm; it is definitely extended (§VIa).

33. Measured with 20" beam only.

34. No photometry of this object was done, so survey magnitudes are given. See RSS.

38. See comment on VS2 (#26).

43. Mean of all observations tabulated, although the star may be slightly variable. 10 μm narrowband magnitudes are: [8.7] = +1.9 ± 0.2, [9.5] = +1.8 ± 0.2, [11.2] = +1.2 ± 0.1, [12.5] = +1.2 ± 0.2

48. See comment on #43.

49. 10 μm narrowband magnitudes are: [7.8] +2.3 ± 0.1, [8.6] = +1.6 ± 0.1, [9.6] ± +1.0 ± 0.1, [10.3] = +0.8 ± 0.1, [11.4] = +0.8 ± 0.1, [12.3] = +1.0 ± 0.1.

TABLE 3

MEASUREMENTS OF ADDITIONAL STARS

OBJECT	POSITION†		INFRARED MAGNITUDES‡					
	α(1950)	δ(1950)	[1.2]	[1.6]	[2.2]	[3.4]	[4.8]	[10]
51*	$16^h14^m14^s.0$	-25°54'55"	5.41	4.43	4.12	3.89	4.1 ± 0.2	4.1 ± 0.5
52*	16 14 49.8	-23 16 38	5.30	4.22	3.94	3.77	4.1 ± 0.2	3.7 ± 0.2
53*	16 15 12.1	-25 33 58	6.50	5.54	5.23	5.1 ± 0.1		
54*	16 15 25.4	-25 57 05	5.55	4.53	4.22	3.94	4.8 ± 0.3	3.7 ± 0.2
55	16 16 39.5	-25 27 31	5.87	4.72	4.40	4.2 ± 0.1		
56*	16 16 41.7	-23 15 22			4.48	4.13	4.0 ± 0.2	3.3 ± 0.2
57	16 16 52.1	-23 58 19	5.6 ± 0.1	4.70	4.40	4.09		
58*	16 17 37.4	-24 03 02	2.25	1.83	1.62	1.42	1.4 ± 0.1	1.5 ± 0.1
59*	16 17 44.0	-23 43 37	4.7 ± 0.1	3.40	2.92	2.43	2.9 ± 0.2	2.5 ± 0.2
60*	16 17 45.4	-25 28 42	5.91	4.85	4.53	4.3 ± 0.1		
61*	16 18 08.7	-25 28 28	2.50	2.39	2.39	2.40	2.47	2.51
62*	16 19 23.2	-23 34 47	5.47	4.07	3.49	3.06	3.35	3.2 ± 0.2
63*	16 19 27.5	-22 59 30	6.73	5.28	4.76	4.46		
64	16 20 12.4	-24 32 24	5.54	4.39	4.02	3.71	4.2 ± 0.3	3.8 ± 0.2
65*	16 20 2?.0	-23 21 06			2.24	1.81	2.1 ± 0.1	1.8 ± 0.1
66*	16 21 55.4	-23 09 02	7.59	6.37	5.95			
67*	16 22 35.0	-23 20 01	3.79	3.51	3.48	3.44	3.4 ± 0.1	
68	16 24 28.5	-25 22 57	6.83	5.59	5.06	4.58		
69	16 25 17.5	-26 29 01	6.08	5.17	4.81	4.5 ± 0.1		
70*	16 25 20.3	-26 21 57	5.90	5.15	4.94	4.7 ± 0.1		
71*	16 25 27.7	-26 06 57	6.04	5.12	4.94	4.7 ± 0.1		
72*	16 25 32.0	-25 05 19	6.02	4.95	4.39	3.73	3.8 ± 0.2	3.0 ± 0.1
73*	16 25 47.4	-23 30 25	6.64	5.29	4.88	4.63	4.9 ± 0.3	>4.7
74*	16 26 20.2	-26 19 22	-2.69	-3.49	-3.82	-4.17	-3.84	-4.54
75*	16 26 36.7	-23 43 37	5.8 ± 0.1	4.60	4.16	3.80	4.0 ± 0.1	4.1 ± 0.3
76*	16 27 09.9	-25 00 24	5.13	5.10	5.16	5.21		
77*	16 28 09.3	-24 33 13	5.85	4.42	3.78	3.27	3.42	2.17
78*	16 28 18.4	-26 25 50	4.19	3.71	3.62	3.54	3.6 ± 0.2	3.5 ± 0.2
79*	16 28 43.8	-23 37 32	6.0 ± 0.1	4.80	4.24	3.68	3.7 ± 0.1	2.9 ± 0.1
80*	16 30 16.7	-23 17 34	5.52	4.28	3.89	3.67	3.7 ± 0.1	3.0 ± 0.2
81	16 31 39.4	-24 18 13	6.57	5.14	4.53	4.06		
82*	16 32 07.5	-26 22 49	6.46	5.58	4.96	4.26	4.1 ± 0.2	3.3 ± 0.1
83*	16 32 26.1	-24 50 40	3.36	2.29	1.90	1.60	1.76	0.66
84*	16 33 06.7	-24 41 40		5.1 ± 0.1	4.8 ± 0.1			
85	16 36 25.3	-24 49 27	5.55	4.56	4.26	3.97	4.2 ± 0.2	3.8 ± 0.2
86	16 37 53.1	-26 31 04	6.59	5.66	5.31	5.0 ± 0.1		
87*	16 38 27.0	-23 34 49	5.48	4.42	4.10	3.88		3.7 ± 0.3

* Indicates the presence of a remark for the object below.

† Positions measured from 48-inch Schmidt plates, except for named stars and star with CoD numbers; positions for these taken from SAO catalog.

‡ Magnitudes given in same format as Table 2.

Remarks (by object number)

51. Mean of 2 days of observations in 1976 June. The 10 μm number is a 2.5σ marginal detections.

52. Not variable. Mean of 2 observations in 1976 June and 1977 July.

53. Possible variable. Single measurement 1976 June 5 (UT). Survey result (1975 June 6) is [1.6] = 5.3, [2.2] = 5.0.

54. Mean of 2 measurements in 1976 June.

56. Variable measurements listed are for 1977 June 27; values for 1977 July 8 are: [1.2] = 6.42, [1.6] = 5.37, [2.2] = 4.90.

58. o Sco = IRC-20311 (Neugebauer and Leighton 1969) = GL1844 (Price and Walker 1976).

59. IRC-20313. Spectral type = M4 (Hansen and Blanco 1975). 10μm narrowband magnitudes (set 2) are: [8.5] = 2.3 ± 0.2, [9.3] = 2.5 ± 0.2, [10.9] = 2.3 ± 0.3, [12.2] = 2.8 ± 0.4.

60. Possible variable. Single measurement 1976 June 5. Survey result (1975 June 6) is [1.6] = 4.5, [2.2] = 4.3.

61. σ Sco = IRC-30260. Used as secondary standard. Identified with GL1845.

62. Mean of 2 measurements in 1976 June.

63. Not variable. Mean of 2 measurements in 1976 June and 1977 July.

65. IRC-20314. Spectral type = M7 (Hansen and Blanco 1975). 10 μm narrowband magnitudes (set 1) are: [8.7] = 1.7 ± 0.2, [9.5] = 1.8 ± 0.1, [11.2] = 1.6 ± 0.2, [12.5] = 1.6 ± 0.2.

66. Variable. Measurement is for 1977 July 8. Other results: 1976 May 27, [1.6] = 5.2 ± 0.1, [2.2] = 4.8 ± 0.1; 1976 June 28, [2.2] = 5.22, [3.4] = 5.02.

67. ρ Oph AB. Position given is that of ρ Oph A.

70. CoD-26°11353.

71. CoD-25°11515.

72. Probably variable. Measurement is for 1976 June 6. Measurements 1976 June 28: [2.2] = 4.61, [3.4] = 4.03, [4.8] = 3.9 ± 0.2, [10] = 2.9 ± 0.2.

73. Not variable. Mean of 2 measurements in 1976 June and 1977 July.

74. α Sco = IRC-30265 = GL1863. Standard star for $\lambda \geq 3.5$ μm. Photometry is the mean of unpublished data from the CIT IR group.

75. Mean of 2 measurements in 1976 June.

76. 22 Sco.

77. Mean of 2 measurements in 1976 June. 10 μm narrowband magnitudes (set 1) are: [8.7] = 2.3 ± 0.2, [9.5] = 2.3 ± 0.2, [11.2] = 1.7 ± 0.2, [12.5] = 1.4 ± 0.2.

78. CoD-26°11379. Mean of 2 measurements in 1976 June.

79. Mean of 2 measurements in 1976 June.

80. Not variable. Mean of 2 measurements in 1976 June and 1977 July.

82. Probably variable. Measurements of 1976 June 5 and 28 have been averaged as they are nearly identical, survey values for 1975 May 7 are: [1.6] = 4.6 ± 0.1, [2.2] < 4.3. May be #62 in the list of Dolidze and Arakelyan (1959) of Hα-emission stars.

83. IRC-20320 = KV Sco. Spectral type = M6 (Hansen and Blanco 1975). Mean of 2 measurements in 1976 June. Probably Dolidze and Arakelyan #63. 10 μm narrowband magnitudes (set 1) are: [8.7] = 0.9 ± 0.2, [9.5] = 0.8 ± 0.1, [11.2] = 0.4 ± 0.1, [12.5] = 0.5 ± 0.2.

84. Magnitudes given are from survey in 1975 July.

87. Mean of 2 measurements in 1976 June.

TABLE 4

OPHIUCHUS B AND AO STARS

Star	Spectral Type*	V*	K†	Estimated Association Membership
HD146331	A0"		7.4±0.3	Probable
HD146706	B9 V	7.55	7.1±0.2	Yes
HD147012	B9 V	9.75	7.6±0.2	Yes
HD147013	A0 V	9.10	7.7±0.3	Yes
HD147084 (o Sco)	A5 II	4.54	1.62±0.06	Yes
HD147165 (σ Sco)	B1 III	2.93	2.39±0.03	Yes
HD147196	B8 Vnnp	7.03	6.3±0.1	No?
HD147384	B9.5 V	8.62	6.4±0.1	Yes
HD147648	B8 V	9.42	6.3±0.1	Yes
HD147701	B5 V	8.35	6.30±0.06††	Yes
HD147888 (ρ Oph D)	B5 V	6.74	5.47±0.05††	Yes
HD147889	B2 V	7.86	4.55±0.04	Yes
HD147932 (ρ Oph C)	B5 V	7.27	5.73±0.05††	Yes
HD147933/4 (ρ Oph AB)	B2 IV + B2 V	4.59	3.48±0.05	Yes
HD147955	B9.5 V	8.07	7.2±0.2	Yes
HD148478/9 (α Sco)	M1Ib+B2.5 V	variable	-3.82±0.05§§	Yes
HD148579	B9 V	7.34	6.1±0.1	Yes
HD148605 (22 Sco)	B2 V	4.79	5.16±0.06	Yes
HD149168	B7 V	9.93	>7.8	No
HD149228	B9 p	9.97	>8.0	No
HD149367	B9 V	8.50	8.0±0.3	No
HD149827	B9"	9.63	>8.0	No
HD150080	A0"#		>8.3	?
HD150193	A0e#		5.40±0.05	?
HD150207	A0"		>8.3	?
S-R 3‡	A0‡	12.00††	6.46±0.06	Yes
S1 §	B3§	17.01‡‡	6.29±0.03	Yes
CoD-24°12698	B9-A1**		6.7±0.1	Yes

*Spectral types and V magnitudes from Garrison (1967) except as noted

†2.2 μm magnitudes from this work, except as noted

‡Struve and Rudkjøbing 1949

§Grasdalen et al. 1973

"HD spectral type from Henry Draper catalog

#Merrill and Burwell (1949)

**Struve and Straka 1962; Vrba et al. 1976

††Carrasco et al. 1973

‡‡Vrba et al. 1975a (VSSG)

§§Neugebauer (unpublished)

TABLE 5

REDDENING

OBJECT NO.	SPECTRAL TYPE*	COLOR EXCESS (MAG)			A_V (MAG)†
		E_{J-H}	E_{H-K}	E_{K-L}	
3	M7 III	0.59	0.30		4.1
4	M1 III	0.50	0.24	0.12	3.4
7(S3)	M8 III	0.89	0.64		7.0
8(S4)	K1 III	1.14	0.61	0.28	8.0
9(HD147889)‡	B2 V	0.66	0.34	0.22	4.6
10	M7 III	0.51	0.36		4.0
11(S16)	K5 III	1.30	0.73		9.3
15	M6 III	1.13	0.78	0.67	8.8
16(S-R3)‡	B6 V	0.85	0.50		6.2
17	K5 III	0.37	0.20	0.08	2.6
25(S1)‡	B3 V	1.69	1.03	0.50	12.5
26(VS2)§	G9 III	1.26	0.88		9.8
31(VS25)§	K0 III	1.42	1.04		11.3
35(VS16)	K5 III	1.51	0.90		11.1
37(VS16)	K0 III	0.94	0.51		6.7
38(VS15)	K3 III	0.99	0.56		7.1
42	M5 III	0.56	0.22	0.19	3.6
44	M4 III	1.01	0.57		7.3
48	M8 III	0.55	0.41		4.4

* Spectral type based on depth of CO band and assumed luminosity class.

† Visual extinction, $A_V = 4.6\ E_{J-K}$.

‡ Association member, not a background star.

§ Spectral type uncertain; may not be a field star.

REFERENCES

Arp, H. C. 1965, Galactic Structure, ed. A. Blaauw and M. Schmidt (University of Chicago), p. 401.

Baldwin, J. R., Frogel, J. A., and Persson, S. E. 1973, Ap. J., 184, 427.

Becklin, E. E., Matthews, K., Neugebauer, G., and Willner, S. P. 1978, Ap. J., in press.

Beckwith, S., Evans, N. J.II, Becklin, E. E., and Neugebauer, G. 1976, Ap. J., 208, 390.

Bertiau, F. C. 1958, Ap. J., 128, 533.

Brown, R. L., and Zuckerman, B. 1975, Ap. J. (Letters), 202, L125.

Carrasco, L., Strom, S. E., and Strom, K. M. 1973, Ap. J., 182, 95.

Chini, R., Elsässer, H., Hefele, H., and Weinberger, R. 1977, Astr. Ap., 56, 323.

Cohen, M. 1975, M.N.R.A.S., 173, 279.

Dolidze, M. V., and Arakelyan, M. A. 1959, Sov. A. J., 3, 434.

Eggen, O. J. 1972, Ap. J., 172, 639.

Elias, J. H. 1978, submitted to Ap. J.

Encrenaz,P. J. 1974, Ap. J. (Letters), 189, L135.

Fazio, G. G., Wright, E. L., Zeilik, M.,II, and Low, F. J. 1976, Ap. J. (Letters), 206, L165.

Frogel, J. A., Persson, S. E., Aaronson, M., and Matthews, K. 1978, Ap. J., in press.

Garrison, R. F. 1967, Ap. J., 147, 1003.

Grasdalen, G. L., Strom, K. M., and Strom, S. E. 1973, Ap. J. (Letters), 184, L53.

Gottlieb, C. A., and Ball, J. A. 1973, Ap. J. (Letters), 184, L59.

Gottlieb, C. A., Gottlieb, E. W., Litvak, M. M., Ball, J. A., and Penfield, H. 1978, Ap. J., 219

Hansen, O. L., and Blanco, V. M. 1975, A. J., 80, 1011.

Haro, G. 1949, A. J., 54, 188.

Herbig, G. H., and Rao, N. K. 1972, Ap. J., 174, 401.

Hidajat, B. 1961, Contr. Bosscha Obs., #11.

Johnson, H. L. 1966, Ann. Rev. Astr. Ap., 4, 193.

Lee, S. W. 1977, Astro. Ap. Suppl., 27, 367.

Lee, T. A. - 1970, Ap. J., 162, 217.

Matsakis, D. N., Evans, N. J.,II, Sato, T., and Zuckerman, B. 1976, A. J. 81, 172; erratum in A.J., 81, 1014.

Merrill, P. W., and Burwell, G. G. 1949, Ap. J., 110, 387.

Neugebauer, G., Becklin, E. E., Beckwith, S., Matthews, K., and Wynn-Williams, C. G. 1976, Ap. J. (Letters), 205, L139.

Neugebauer, G., and Leighton, R. B. 1969, Two-Micron Sky Survey, NASA SP-3047 (Washington, D. C.).

Persson, S., Frogel, J. A., and Aaronson, M. 1976, Ap. J., 208, 753.

Price, S. D., and Walker, R. G. 1976, AFGL Four Color Infrared Sky Survey, AFGL-TR 76-0208 (Washington, D. C.).

Racine, R. 1968, A. J., 73, 233.

Rydgren, A. E., Strom, S. E., and Strom, K. M. 1976, Ap. J. Suppl., 30, 307.

Schlesinger, F., and Barney, I. 1943, Trans. Astr. Obs. Yale, 14, 1.

Spitzer, L., Jr., and Jenkins, E. B. 1975, Ann. Rev. Astr. Ap., 13, 133.

Strom, S. E., Grasdalen, G. L., and Strom, K. M. 1974a, Ap. J., 191, 111.

Strom, K. M., Strom, S. E., and Kinman, T. D. 1974b, Ap. J. (Letters), 191, L93.

Struve, O., and Rudkjøbing, M. 1949, Ap. J., 109, 92.

Struve, O., and Straka, W. C. 1962, P.A.S.P., 74, 474.

The, P.-S., and Lim, H.-K. 1964, Contr. Bosscha Obs., #23.

Vrba, F. J. 1977, A. J., 82, 198.

Vrba, F. J., Strom, K. M., Strom, S. E., and Grasdalen, G. L. 1975a, Ap. J., 197, 77.

Vrba, F. J., Strom, S. E., and Strom K. M. 1975b, P.A.S.P., 87, 337.

Vrba, F. J., Strom, S. E., and Strom, K. M. 1976, A. J., 81, 958.

Wilson, W. J., Schwartz, P. R., Neugebauer, G., Harvey, P. M., and Becklin, E. E. 1972, Ap. J., 177, 523.

Whittet, D. C. B. 1974, M.N.R.A.S., 168, 371.

FIGURE CAPTIONS

Fig. 1a Regions surveyed in the near infrared. The area covered by the main survey is indicated by the large irregular outline. The north-south dimension of this region is 3.7^{o}; north is at the top, east is to the left. The two small boxes in the upper left and lower center of the figure are the unobscured regions surveyed at higher sensitivity around HD 150714 and HD 148760. The larger box in the middle of the figure is an approximate outline of the region studied by GSS/VSSG; HD 147889 is the bright star in the nebulosity near the right edge of the box.

Fig. 1b The spatial distribution sources brighter than K = 75 is shown. Point sources with $7.0 < K < 7.5$ are shown as a +, sources with $5.0 < K < 7.0$ as an X, sources with $3.0 < K < 5.0$ as an open triangle, and sources with $K < 3.0$ are shown as filled triangles. The two globular clusters detected in the survey are shown as open squares. The two dashed lines at $16^{h}17^{m}$ and south of -26^{o} at $16^{h}28^{m}.5$ represent the boundaries of the unobscured regions referred to in the text.

Fig. 1c Red sources with $K < 7.0$ detected in the survey. Sources with $0.5 \leq H-K < 0.70$ are shown as a + and sources with $H-K \geq 0.70$ are shown as circles.

Fig. 2 Cumulative 2.2 μm source counts per square degree in Ophiuchus corrected for coincidence. The globular clusters have been omitted.

Fig. 3 Cumulative 2.2 μm source counts for the unobscured regions only. The prediction of the model from Paper I are shown as a solid curve; the observed cumulative counts over the whole region (Fig. 2) are shown as a dashed curve. The lower dotted line indicates the predicted counts for M giants, while the upper dotted line indicates the predicted counts for K and M giants combined.

Fig. 4a 2 μm spectrophotometry of Ophiuchus objects. Numbers identifying spectra refer to entry numbers in Table 2. Note that log (F_ν) is plotted against λ, with an arbitrary vertical scale shift. Objects with similar spectra are plotted together. The true uncertainties at the ends of the spectra are not necessarily as small as indicated.

Fig. 4b Same as Fig. 4a.

Fig. 5 Energy distributions of selected objects. Except for the 3.4 μm measurement of VS 17 (#33) taken from VSSG, all values are from this work.

Fig. 6 Distribution and association of objects with $K < 7.0$ and $H-K \geq 0.70$. Stars associated with the dark cloud are shown as circles, field stars are shown as a +, and uncertain cases are shown as an X.

Fig. 7 Distribution and association of identified stars with spectral types of A0 or earlier. The two evolved stars α Sco and o Sco are also shown. Symbols are as in Fig. 6.

Fig. 8 Multi-aperture measurements of extended objects. Filled symbols are measurements where the two beams were spaced in right ascension, open symbols are measurements where the spacing was in declination. Circles represent measurements made with a 36" beam separation, and triangles represent measurements made with an 18" beam separation. The plots are: a) object 21 (S29), 2.2 μm; b) object 21, 1.5 μm; c) object 21, 1.2 μm; d) object 32 (VS 18), 2.2 μm; e) object 32, 1.6 μm; f) object 29, 2.2 μm; g) object 29, 1.6 μm. The two sets of measurements of S29 were made on different nights. All measurements have been corrected for beam profile effects; flux in the reference beams has not been corrected for.

Fig. 9 Color vs. beam diameter plots. H-K is plotted in the top three panels for objects 21(a), 32(b), and 29(c), and J-K for object 21 is plotted in (d). Symbols are as in Fig. 8.

Fig. 10 Surface brightness plots for object 21 (S29). The surface brightness and associated uncertainties are indicated by the vertical error bars; the annular regions to which points refer are indicated by the horizontal bars. The open circles, filled circles, and triangles refer to wavelengths of 2.2 μm, 1.6 μm and 1.2 μm respectively.

Fig. 11 2.2 μm magnitude vs. time for object 29(a) and object 21(b). Open circles are measurements with a 9" beam, filled circles are measurements with a 20" beam, corrected by +0.10 mag for object 29 and by +0.55 mag for S29.

Fig. 12 2.2 μm magnitude vs. time for object 1(a) and object 43(b).

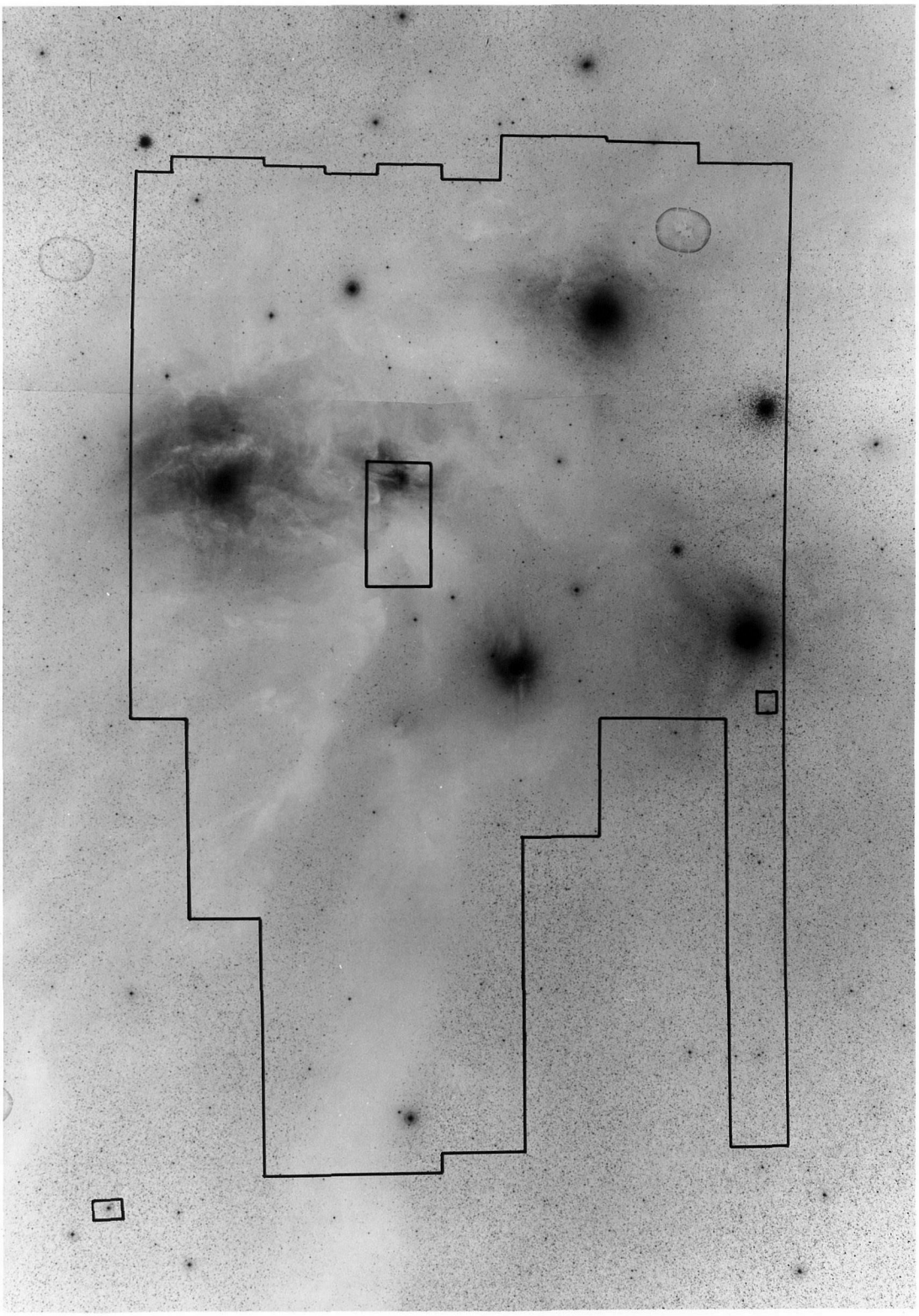

Fig. 1a

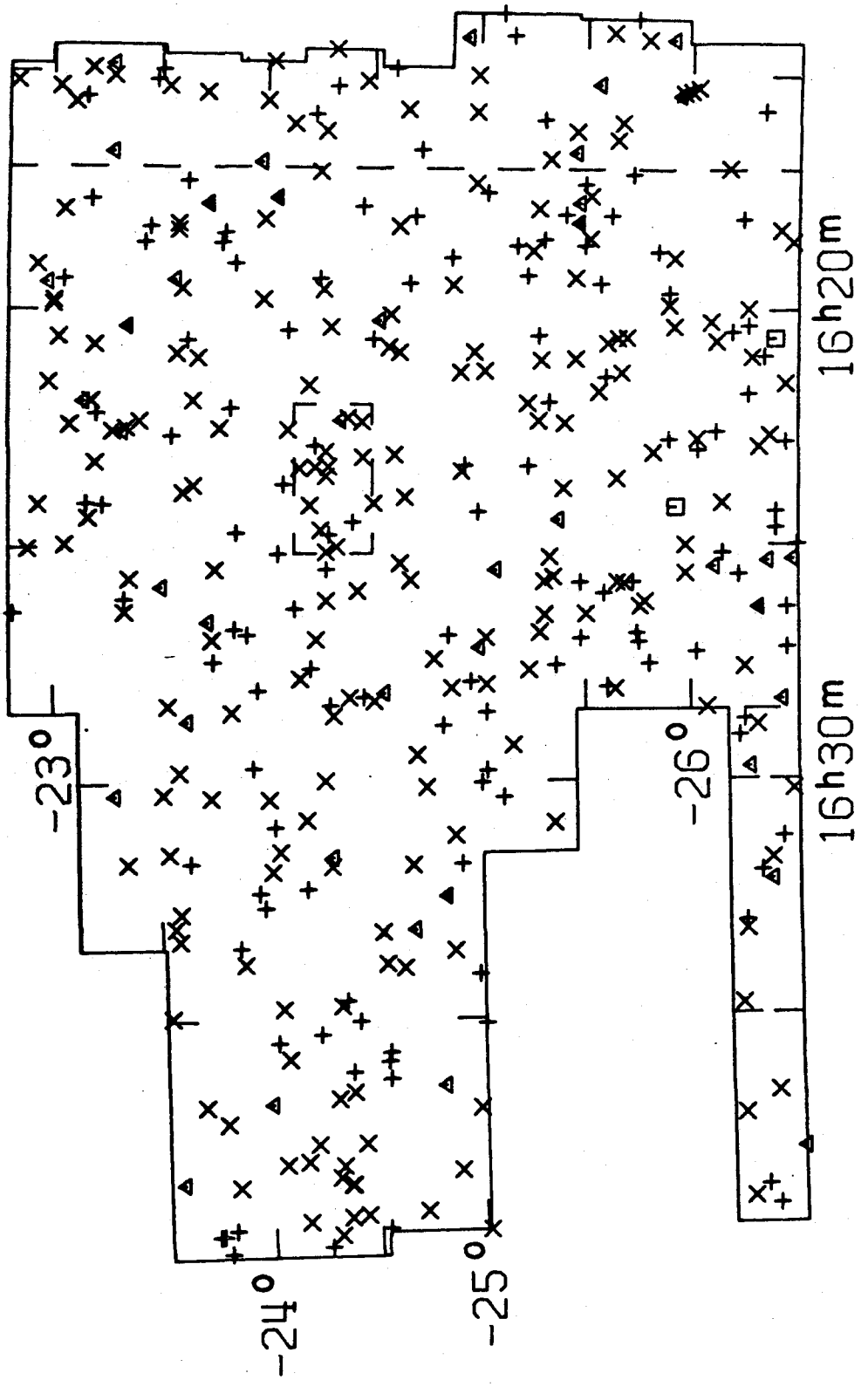

Fig. 1b

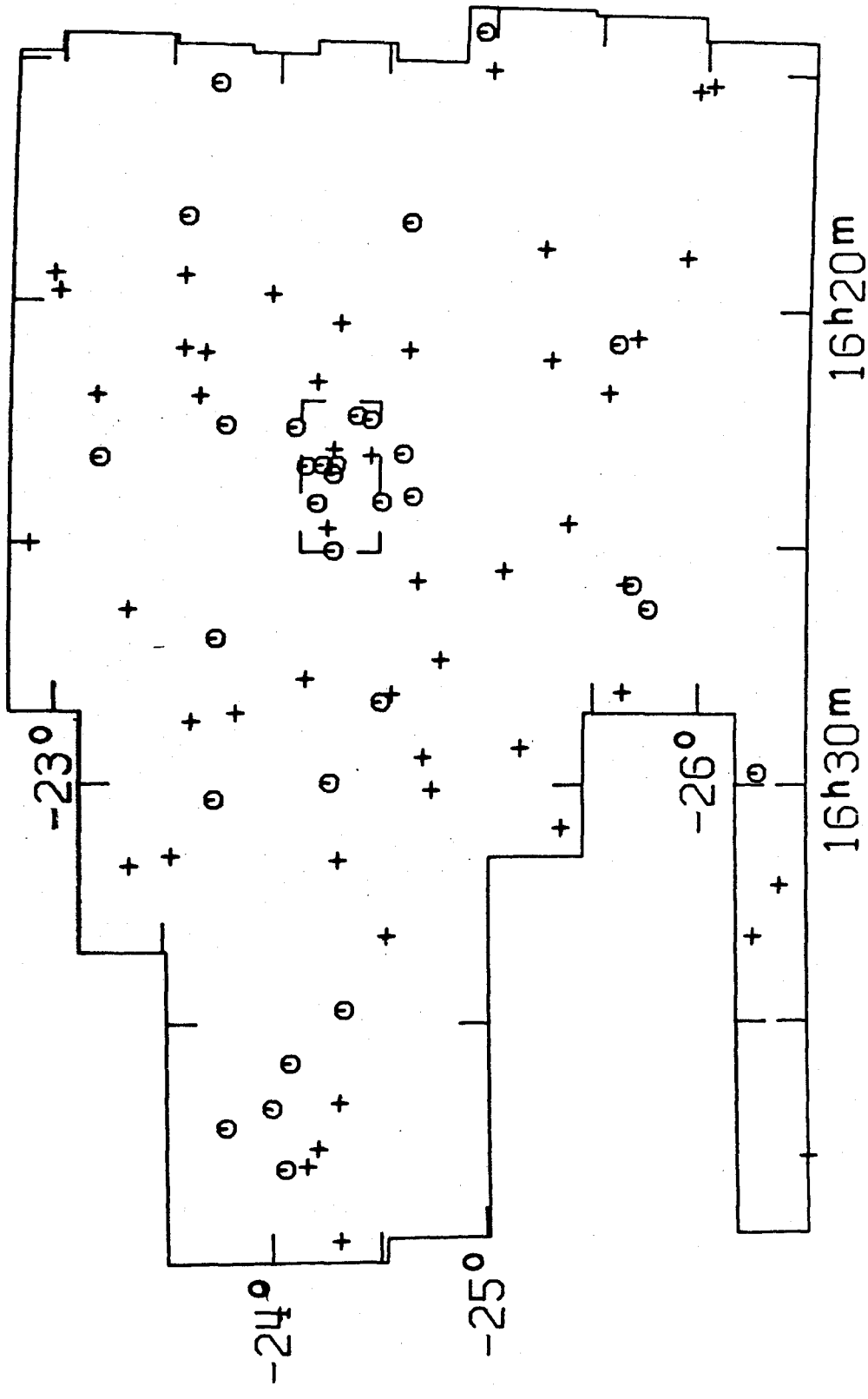

Fig. 1c

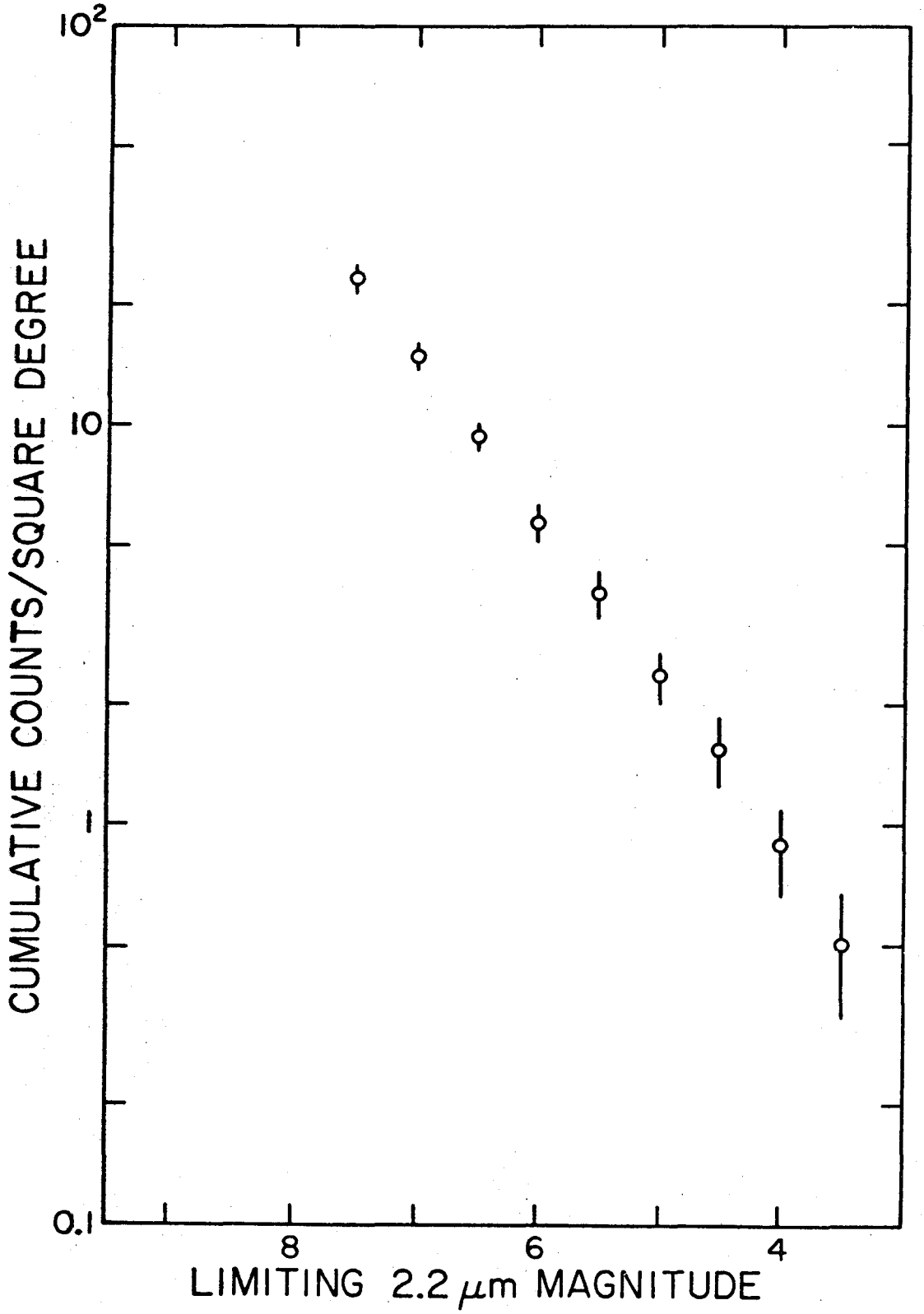
10^2
10
1
0.1
CUMULATIVE COUNTS/SQUARE DEGREE
8
6
4
LIMITING 2.2 μm MAGNITUDE

Fig. 2

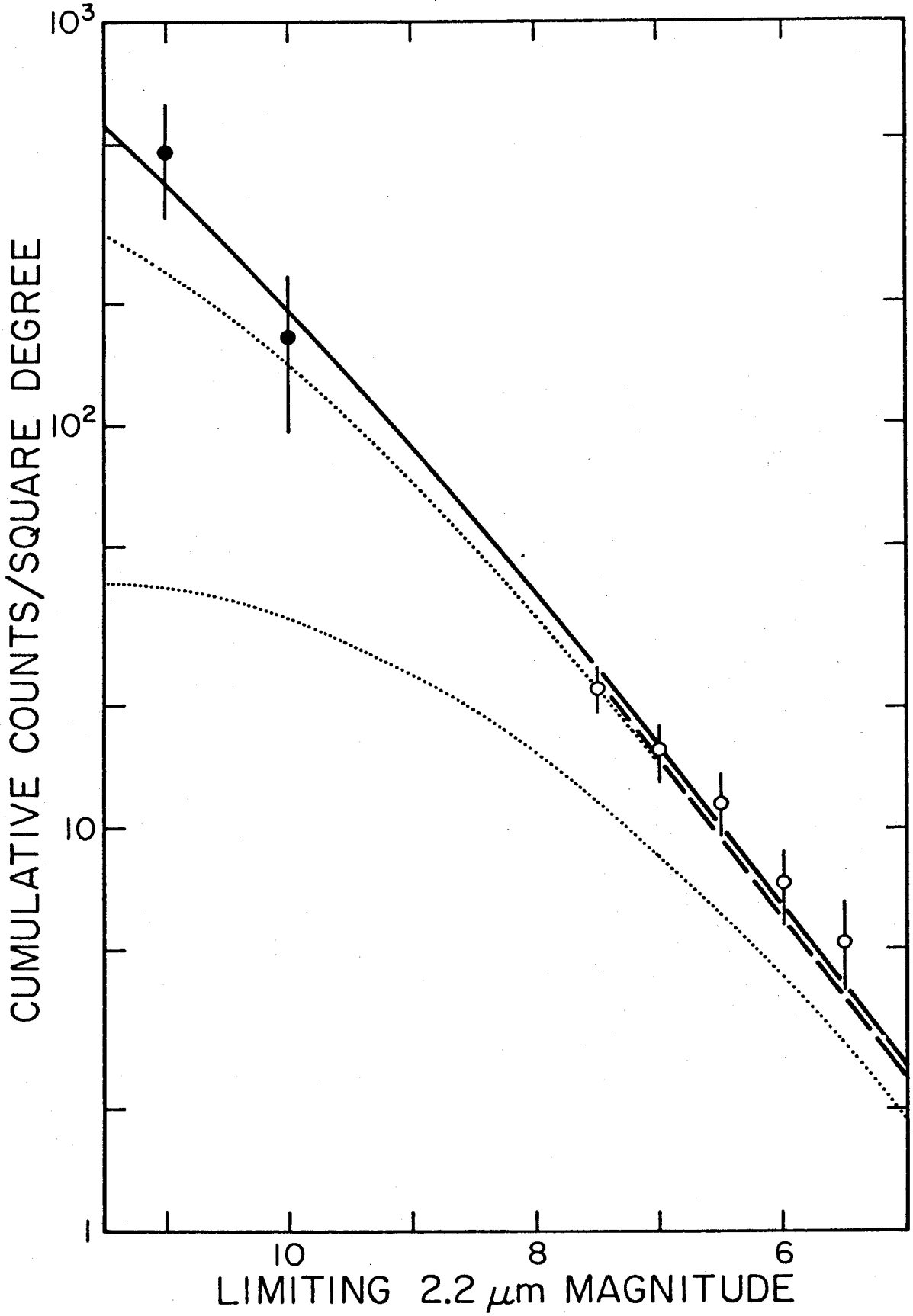
10^3
10^2
10
1
CUMULATIVE COUNTS/SQUARE DEGREE
10
8
6
LIMITING 2.2 μm MAGNITUDE

Fig. 3

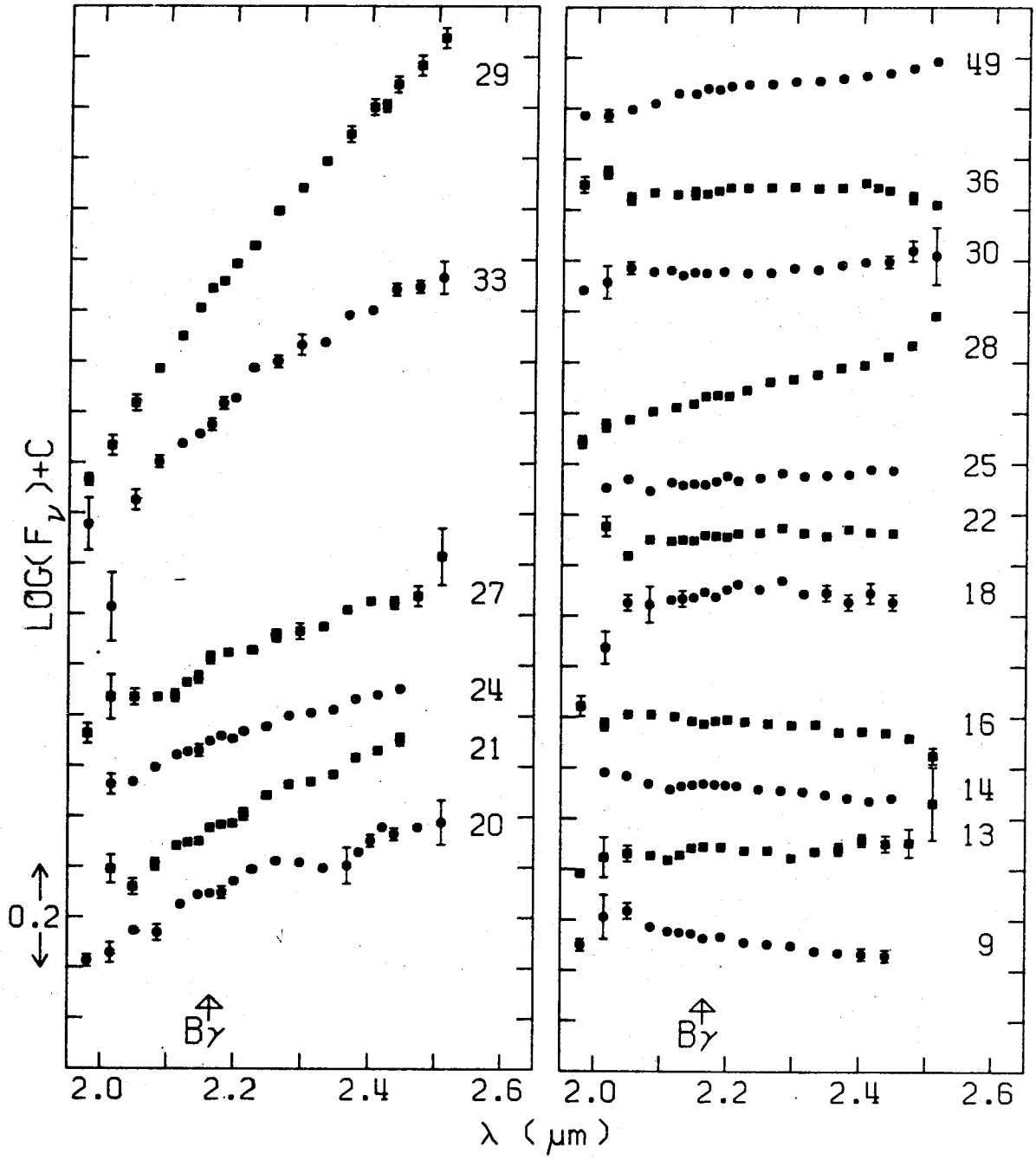
LOG(F_ν)+C
0.2
29
33
27
24
21
20
49
36
30
28
25
22
18
16
14
13
9
Bγ
Bγ
2.0
2.2
2.4
2.6
2.0
2.2
2.4
2.6
λ (μm)

Fig. 4a

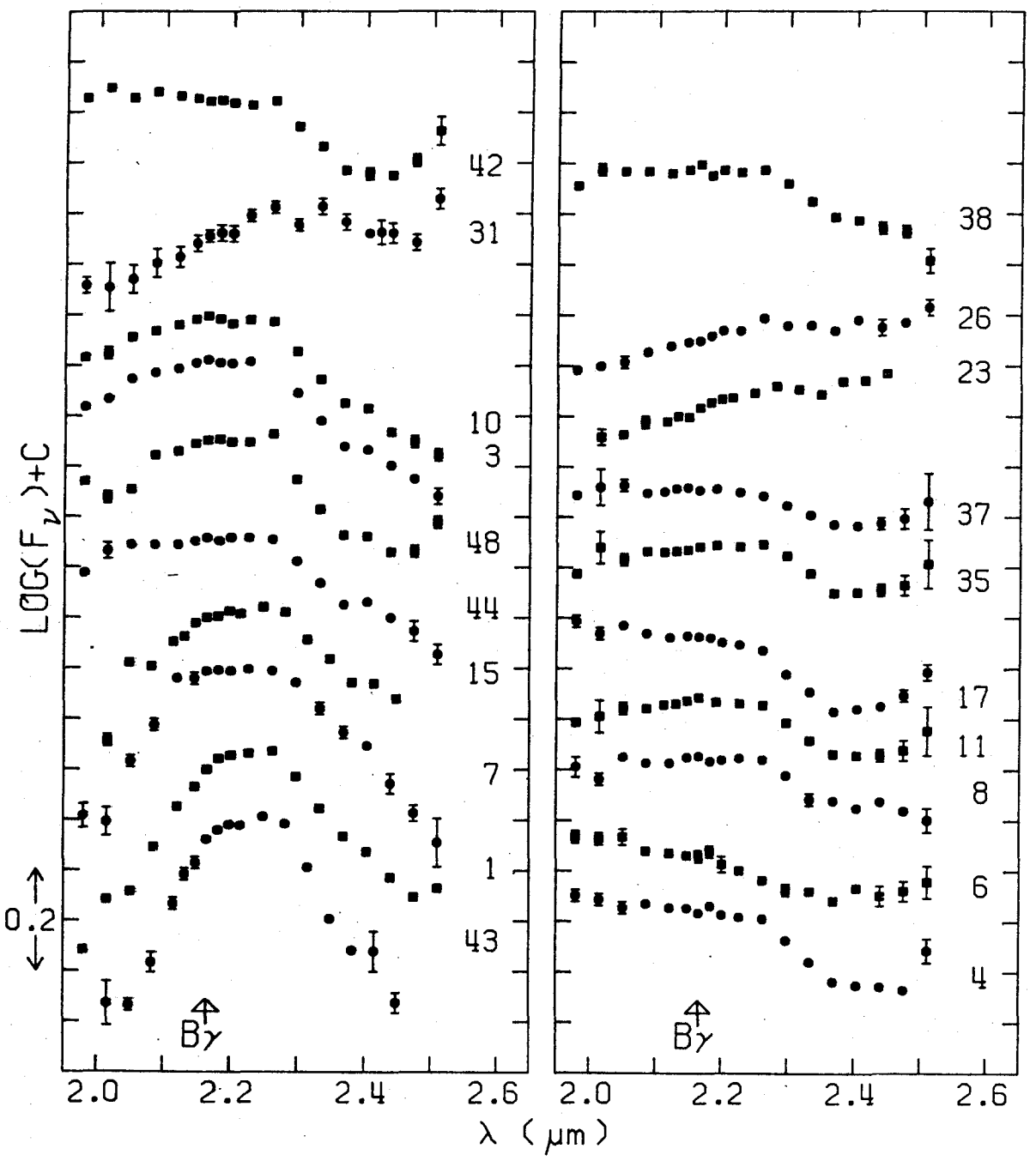
LOG(F_ν)+C
0.2
Bγ
Bγ
42
31
10
3
48
44
15
7
1
43
38
26
23
37
35
17
11
8
6
4
2.0
2.2
2.4
2.6
2.0
2.2
2.4
2.6
λ (μm)

Fig. 4b

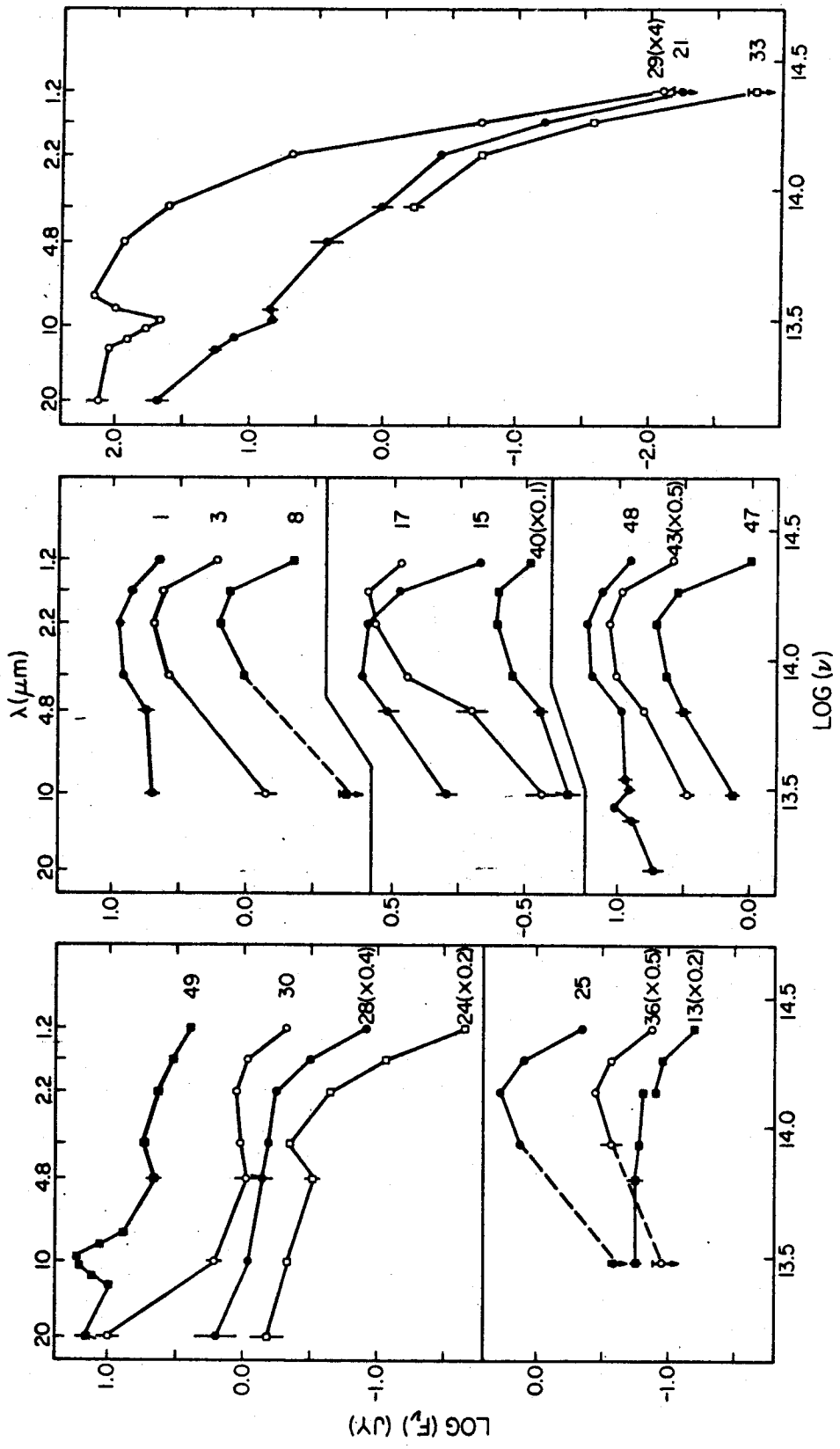
λ(μm)
20
10
4.8
2.2
1.2
LOG (ν)
14.5
14.0
13.5
LOG (F_ν) (JY)
1
3
8
17
15
40(X0.1)
48
43(X0.5)
47
49
30
28(X0.4)
24(X0.2)
25
36(X0.5)
13(X0.2)
29(X4)
21
33

Fig. 5

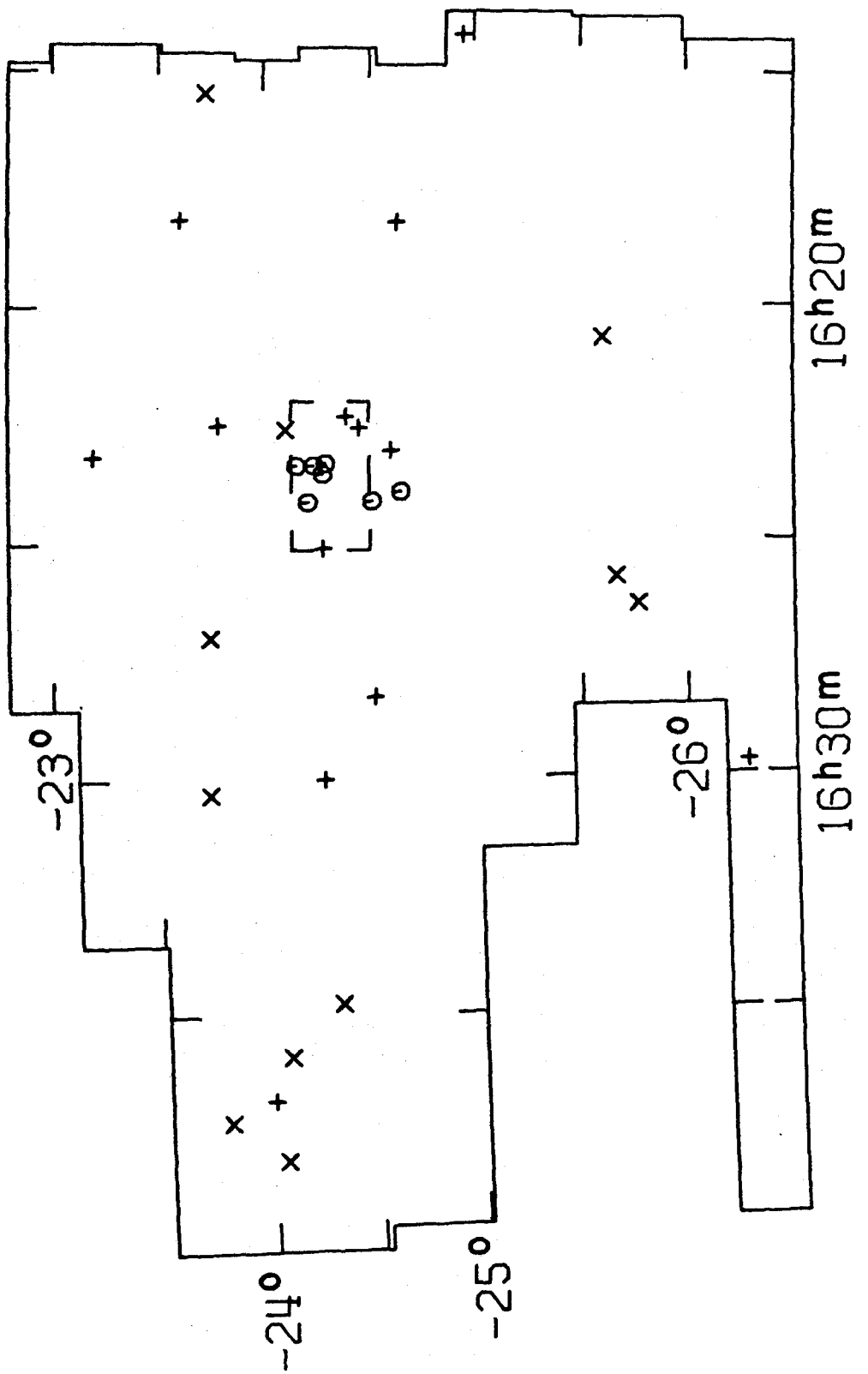

Fig. 6

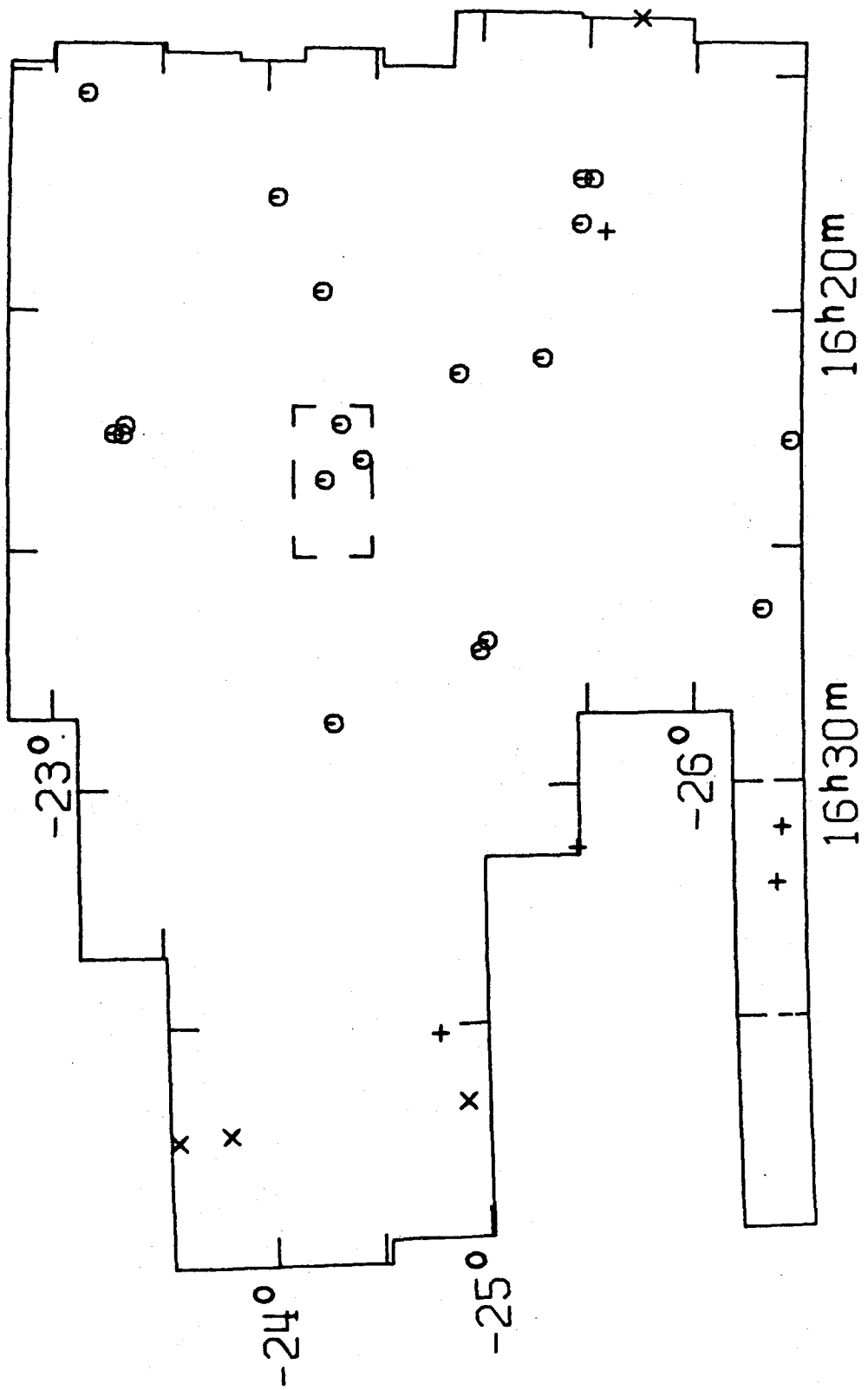

Fig. 7

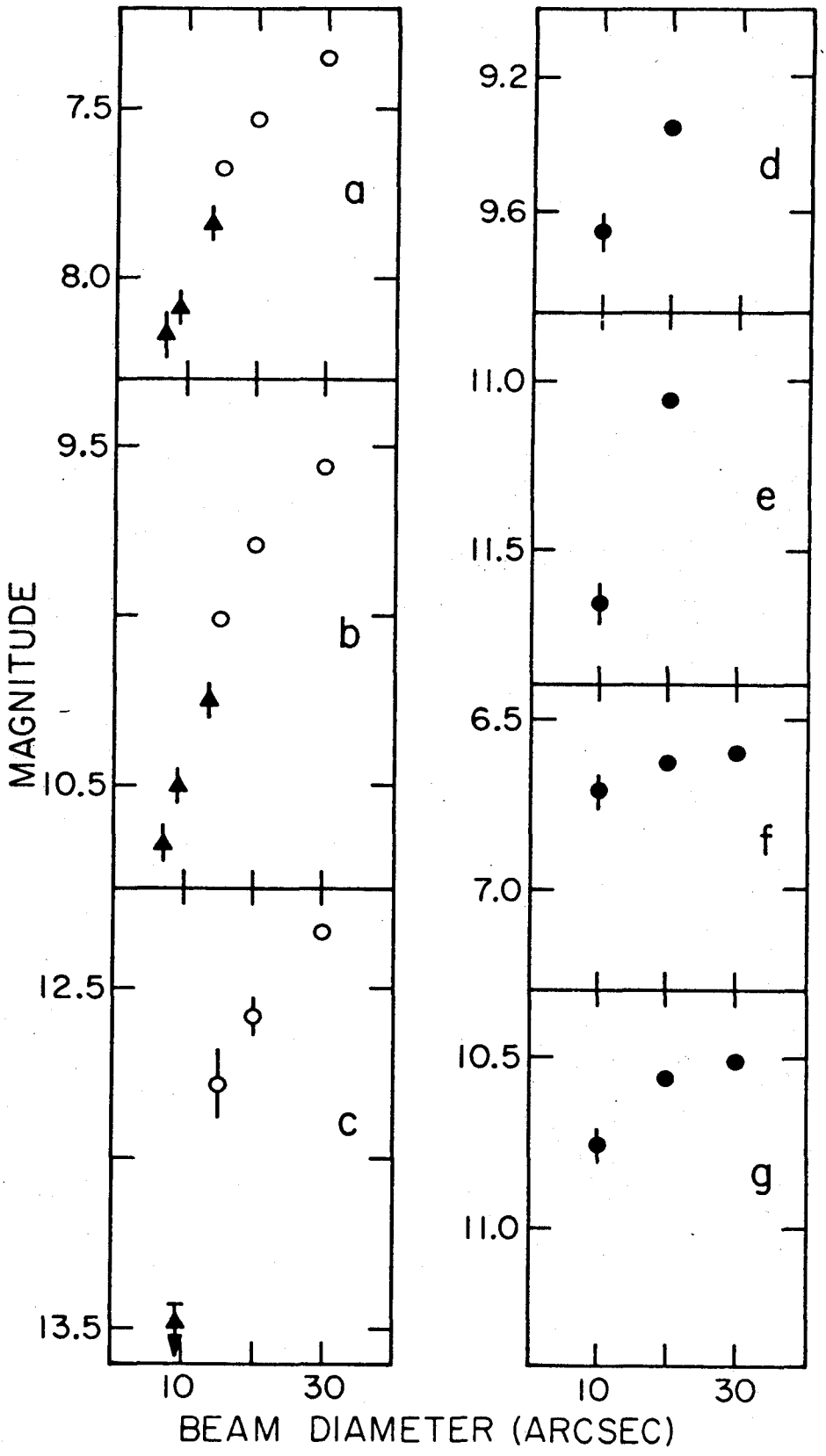
7.5
8.0
9.5
10.5
12.5
13.5
a
b
c
9.2
9.6
11.0
11.5
6.5
7.0
10.5
11.0
d
e
f
g
MAGNITUDE
10
30
10
30
BEAM DIAMETER (ARCSEC)

Fig. 8

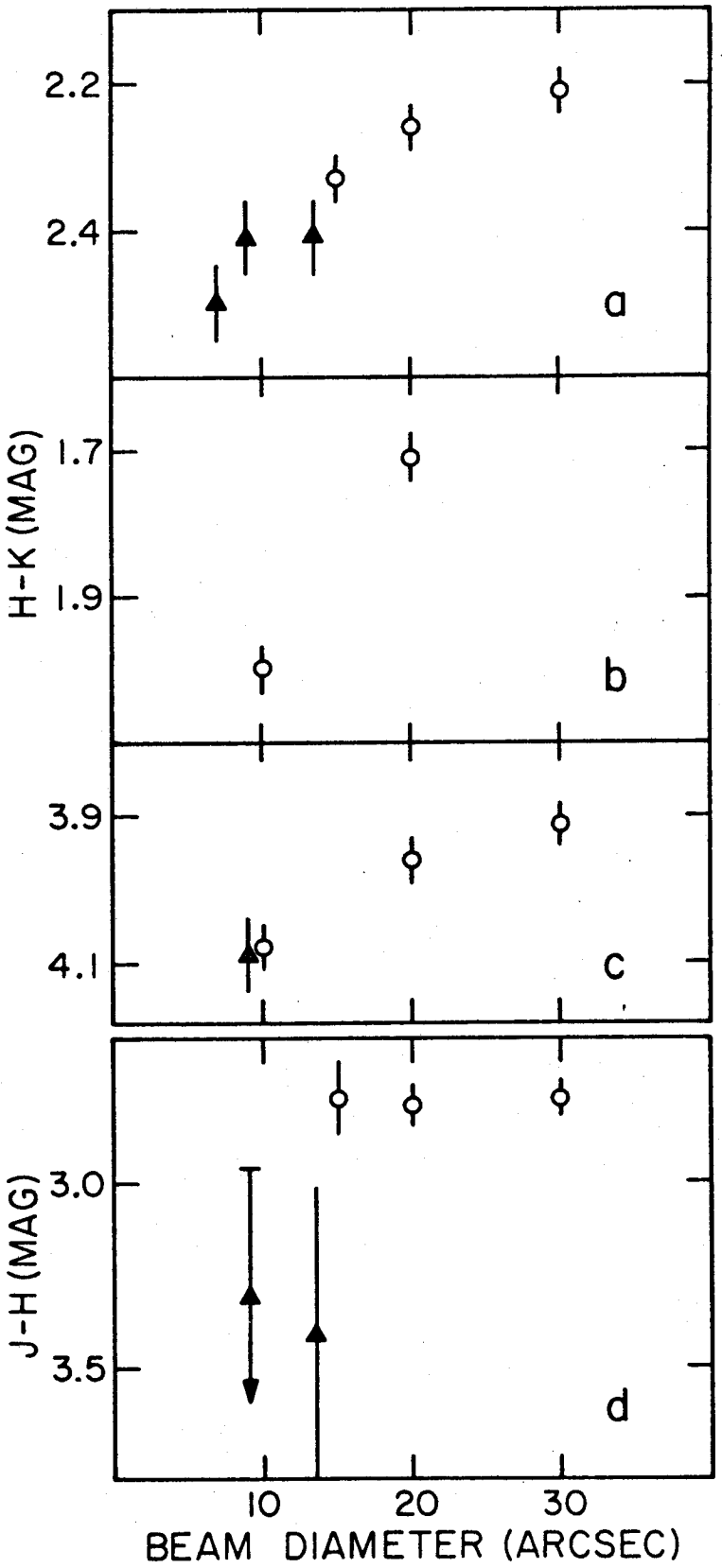
2.2
2.4
a
H-K (MAG)
1.7
1.9
b
3.9
4.1
c
J-H (MAG)
3.0
3.5
d
10
20
30
BEAM DIAMETER (ARCSEC)

Fig. 9

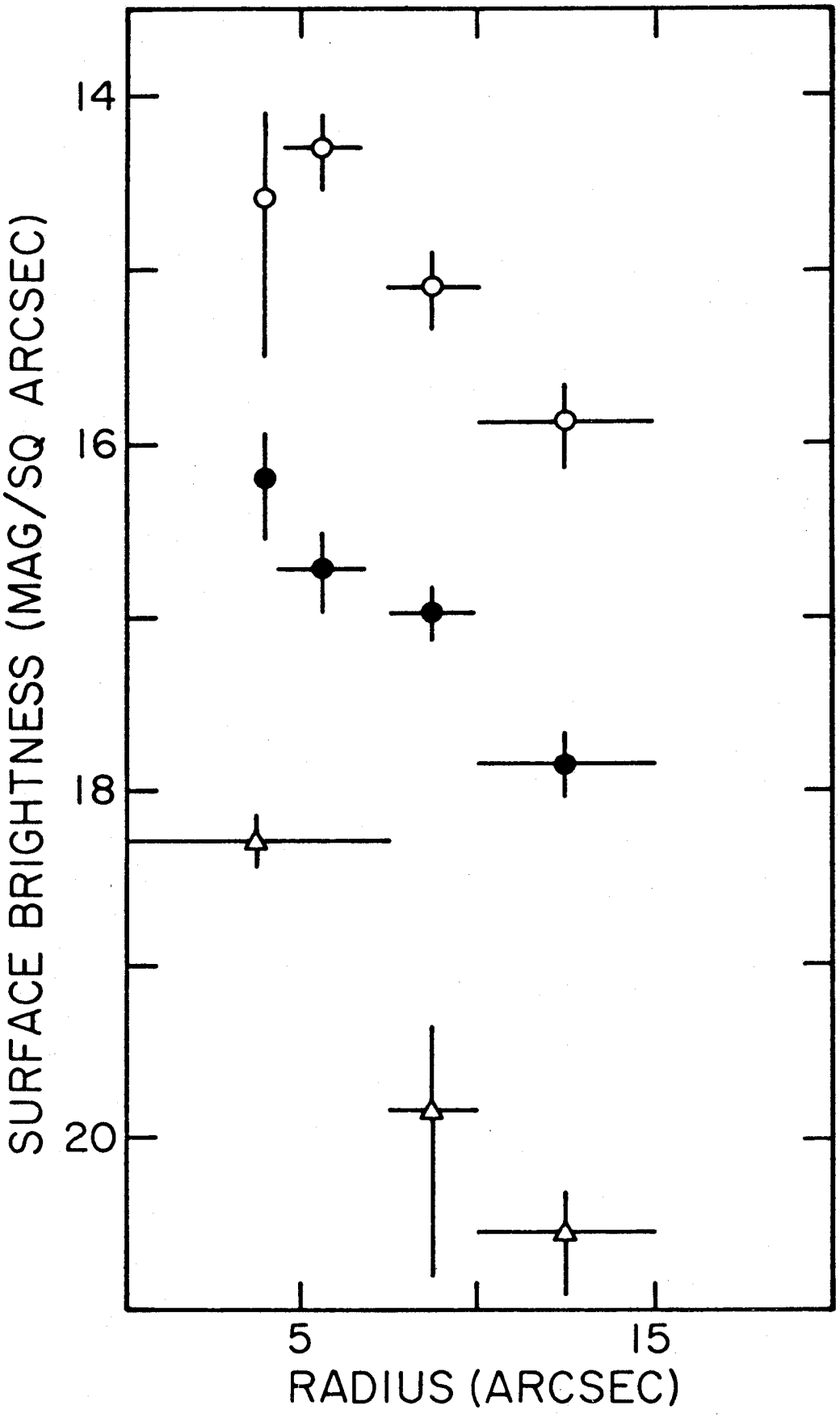
14
16
18
20
SURFACE BRIGHTNESS (MAG/SQ ARCSEC)
5
15
RADIUS (ARCSEC)

Fig. 10

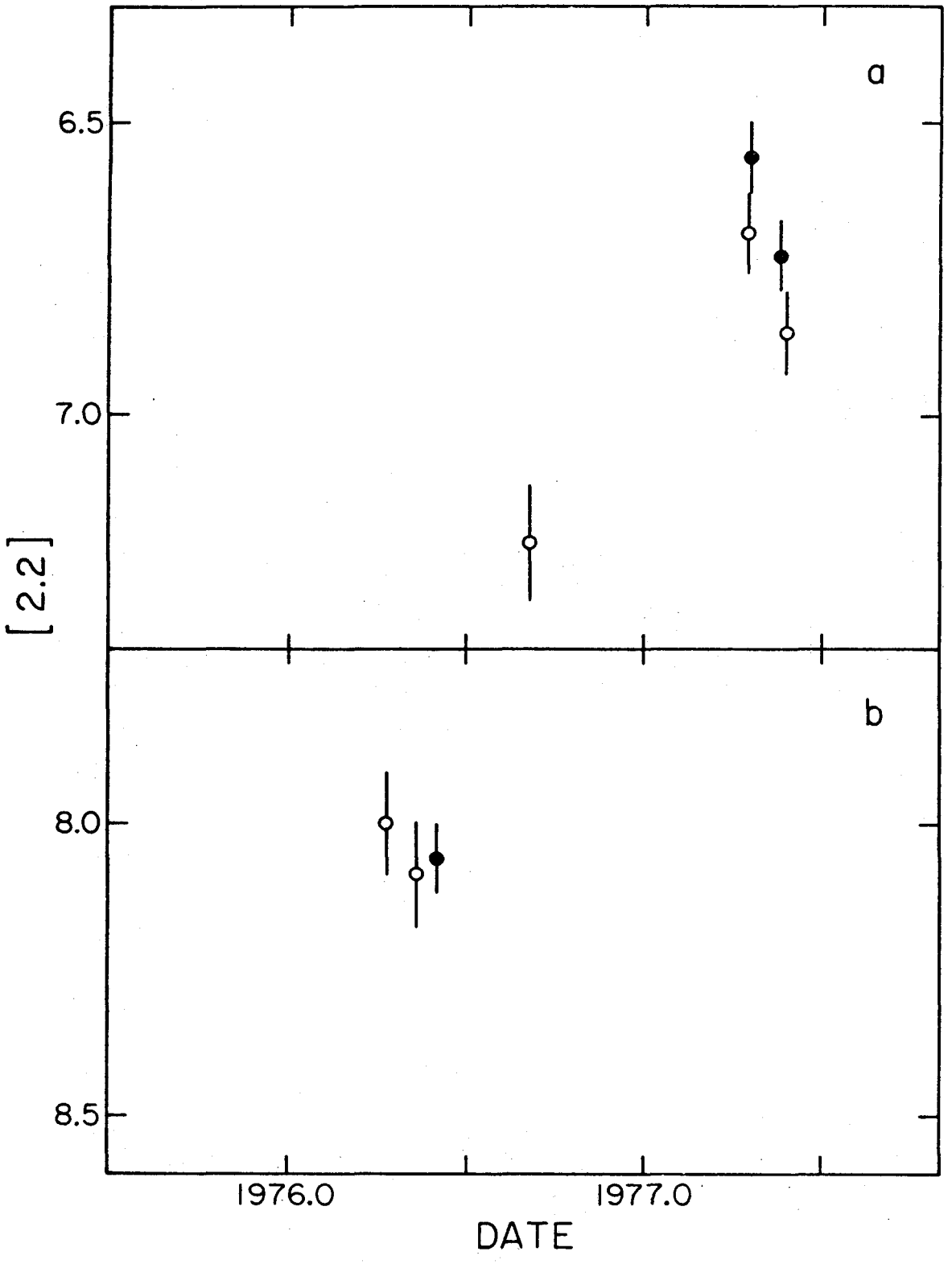

Fig. 11

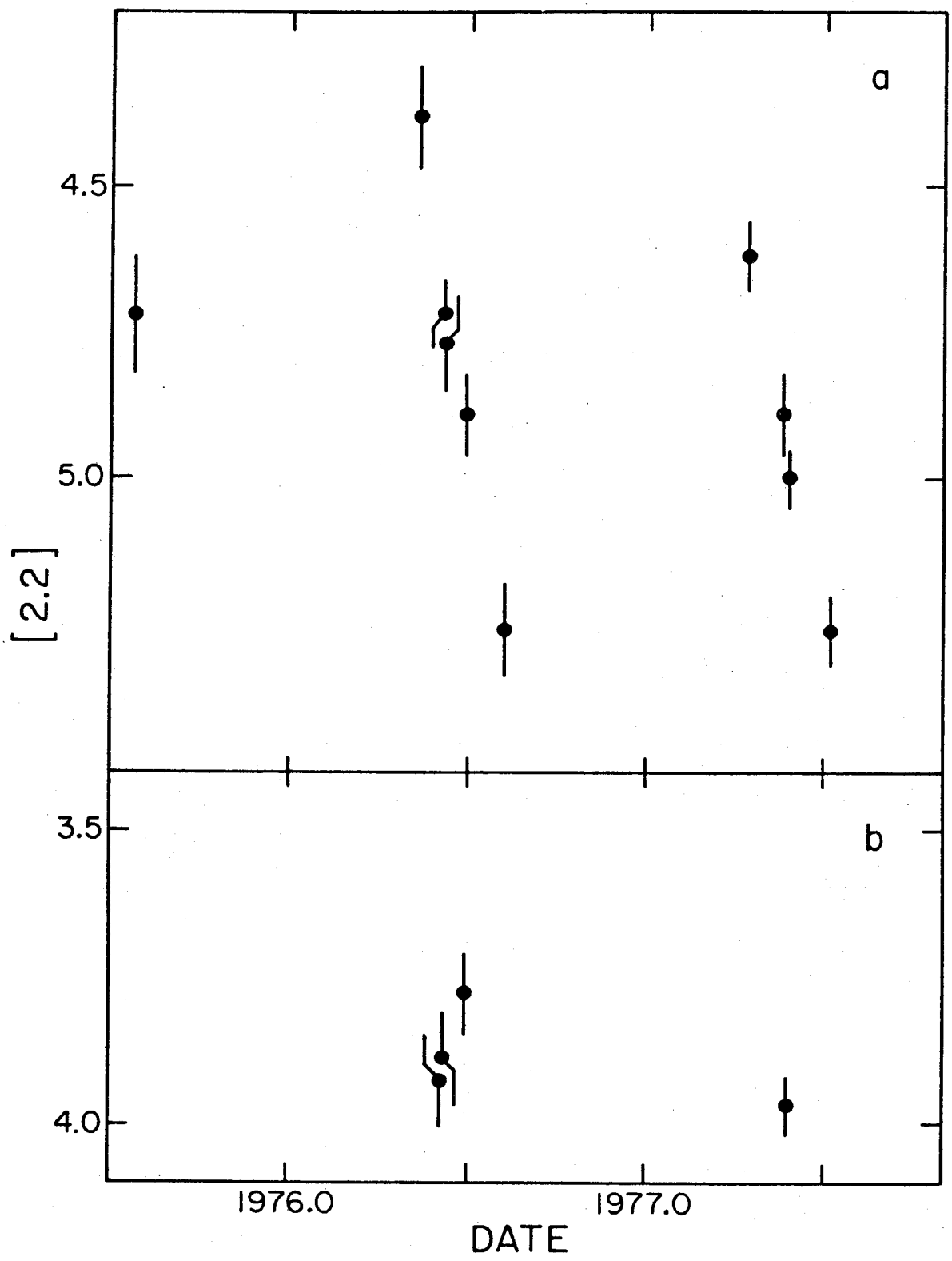

Fig. 12